Using Microsimulation to Estimate the Impact of Transportation Improvements and Operational Policy Changes on Travel Time Reliability

by

Reza Golshan Khavas

A thesis

presented to the University of Waterloo

in fulfillment of the

thesis requirement for the degree of

Doctor of Philosophy

in

Civil Engineering

Waterloo, Ontario, Canada 2017

Author's Declaration

This thesis consists of material all of which I authored or co-authored: see Statement of Contributions included in the thesis. This is a true copy of the thesis, including any required final revisions, as accepted by my examiners.

I understand that my thesis may be made electronically available to the public.

Statement of Contributions

Chapter 4 of this thesis consists of a paper that was co-authored by myself, my supervisor, Dr. Bruce Hellinga, and a PHD student, Mr. A. Zarinbal. I developed and documented the methodology. Mr. Zarinbal assisted with implementing the method within software. He also designed a website to demonstrate the output.

Abstract

Traditionally, traffic engineers have designed roadway networks and operational strategies to manage congestion and minimize delays during the peak demand period for some "average" or "typical" day. However, increasingly, there is concern about not only the average traffic conditions along a route (during some period of the day), but also about the variability of the required time to traverse the route. Travel times vary as a function of the departure time according to relatively predictable changes in the traffic demands (i.e. travel times are longer during the peak commuting periods than during off peak periods). However, the time to complete the same trip at the same departure time also varies from day to day. The variability of travel time, and the associated additional costs, has introduced another performance measure in transportation engineering called *travel time reliability (TTR)*. Travel time reliability has gained significant attention among the transportation researchers and practitioners recently. In this research, we aimed to implement traffic microsimulation models in order to model travel time reliability and finally to incorporate it into the alternative comparison. The contribution areas of this research are explained briefly in the following paragraphs.

Previous work that has examined the impact of weather on the characteristics of the speed-flow-density relationship has defined the weather conditions *a priori* and then attempted to determine the macroscopic traffic stream characteristics for these categories. However, for the purposes of modeling travel time reliability, it is necessary to only capture those weather conditions for which the associated macroscopic characteristics are statistically different. In this research we develop a technique to distinguish distinct weather categories through an innovative method.

Also, the process of determining macroscopic traffic stream characteristics requires the calibration of a macroscopic speed-flow-density model to field data. In employing this approach, we observed that the errors associated with the estimated parameters are impacted by the number and distribution of the observation points that used to calibrate the model. Therefore, we developed models to estimate the corresponding errors of the estimated traffic parameters and found that for most practical applications, the estimation of the jam density is most sensitive to the distribution of the calibration

data. As a result, we suggested some specific conditions for which the jam density value should be assumed *a priori* rather than calibrated on the basis of the available field data.

We additionally wanted to be able to model specific weather categories. We knew the traffic flow parameters of those weather conditions from the field data and we wanted the same traffic characteristics to be simulated in the traffic microsimulation model. Therefore, we proposed and evaluated a method to map the traffic flow characteristics to the TMM input parameters. The model developed in this research is not only applicable to simulate different weather categories, but also can be used to simulate any traffic condition -within the acceptable range of the model- when the traffic flow parameters are known.

Furthermore, we aimed to monetize travel time (un)reliability. To do this we have adopted the unreliability cost in terms of the costs of arriving early or arriving late. This approach has been widely used to quantify the costs of unreliability of public transport system; however, for road transport, this construct requires that we know the *scheduled travel time* which, from the user's perspective is the *anticipated* travel. We carried out a stated preference survey to estimate the anticipated travel time based on the travel time distribution. On the basis of the survey responses, we proposed two models in which travelers ignore unusually long travel times when determining their anticipated travel time.

Finally, we incorporated all of these findings to create an approach to quantify the cost of travel time (un)reliability using traffic microsimulation tools. We demonstrate this approach to evaluate two road improvement alternatives. We used the traffic simulation model VISSIM to compare these two alternatives based on the travel time cost and travel time reliability cost together.

Acknowledgement

First of all, I wish to praise and thank God for all His blessings. I would not have made any progress without His providence.

I would like to express my sincere gratitude to my supervisor, Professor Bruce Hellinga, for his invaluable guidance, brilliant ideas, continuous motivation and the financial support. I learned a lot from his profound knowledge and great personality. I would also like to thank my PHD examining committee members, Dr. Matthew Roorda, Dr. Jeffrey Casello, Dr. Carl Haas, and Dr. Clarence Woudsma for their time and valuable comments.

I am grateful to my friends and colleagues Wenfu Wang, Reza Noroozi, Ehsan Bagheri, Sajad Shiravi, Soroush Salek Moghaddam, Ali Sarhadi and Babak Mehran for their kind support and great friendship. My special thanks go to Mr. Amir Zarinbal for the fruitful discussions we had together and also his invaluable assistance especially in IT-related areas of my research. I additionally appreciate the Iranian Ministry of Science, Research and Technology for partially funding this research.

I am deeply indebted to my beloved parents who were my first teachers. Their unconditional love and support always inspired me through my life.

Finally, I would like to thank my wonderful wife, Maryam and my lovely daughter Zahra, for their endless love, unconditional support, encouragement, and patience which made this research possible.

Dedication

Dedicated to my family:

My dearest wife, Maryam,

and my lovely daughter, Zahra

Table of Contents

List of Figures

List of Tables

Chapter 1

Introduction

1.1. Background

Traditionally, traffic engineers have designed roadway networks and operational strategies to manage congestion and minimize delays during the peak demand period for some "average" or "typical" day. However, increasingly, there is concern about not only the average traffic conditions along a route (during some period of the day), but also about the variability of the required time to traverse the route. Travel times vary as a function of the departure time according to relatively predictable changes in the traffic demands (i.e. travel times are longer during the peak commuting periods than during off peak periods). However, the time to complete a trip along a particular route between a specific origin and destination when the trip starts at a certain departure time (e.g. between 5 and 5:15 pm) also varies from day to day.

The variability of travel time is caused by various factors including: demand variation; insufficient road capacity; weather impacts; special events; road works; traffic management policies; and road incidents. Sources of variability have been categorized in Figure 1-1. In this figure the sources of travel time variation have been divided in two main groups: demand related and supply related sources.

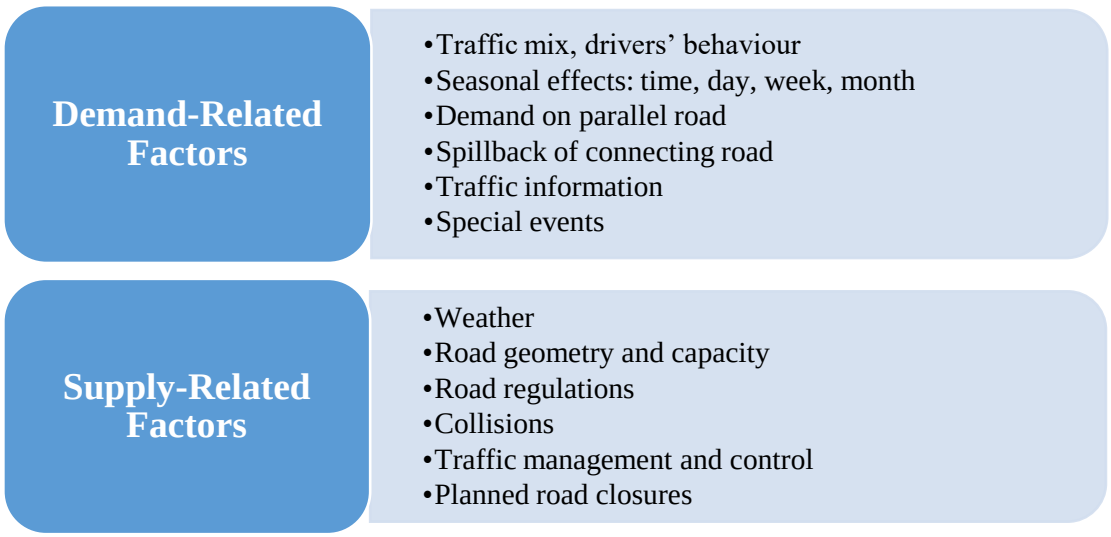

Figure 1-1-Sources of travel time variation

The importance of arriving at the destination at a specific time is known to vary by trip type (e.g. much more important for a trip to the airport to catch a flight than a trip to the mall for shopping). Nevertheless, if the traveler has a desired arrival time, and is uncertain about the time required to travel to the destination (e.g. because of variations in travel time) then the traveler typically budgets extra time in order to be more certain of arriving on time, which increases the total travel cost considering the value of travel time (VOT) for different road users. Not only does this additional cost impact commuters, but it also impacts businesses for which punctuality is important (e.g. freight companies).

The variability of travel time, and the associated additional costs, has introduced another performance measure in transportation engineering called *travel time reliability (TTR)*. Generally speaking, travel time is more reliable when it is less variable; meaning that the TTR is inversely proportional to travel time variability. Travel time reliability has several definitions in the literature; one of them being "the consistency or dependability in travel times, as measured from day to day and/or within different times of day" (U.S. Federal Highway Administration (FHWA), 2009).

Reliability of travel time is valuable. Casello et al.(2009) developed models that included the cost of (un)reliability as a part of the generalized cost of the transit mode while they assumed the difference between the necessary arrival time and the actual arrival time as the measure of reliability. They

suggested that developed models would improve the estimation of modal split in the models used for transportation forecasting.

Empirical research projects verify that the value of reliability (VOR) is larger than the value of travel time (VOT) for business trips (Warffemius, 2013). Other studies confirm that improvements made in travel time reliability are worth more than improvements of the average travel time. For instance, one study found that the cost a driver considers for mean travel time is $2.60 to $8 per hour while it is $10 to $15 per hour for standard deviation of travel time, where standard deviation is a measure of TTR (Small, 1999). The reason is that the travel time unreliability brings "scheduling cost"- the extra time the traveler budgets for the uncertainty of a route travel time - and makes the travel more expensive (Chen et al., 2003).

Travel time reliability was not the focus area in transportation engineering until the beginning of this millennium. For years, when authorities aimed to improve the performance of a road, the main objective was to increase the capacity and thereby to improve (reduce) the average travel time. Although the average travel time is still considered as the traditional road performance measure, travel time reliability has started to be used by practitioners as an additional measure of performance. There are several reasons for the increasing importance of travel time reliability. The most significant factor is that decision makers now consider a wider range of potential treatments for improving roadway performance. Road improvement options are no longer limited to capacity expansion through the addition of lanes. In fact, roadway expansion is becoming increasingly expensive and consequently impractical, particularly within developed urban centers. There are varieties of alternative improvement options. One example is the use of technologies to provide real-time information to travelers so that they are able to make optimal travel decisions (e.g. departure time, mode, route, etc.). Also, among the alternatives is the use of advanced traffic management strategies that are able to pro-actively control roadway corridors. The challenge with many of these alternative treatments is that although they may have significant benefits in terms of improving travel time reliability, they may have only a small impact on mean travel time. Consequently, when one is applying traditional cost-benefit evaluation methods, which rely on computing benefits only in terms of improvements in the mean travel time, the associated benefits may be substantially underestimated for such alternatives.

Thus, ignoring the value of improving travel time reliability may bias the economic evaluation of some types of treatments which leads to the inefficient allocation of roadway improvement budgets. Furthermore, these types of treatments may also be undervalued when compared to other types of public sector investments.

There are a number of travel time reliability measures in the literature, all defined based on the characteristics of the travel time distribution. If the objective is to quantify the reliability of an existing corridor, then the travel time distribution can be determined by obtaining travel times from all (or a sample) of the vehicles travelling along that corridor over a period of many days. The common practice is to obtain field data for a period of at least one year.

However, if the objective is to evaluate the impact that one or more proposed roadway improvements or changes in policy (i.e. alternatives) will have on travel time reliability, then it is necessary to use models to estimate the travel time reliability for each potential future alternative.

Analytical models and traffic micro-simulation models (TMM) are two different tools that can be used to estimate the travel time reliability.

One of the earliest attempt to develop an analytical model to explain travel time variation was suggested by Herman and Lam (1974). They suggested the relationship between the mean ($\bar{\tau}$) and the standard deviation (σ) of travel time could be explained with the following empirical regression:

$$\sigma = a(\bar{\tau})^b \tag{1-1}$$

in which a and b are estimated regression parameters. Other researchers including Richardson and Taylor (1978) and Eliasson (2007) developed analytical models to relate the mean and the standard deviation of travel times. Some other researchers including Park et al (2010), and Tu et al (2008) studied the relationship between travel time variation and road incidents, while other researchers such as Kwon (2011) investigated the weather-related impacts on the travel time variation. Some of these models consider the TTR metrics as the dependent variable, and the factors that impact TTR as independent variables. Other analytical models estimate travel times for different situations (e.g.

roadway geometry, traffic demands, weather, etc.) and calculate the distribution of travel times based on the probability of those situations (Cambridge Systematics, 2013).

1.2. Problem Statement

Analytical models offer the following advantages:

- They are typically easy to apply and require relatively little field data for input.
- The relationships between the independent variables (e.g. sources of variation) and the dependent variable (e.g. TTR) are explicitly defined by the analytical model and therefore are easier to understand.

However, analytical models typically suffer from the following limitations:

- They require an extensive set of field data, including a wide range of locations, on which to calibrate the model;
- The model may not be transferable to locations that were not included in the original calibration data set;
- They cannot be used to evaluate the impacts of new designs, technologies, or policies for which no field data are available; and
- They typically only estimate a single characteristic of the travel time distribution (e.g. Standard deviation) rather than the distribution itself.

In contrast, traffic micro-simulation models could be used to estimate the impact of roadway improvements or policy changes on travel time reliability. The conceptual approach is to use the TMM to simulate a large number of "days". TMM inputs would be varied so that each "day" would reflect different demand and supply factors which impact the travel time distribution. Essentially this is a Monte Carlo simulation approach (Bindel and Goodman, 2009) for estimating distributions given a model (in this case the TMM) and distributions for a number of model input parameters (in this case parameters to reflect the demand and supply factors that impact travel time reliability). Monte Carlo simulation consists of running the model multiple times (trials); each time randomly selecting the values from the input parameter distributions. As the number of runs increases, the estimation of the

distribution of the output measure of performance begins to more closely approximate the true distribution. Consequently, the use of TMM offer the following advantages:

- Field data are required only from the site being investigated;
- TMM permit the incorporation of as many factors as desired into the analysis process by designing different scenarios;
- TMM permit estimation of the entire travel time distribution (for each O-D, each route, each link, etc.); and
- TMM are already commonly being used to perform evaluations of the impacts (e.g. average travel time; emissions, etc.) of potential roadway improvements and therefore extracting measures that capture the impact on TTR might be done with very little additional effort.

However, the use of traffic micro-simulation models presents the following challenges:

- Input factors (e.g. weather) required to be characterized clearly; however, it is not clear how they should be characterized. For instance, it is not clear how many distinct weather categories are really available to be simulated in TMM.
- Most TMM do not define input parameters that map directly to factors that cause travel time variability in the real world (e.g. weather). Consequently, there is a need to map variations in these factors to model input parameters.

Finally, even when the travel time distribution can be estimated (whether by TMM or some analytical model), there is a question of how this distribution can be used to make decisions about the relative preference of one alternative versus another.

This thesis addresses these challenges. Figure 1-2 illustrates the conceptual process of performing an evaluation of alternatives using TMM. The following provides a brief introduction of each stage in this process and identifies the areas in which this thesis makes novel contributions to the state of art.

Field Data

The study area in which the travel time reliability is computed is introduced to the traffic microsimulation models through the field data. The field data required for the travel time reliability is

usually the archived data of at least one year or more. The data should be cleaned and prepared for the further steps.

Scenario Generation

To incorporate the impact of the travel time variability factors, TMM scenarios should be generated. In this research, we considered the demand variation as the demand-side traffic variation factor as well as weather variation and vehicle collisions as the two supply-side variability factors.

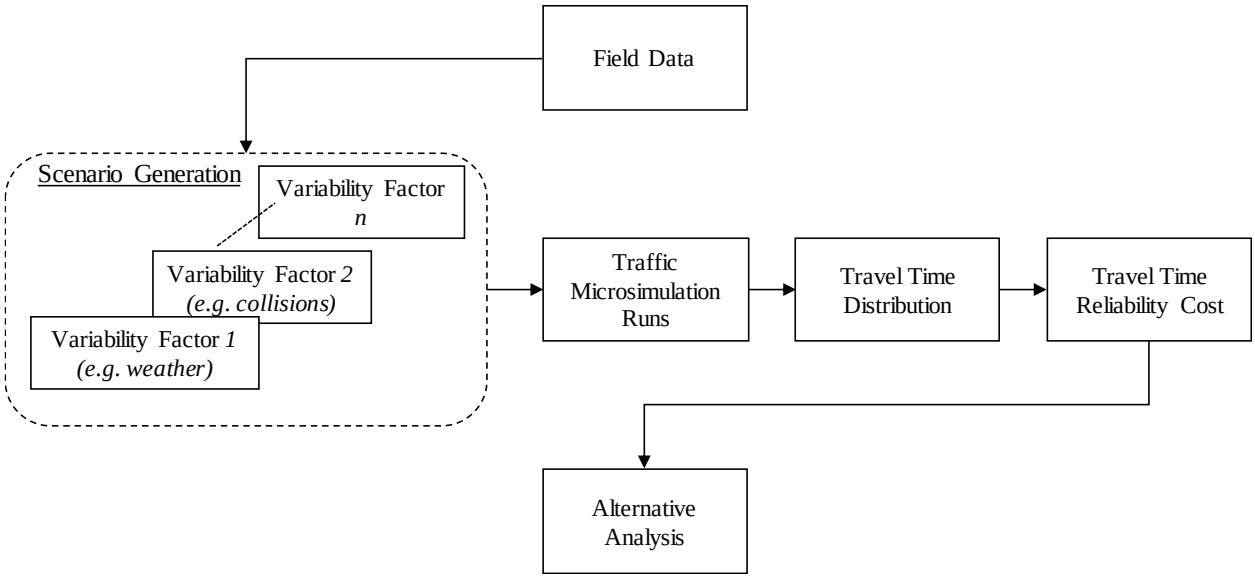

Figure 1-2- Conceptual stages from data preparation to alternative analysis

One of the significant areas of contribution of this research is the development of methods for incorporating the effects of weather within the TMM. There are three contributions in this area, namely (1) a method was developed to determine the preferred approach for calibrating a macroscopic speed-flow-density model on the basis of field data reflecting a specific weather/road surface condition; (2) a method was developed to determine statistically distinct weather/road surface condition categories; and (3) models were developed to permit the estimation of TMM input parameter values that represent a traffic stream with a set of desired characteristics (i.e. a traffic stream with characteristics reflecting a specific weather/road surface condition).

Traffic Microsimulation Model

Within this research, we have chosen to use the VISSIM TMM. However, the proposed methods are applicable to any TMM.

Travel Time Distribution

The travel time values obtained from simulation runs are captured to compute the travel time distribution. Within this thesis, we propose methods for compiling and aggregating these data to be computational and data storage efficient.

Travel Time Reliability Cost

One of the challenges is translating the estimated travel time distribution into a cost value to be used within cost-benefit analyses. We propose a new method to compute the travel time reliability cost which determines cost as a function of the difference between the actual travel time and the anticipated travel time. In most previous work, anticipated travel time is considered to be the mean travel time; however, one of the contributions of this research is the use of stated preference survey data to determine a model which estimates the anticipated travel time on the basis of the travel time distribution.

Alternative Analysis

We demonstrate the proposed approach through a sample application. We compared two traffic improvement alternatives based on their travel time cost and travel time reliability cost.

Figure 1-3 shows how different modules of this research are implemented to enable us to perform alternative analysis. The contributions of this research as associated with the modules shown in green.

1.3. Thesis Outline

This dissertation is organized into seven chapters as follows:

1. Introduction
2. Determining the preferred approach for calibrating a macroscopic speed-flow-density model on the basis of empirical data

3. Determining road surface and weather conditions which have a significant impact on traffic stream characteristics
4. Identifying parameters to model traffic during inclement weather using microsimulation
5. Incorporate drivers' anticipated travel time in estimating travel time reliability cost
6. Demonstrating the methodology: alternative analysis
7. Conclusions and recommendations

Note that a review of the relevant literature is provided within each chapter rather than extracted into a single separate chapter.

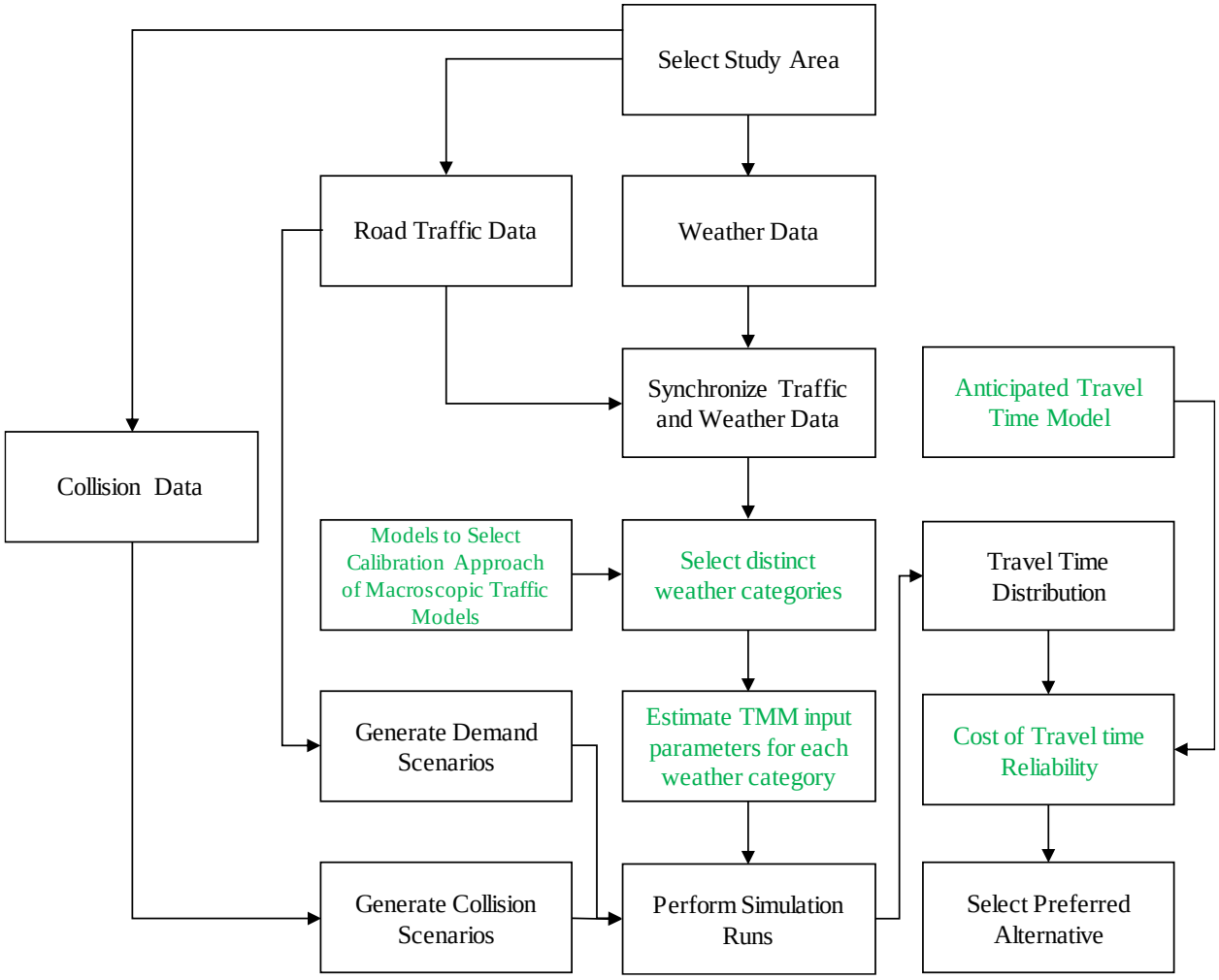

Figure 1-3-Incorporation of research findings in the alternative analysis

Chapter 2

Calibrating a macroscopic speed-flow-density relationship using field data

2.1. Introduction

In order to incorporate different weather conditions within a microscopic traffic simulation model, it is necessary to (i) characterize the weather conditions; (ii) determine the effect that this weather condition has on driver behavior; and (iii) select appropriate values for the simulation input parameters so that the model reflects the desired behavior. This chapter addresses step (ii) from the above list.

It is (currently) impractical to make observations regarding the behavior of individual drivers under different weather conditions. However, most large urban centers have deployed systems and sensors (e.g. induction loop detectors) to collect data regarding the characteristics of the traffic stream such as average speed and flow rate. When these data are combined with meteorological weather and/or road surface condition data, it is possible to determine the traffic stream characteristics associated with specific weather conditions.

The relationship between traffic stream speed, density and flow has been under investigation since the early 20th century. In 1935, Greenshields proposed a linear relationship between speed and density for the whole range of the density in which the parameters of the model were free-flow speed and jam density (Greenshields et al., 1935). During the following years, other researchers such as Greenberg (1959), Underwood (1961), Edie (1961), etc. suggested that speed-density relationship is nonlinear (i.e. exponential, logarithmic, or both). Some researchers (including Edie) suggested piecewise models for different ranges of the traffic density.

More recently, Van Aerde and Rakha (1995) suggested a four-parameter nonlinear model which provides a continuous relationship between the speed and the density. The parameters of Van Aerde's model are free-flow speed (u_f), speed-at-capacity (u_c), jam density (k_j), and capacity (q_c). Figure 2-1 consists of two-dimensional projections of the calibrated Van Aerde's model in terms of the relationships between: (a) speed as a function of flow; (b) speed as a function of density; and (c) flow as a function of density. The blue dots represent the observed traffic data aggregated at 5-minute intervals. The red curve is the calibrated Van Aerde's traffic flow relationship.

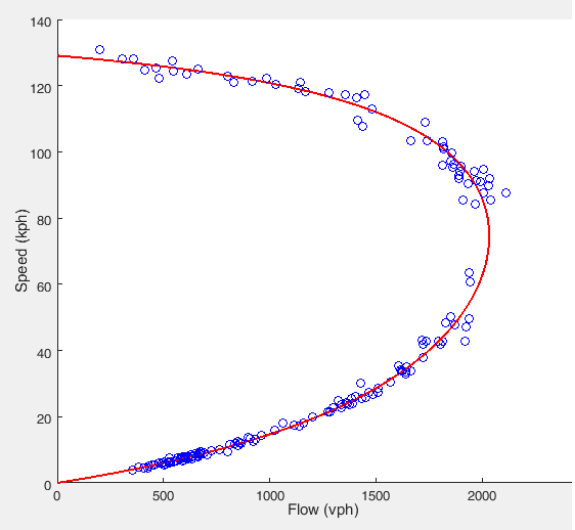

(a)Speed and Flow

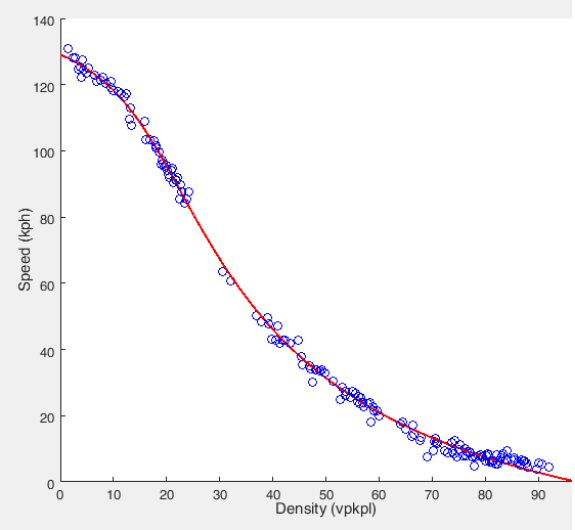

(b) Speed and Density

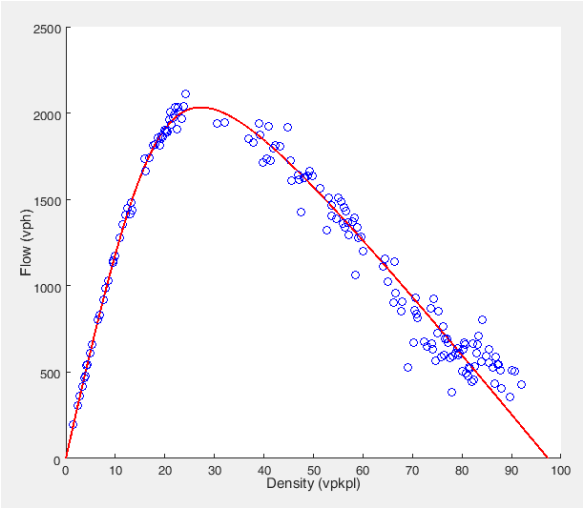

(c) Flow and Density

Figure 2-1-Illustration of Van Aerde's macroscopic speed-density-flow model

In this thesis, we use Van Aerde's model to characterize the traffic stream because the model is continuous and permits all four traffic stream characteristics to be specified as parameters to the model. We point out here that from a conceptual perspective, any other continuous macroscopic traffic model could have been used. However, using a model with fewer degrees of freedom, such as Greenshields' model, restricts the ability to reflect differences in traffic stream behavior under different weather conditions, and therefore is less desirable.

Thus, given a set of observed traffic data, we can calibrate Van Aerde's model and find the associated values for the four model parameters (i.e. u_f, u_c, k_j, and q_c). Ultimately, our goal is to determine the set of weather conditions which cause statistically significant differences in these traffic stream parameters. Consequently, we want to ensure that the model parameter estimates are reliable.

We hypothesize that there are two characteristics of the calibration field data set that impact the reliability of the estimated traffic stream parameters, namely: (i) the number of observations; and (ii) the distribution of the observations across density. We further hypothesize that the jam density parameter is most sensitive to these two factors and that under some conditions, it is best to fix the value of jam density rather than try to calibrate the value from the field data.

To test these hypotheses, we study the impact of the distribution of the field data over the range of the density on the error of the whole model calibration process as well as the error of each traffic parameters (i.e. free-flow speed (u_f), speed-at-capacity (u_c), jam density (k_j), and capacity (q_c)).

2.1.1. Calibrating Van Aerde's Model

In this research, we are required to estimate the traffic flow parameters in several occasions. Here we explain how we estimate these parameters. Rakha and Arafeh (2007) showed that the functional form of the Van Aerde's traffic flow model can be shown as:

$$h_n = c_1 + c_3 u_n + \frac{c_2}{u_f - u_n} \tag{2-1}$$

where:

h_n : distance headway (km) between two consecutive vehicles (i.e. *n-1* and *n*) travelling in the same lane

u_n: speed of vehicle *n* (km/h)

u_f: free-flow speed (km/h)

c_1, c_2, c_3: constants

Then as per Rakha and Arafeh (2007), Van Aerde's model can be calibrated by solving the following optimization problem:

$$Min \quad E = \sum_i \left\{ \left[\frac{u_i - \hat{u}_i}{\tilde{u}} \right]^2 + \left[\frac{q_i - \hat{q}_i}{\tilde{q}} \right]^2 + \left[\frac{k_i - \hat{k}_i}{\tilde{k}} \right]^2 \right\} \tag{2-2}$$

S.T.

$$\hat{k}_i = \frac{1}{c_1 + \frac{c_2}{u_f - \hat{u}_i} + c_3 \hat{u}_i} \quad , \forall i$$

$$\hat{q}_i = \hat{k}_i \times \hat{u}_i \quad , \forall i$$

$$\hat{q}_i, \hat{k}_i, \hat{u}_i \geq 0 \quad , \forall i$$

$$\hat{u}_i < u_f \quad , \forall i$$

$$0.5u_f \leq u_c \leq u_f$$

$$q_c \leq \frac{k_j u_f u_c}{2u_f - u_c}$$

$$c_1 = \frac{u_f}{k_j {u_c}^2}(2u_c - u_f); \quad c_2 = \frac{u_f}{k_j {u_c}^2}(u_f - u_c)^2; \quad c_3 = \frac{1}{q_c} - \frac{u_f}{k_j {u_c}^2}$$

$${u_f}^{min} \leq u_f \leq {u_f}^{max}; \; {u_c}^{min} \leq u_c \leq {u_c}^{max}; \; {k_j}^{min} \leq k_j \leq {k_j}^{max}; \; {q_c}^{min} \leq q_c \leq {q_c}^{max}$$

where u_i, k_i and q_i are space-mean speed, flow, and density from the field, variables with hat (^) are estimations, and variables with tilde (~) are the maximum observations. Other variables were defined earlier. We use this formulation whenever we calibrate Van Aerde's model in this research. Moreover, to reduce the computational cost, Rakha and Arafeh (2007) suggested to aggregate the observation points at user-defined density bins. We set the size of this density bins throughout this research at 0.25 vpkpl. We also used the built-in MultiStart algorithm in Matlab software to find the global minima of the above optimization problem in this research.

2.2. Problem Formulation

Consider that *B* is the set of traffic observations obtained from a traffic sensor at a location on a freeway. Observations (speed, density, flow) are aggregated and obtained over discrete time intervals (e.g. 5 minutes). *B* consists of observations from *n* time intervals such that we obtain speed (u_i^o), density

(k_i^o), and flow rate (q_i^o) where $i = 1, n$. In practice, the traffic sensors typically measure speed and flow, and then density is computed.

We calibrate Van Aerde's traffic model using the observations in set *B*. The fitted curve is a line in three-dimensional space. For each observed point (u_i^o, k_i^o, q_i^o) we can identify the nearest point on the fitted curve (u_i^c, k_i^c, q_i^c), and the normalized Euclidean distance between these two points is designated as $\|d_i\|$ and computed as follows (H. A. Rakha and Arafeh, 2007):

$$\|d_i\| = \sqrt{\left(\frac{u_i^o - u_i^c}{\tilde{u}}\right)^2 + \left(\frac{k_i^o - k_i^c}{\tilde{k}}\right)^2 + \left(\frac{q_i^o - q_i^c}{\tilde{q}}\right)^2} \quad (2\text{-}3)$$

In which the parameters with tilde (~) are the maximum field observation values.

The model calibration error (ε^c) is computed as

$$\varepsilon^c = \frac{\sum_{i=1}^{n} \|d_i\|}{n} \quad (2\text{-}4)$$

where *n* is the number of observation points.

To test our hypothesis, we wish to determine the following relationship:

$$\varepsilon^c = f(B_D, n) \quad (2\text{-}5)$$

In which B_D is some measure of the distribution of the traffic observations (i.e. set B) across density, *n* is the number of observations and *f* is a function that relates the calibration error to the distribution.

2.3. Data Generation

2.3.1. Generation of traffic data for calibrating the macroscopic speed-flow-density relationship

Applying the above equations to field data is challenging because: (i) the true value for the traffic stream parameters is unknown; and (ii) only a limited range of traffic conditions can be observed. Consequently, the set of traffic observations was generated from the VISSIM traffic microsimulation software. A hypothetical freeway section was coded in VISSIM (shown in Figure 2-2) and demands were varied to simulate the entire spectrum of traffic states (i.e. uncongested, capacity, and congested). The network consisted of two one-way roads: (1) and (2). The road (1) consisted of two sections. The

upstream section had three lanes and the downstream section had two lanes. The measurement point (i.e. location at which a traffic sensor was modelled) was located at the latter section. The road (2) had two lanes and both roads merged. The following techniques were used to create a wide range of traffic states:

1- Free flow: we defined a range of traffic demands during a number of time intervals in a way that the flow was always less than the capacity along all road sections.
2- Flow at Capacity: to experience the capacity state at the measurement point, we modelled a lane-drop upstream of the measurement point. By increasing the traffic demand entering roadway 1 to above the capacity of the two-lane section, a queue formed at the lane drop and the flow at the measurement point was equal to the capacity.
3- Traffic Congestion: we modelled a merging section downstream of the measurement point. By increasing the demand on roadway 2, it was possible to create a queue at the merging link, which would grow upstream until it spilled over the measurement point.

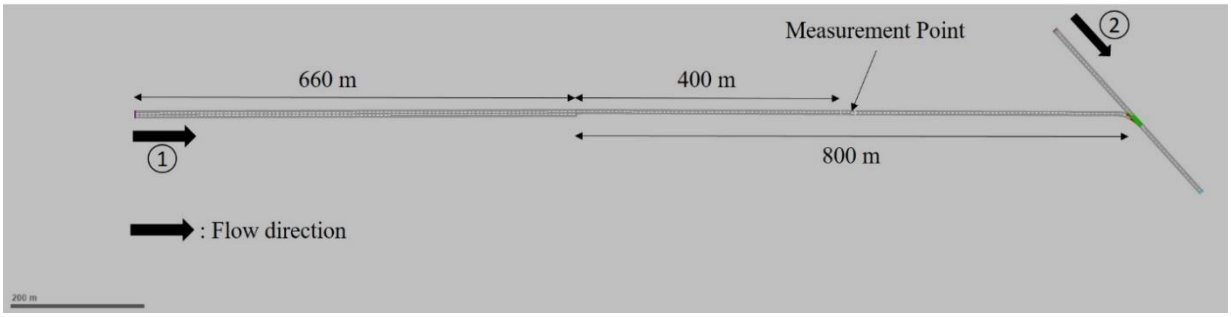

Figure 2-2-Simulated freeway section

The simulation time was 3.5 hours divided into 42 five-minute intervals. The simulation resolution was set to 5 time steps in each simulation second and the VISSIM default parameters were used. The first five-minute time interval was considered as warm-up period to load the network. We captured the aggregated five-minute speed, flow, and density measurements for all of the other 41 time intervals. The traffic demand values at each time interval are shown in Table 2-1.

Table 2-1-Time Variant Demand in Simulated Network

#	Time Interval (s)	Traffic Demand (vph)		#	Time Interval (s)	Traffic Demand (vph)	
		Road (1)	Road (2)			Road (1)	Road (2)
1	300-600	500	0	22	6600-6900	5200	200
2	600-900	750	0	23	6900-7200	5200	400
3	900-1200	1000	0	24	7200-7500	5000	600
4	1200-1500	1250	0	25	7500-7800	1500	800
5	1500-1800	1500	0	26	7800-8100	1500	1000
6	1800-2100	1750	0	27	8100-8400	1500	1200
7	2100-2400	2000	0	28	8400-8700	1500	1400
8	2400-2700	2250	0	29	8700-9000	1500	1600
9	2700-3000	2500	0	30	9000-9300	1500	1800
10	3000-3300	2750	0	31	9300-9600	1500	2000
11	3300-3600	3000	0	32	9600-9900	1400	2200
12	3600-3900	3250	0	33	9900-10200	1300	2000
13	3900-4200	3500	0	34	10200-10500	1200	1800
14	4200-4500	3750	0	35	10500-10800	1100	1600
15	4500-4800	4000	0	36	10800-11100	1000	1400
16	4800-5100	4250	0	37	11100-11400	900	1200
17	5100-5400	4500	0	38	11400-11700	800	0
18	5400-5700	4750	0	39	11700-12000	600	0
19	5700-6000	5000	0	40	12000-12300	400	0
20	6000-6300	5200	0	41	12300-12600	200	0
21	6300-6600	5200	0				

The simulation was run 570 times (each with a different random number seed) and therefore 41×570=23,370 data points were captured. This dataset formed our “population”. Figure 2-3 shows the speed-flow and speed-density plots of the population data points.

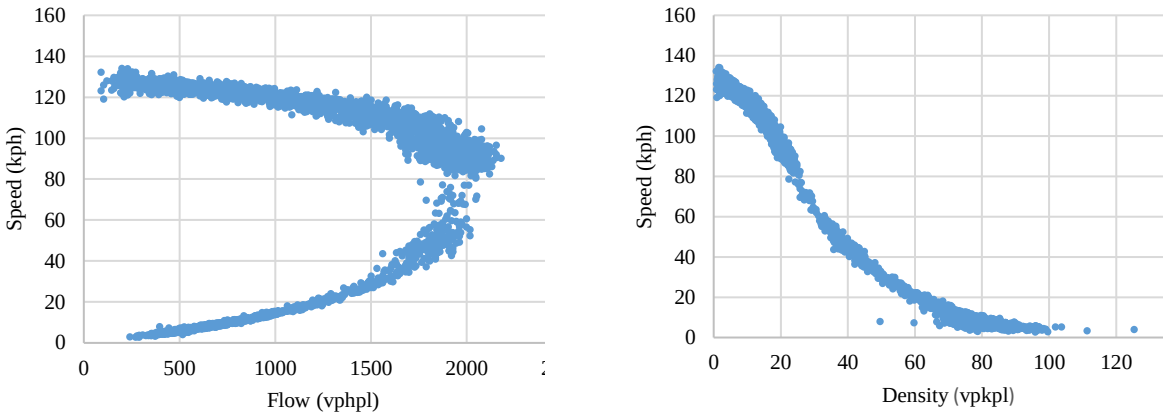

Figure 2-3- Fundamental diagrams of the traffic flow in the simulated network

Then we calibrated Van Aerde's traffic stream model using the technique introduced by Rakha (2010). The estimated traffic flow parameters were u_f=126.9 (kph), u_c=76.3 (kph), k_j=106.9 (vpkpl), and q_c=1969 (vph).

2.3.2. Characterizing the distribution of calibration data across the density space

To investigate the impact of the distribution of the calibration data on the estimation error we considered five bins on the density axis:

bin1: (0,20) vpkpl

bin2: (20,40) vpkpl

bin3: (40,60) vpkpl

bin4: (60,80) vpkpl

bin5: (80, max) vpkpl

The actual distribution of the entire population of calibration data across the five bins is provided in Table 2-2.

Table 2-2-distribution of calibration data across the density bins

Bin #	Density Range (vpkpl)	# of points in the bin	Proportion of the population in the bin
1	(0,20)	9256	40%
2	(20,40)	4313	18%
3	(40,60)	1018	4%
4	(60,80)	5487	23%
5	(80, 125.3)	3296	14%

We took samples from our "population" by specifying the proportion of the sampled points taken from each density bin (p_i, i = 1, 5) and where the proportions were restricted to one of six values ($p_i \in$ {0%, 20%, 40%, 60%, 80%, and 100%}). Naturally, the sum of the proportions across the five bins must equal 100%. For instance, one sampling schemes could be 20%, 20%, 0%, 0%, 60% in bin1 to bin5 respectively. If the sample size was 200 in one iteration, then the number of samples in bin1 to bin 5 would be 40, 40, 0, 0 and 120 respectively. The total number of individual sampling schemes is obtained from $\binom{(m-1)+(n_p-1)}{m-1}$ where m is the number of bins (i.e. m = 5) and n_p is the number of possible levels of proportion of samples in each bin (i.e. n_p = 6). Therefore, 126 different sampling schemes are possible.

Also, we investigate the impact of the number of observations in our sample. We consider 24 different sample sizes (i.e. $n \in$ {5, 10, 15, 20, 25, 30, 50, 100, 150, 200, 250, 300, 350, 400, 450, 500, 550, 600, 650, 700, 750, 800, 850, and 900}) from the population. To account for randomness, we repeated each sample scheme 50 times for each sample size. The sampling from the population within each bin was performed completely randomly at each repetition. In total, 126×24×50=151,200 samples were taken and for each sample j, Van Aerde's macroscopic model was calibrated following the method explained earlier to obtain the values u_{fj}, u_{cj}, k_{jj}, and q_{cj}.

2.4. Investigating Sensitivity

2.4.1. Investigating the impact of the distribution of calibration data on the calibration accuracy

For each sample j the model calibration error ε_j^c was computed using Equation (2-4). We then computed the arithmetic average calibration error across the 50 repetitions to obtain a single average value ($\bar{\varepsilon}_{d,e}^c$) for each combination of sample scheme (d = 1, 126) and number of observations in the sample (e = 1, 24).

Further, we define binary variables db_1 to db_5 (where db_i is 0 when p_i = 0 and 1 otherwise). In order to investigating the impact of the distribution of the points regardless the sample size impact, we initially aggregate the results over all sample sizes based on the values of *db1* to *db5*. Thirty-one sampling scheme groups (g_1 to g_{31}) were formed which are shown in Table 2-3. Each group has a representative $\bar{\varepsilon^c}$ which is the average of ε^c values of the samples that fall in that group.

Table 2-3-Average calibration error as a function of the distribution of the calibration data across density(Calibration error averaged across all sample sizes and groups sorted in ascending order of average calibration error)

Group	*db1*	*db2*	*db3*	*db4*	*db5*	Average Error
g_{16}	1	1	1	1	1	0.02
g_{3}	1	0	1	0	0	0.03
g_{4}	1	0	0	1	0	0.03
g_{5}	1	0	0	0	1	0.03
g_{6}	1	1	1	0	0	0.03
g_{7}	1	1	0	1	0	0.03
g_{8}	1	1	0	0	1	0.03
g_{9}	1	0	1	1	0	0.03
g_{10}	1	0	1	0	1	0.03
g_{11}	1	0	0	1	1	0.03
g_{12}	1	1	1	1	0	0.03
g_{13}	1	1	1	0	1	0.03
g_{14}	1	1	0	1	1	0.03
g_{15}	1	0	1	1	1	0.03
g_{21}	0	1	1	1	0	0.06
g_{22}	0	1	1	0	1	0.07
g_{24}	0	1	1	1	1	0.07
g_{19}	0	1	0	1	0	0.08
g_{2}	1	1	0	0	0	0.09
g_{18}	0	1	1	0	0	0.10
g_{23}	0	1	0	1	1	0.10
g_{17}	0	1	0	0	0	0.14
g_{1}	1	0	0	0	0	0.16
g_{20}	0	1	0	0	1	0.20
g_{26}	0	0	1	1	0	0.28
g_{25}	0	0	1	0	0	0.39
g_{27}	0	0	1	0	1	0.43
g_{28}	0	0	1	1	1	0.45
g_{30}	0	0	0	1	1	0.53
g_{29}	0	0	0	1	0	0.54
g_{31}	0	0	0	0	1	0.54

An examination of the data in Table 2-3 reveals that most of the groups with very low average calibration errors are those which have observations in bin 1 and at least one of the bins 3 to 5 (i.e. data representing both the uncongested and the congested traffic regimes). On the other hand, groups with the largest calibration errors have no observations in bins 1 and 2.

It is also instructive to examine the relative magnitude of the average calibration errors (Figure 2-4). The first set of 14 groups has very low calibration errors and the differences in the calibration errors between different groups are small. However, the last 7 groups have calibration errors as much as 25 times the calibration errors in the first set of groups. These results indicate that the distribution of the calibration data across the density has a substantial impact on the accuracy of the calibration of the macroscopic flow-speed-density model (i.e. Van Aerde's model).

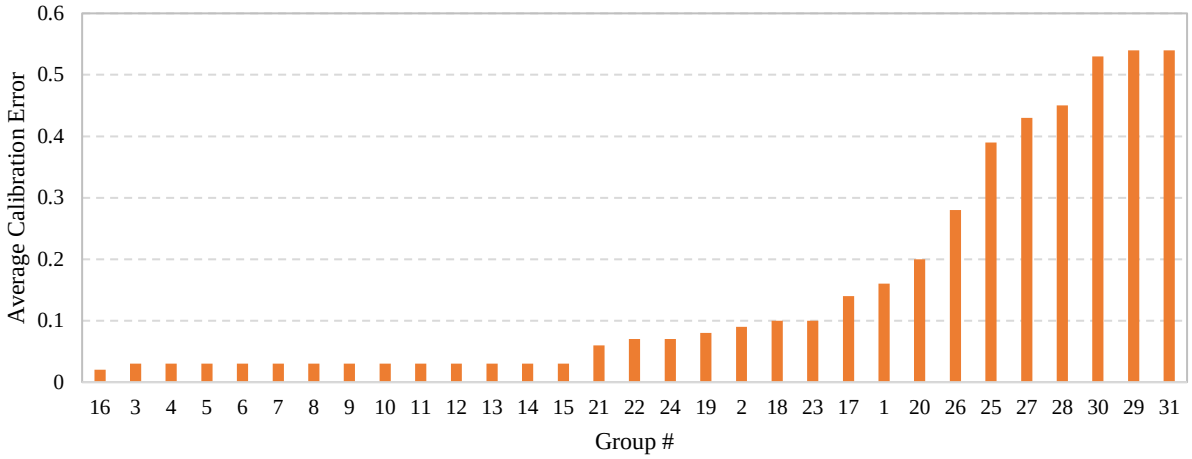

Figure 2-4- Average calibration error as a function of calibration data group number

We further aggregate the data by considering just three categories for the distribution of the calibration data:

1. Data from both the Uncongested and Congested traffic regimes,
2. Data from only the Uncongested traffic regime, and
3. Data from only the Congested traffic regime.

From the calibration of Van Aerde's model to the population of data we have u_c=76.3 (kph) and q_c=1969 (vph) and therefore the density at capacity (k_c) = 25.8 (vpkpl). Density less than k_c are considered in the uncongested traffic regime and density greater than k_c are considered in the congested traffic regime. Therefore, we can classify the groups from Table 2-3 into one of the three categories identified above. Data in *bin1* have density < 20 vpkpl and therefore are entirely in the uncongested regime. Data in bins 3 – 5 have density ≥ 40 vpkpl and therefore are entirely in the congested regime.

However, data in bin 2 span both the uncongested and congested regimes and consequently Group 17 from Table 2-3 cannot be classified. Descriptive statistics related to the calibration errors for the 30 classified groups are provided in Table 2-4. To calculate the statistics, we use the data from individual simulation runs performed in data generation section.

Table 2-4 Calibration error as a function of the distribution of the calibration data across traffic regimes

Distribution of Data	Average Error	Number of Groups	Number of samples	Standard Deviation	Lower Bound at 95% CL	Upper Bound at 95% CL
Congested and Uncongested Regimes	0.0512	21	118800	0.073	0.0508	0.0516
Uncongested Regime only	0.1040	2	6000	0.053	0.1027	0.1053
Congested Regime only	0.4346	7	25200	0.160	0.4326	0.4366

As is evident from Table 2-4, on average the lowest calibration errors are obtained when the calibration data represent both the uncongested and congested regimes. When the calibration data represent only the uncongested traffic regime then average calibration errors are almost double the previous category, and when the calibration data represent only the congested traffic regime, then the average calibration error is much greater. The confidence intervals of each of these categories at 95% confidence level confirms that the average errors of these categories are significantly different from each other.

2.4.2. Investigating the impact of the sample size on the calibration accuracy

To understand the impact of the sample size on the estimation error, Figure 2-5 shows the calibration error as a function of sample size for three different sampling distributions, one for each of the three distributions specified at the first column of Table 2-4: group 16 as an ideal instance that have both congested and uncongested regimes; group 2 as an instance of only uncongested regimes; and group 30 as an instance of only congested regimes. We observe from Figure 2-5:

1- Sample size does not have a large impact on the calibration error when sample size exceeds 100.

2- When calibration data are from (i) uncongested and congested regimes or (ii) from the uncongested regime only, then calibration error decreases as the sample size increases.

However, when calibration data are from just the congested regime, calibration error appears to slightly increase as the sample size increases. We also note that in practice, it is very unlikely to have only data from the congested regime. It is much more likely to have too little (or no) data from the congested regime.

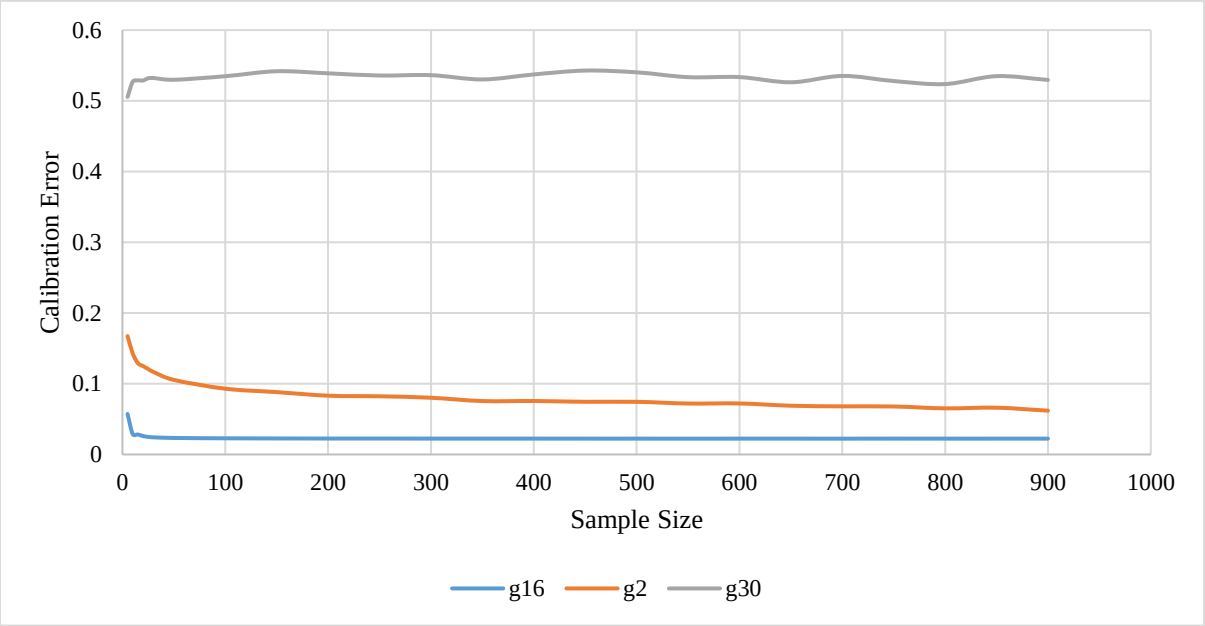

Figure 2-5-Model calibration error as a function of sample size in instances of uncongested-only (g_2), congested-only (g_{30}), and both congested-uncongested regime (g_{16})

Figure 2-6 shows the estimation error of ε^{u_f}, ε^{u_c}, ε^{k_j}, and ε^{q_c} (shown as Euf, etc.) in the same groups as Figure 2-5 (i.e. groups 16, 2, and 30). It should be noted that the parameter estimation error which is shown in Figure 2-6 is different from the errors in Table 2-3 which are the averages of the model calibration error. To compute the estimation error of traffic parameters, assume that the "true" value of each traffic stream parameter X (u_f, u_c, k_j, q_c) is $\hat{X}$ and their estimated value is $\dot{X}$, then the error in the value of the traffic stream parameter is computed as:

$$\varepsilon^X = \frac{\left|\hat{X} - \dot{X}\right|}{\dot{X}} \tag{2-6}$$

As shown in Table 2-3, the group 16 has the lowest calibration error; therefore, we assume that the "true" values of traffic parameters (i.e. $\hat{X}$) pertains to a sampling with the same distribution of the group 16. The group 16 is made by sampling equally from all density bins (i.e. bin1 to bin5). As shown in Table 2-2, bin3 has the lowest number of observations with slightly over 1000 data points; therefore, to create a *base sampling* we sample 1000 data points without replacement from each density bin1 to bin5 shown in Table 2-2. Then we calibrate the Van Aerde's model on this five-thousand-point *base sample* to estimate the "true" parameter values. The values are: u_f=126.9; u_c=76.2; k_j=103.4; q_c=1996.

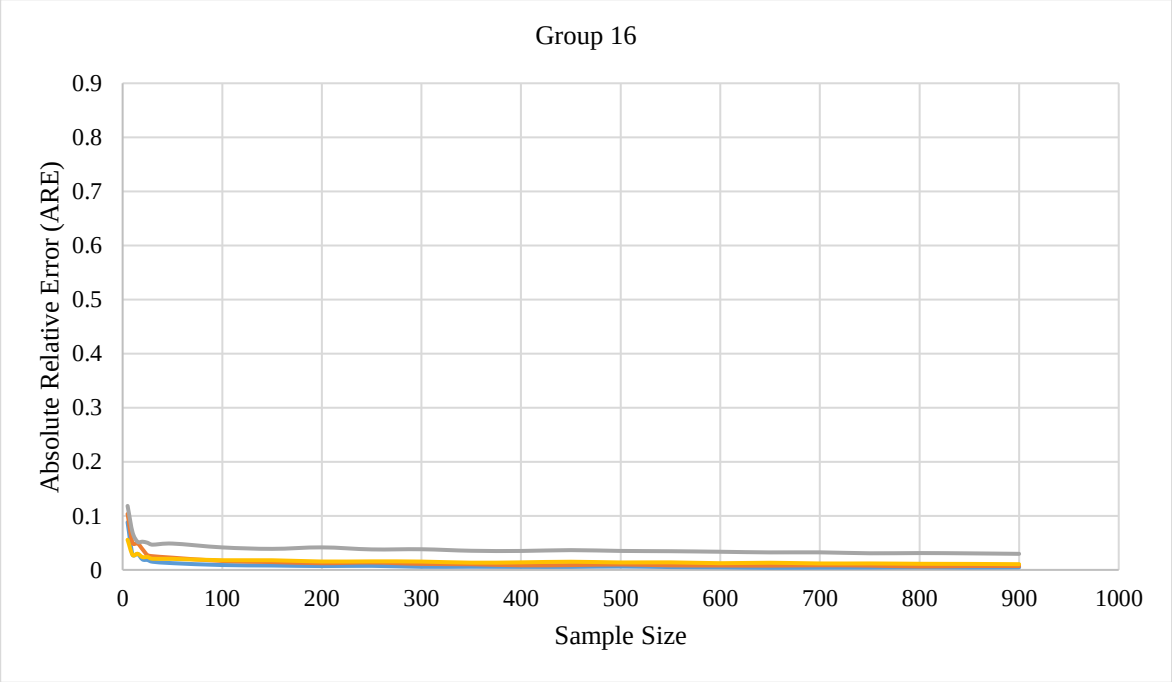

(a)

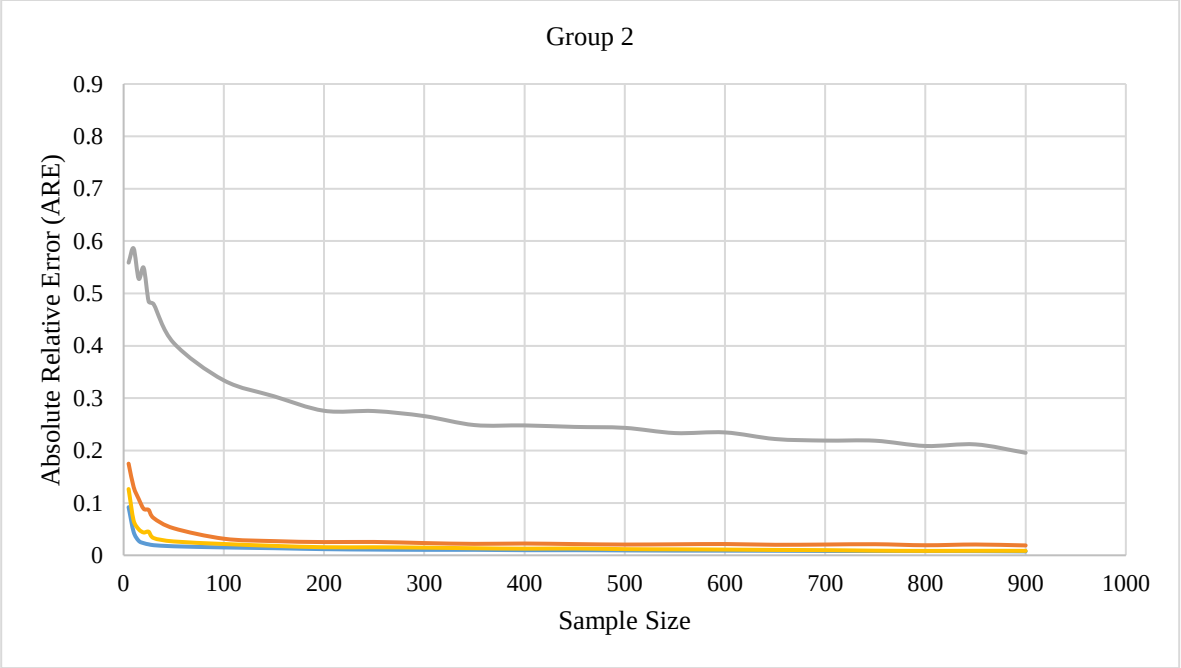

(b)

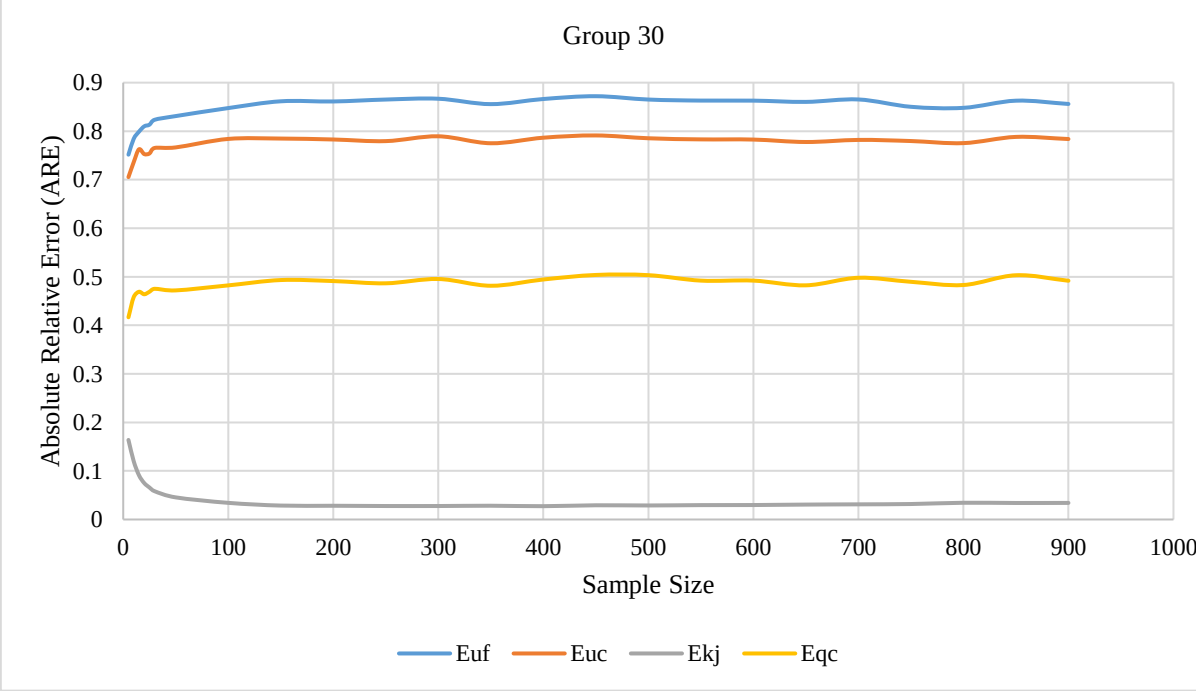

(c)

Figure 2-6- Traffic parameter estimation error as a function of sample size in group 16 (a), group 2 (b), and group 30 (c)

We observe from Figure 2-6 that:

1- The estimation error of all traffic parameters generally decreases when the sample size increases for the categories that include both congested and uncongested regimes and for the categories that include uncongested-only regimes; however, the rate of the decrease of the estimation error is greater when samples sizes are relatively small (up to approximately 100 observations). For larger sample sizes, adding more observations has less impact on the estimation error.
2- When (i) the calibration data are from both the uncongested and congested regimes; and (ii) when the calibration data are from the uncongested regime only; the estimation errors for kj are much larger than the estimation errors for the other three parameters.
3- When the calibration data are only from the congested regime, then the estimation errors associated with the free speed are largest.

2.4.3. Investigating the impact of the sample size and the distribution of calibration data on the accuracy of parameter estimates

Having demonstrated that calibration accuracy is highly influenced by the sample size and the distribution of the calibration data across density, we now investigate the influence that the sample size and the distribution of the calibration data across the density regime have on the accuracy of the parameter estimates.

As we observed from Figure 2-6, the estimation error (i.e. absolute relative error) for the jam density (k_j) parameter is higher than for the other three traffic flow parameters in groups that include data points from: (i) both congested and uncongested regimes (ii) uncongested-only regime. From these observations, and the expectation that in practice we most often have data from either (i) both the congested and uncongested regimes; or (ii) just the uncongested regime; it appears that the estimation errors associated with k_j are most problematic. Table 2-5 shows the mean, the standard deviation, and the coefficient of variation of the four traffic parameters estimated for: (i) two groups that only include data points from uncongested regime (i.e. groups 1, 2) (ii) two groups which have data from both congested and uncongested regimes (i.e. groups 3, 6) at the sample size of 900. The values are

calculated using the data of 50 replications in data generation procedure. As shown in Table 2-5, the coefficient of variation for k_j parameter is significantly higher than three other parameters.

Table 2-5-Characteristics of The Estimated Traffic Flow Parameters in the Sampling Instances from Uncongested-only Regime (g1 & g2) and Both Congested-Uncongested Regimes (g3 & g6)

Group	$\mathbf{u_f}$				$\mathbf{u_c}$			
	mean	std	cov	ε^{uf}	mean	std	cov	ε^{uc}
g1	127.99	0.33	0.0026	0.0086	81.96	7.97	0.0972	0.1169
g2	127.84	0.48	0.0037	0.0075	77.62	0.66	0.0085	0.0188
g3	128.13	0.35	0.0027	0.0097	74.48	0.51	0.0068	0.0226
g6	127.53	0.44	0.0034	0.0052	75.49	0.65	0.0086	0.0107
	$\mathbf{k_j}$				$\mathbf{q_c}$			
	mean	std	cov	ε^{kj}	mean	std	cov	ε^{qc}
g1	70.21	48.95	0.6972	0.5295	1951	69.70	0.0357	0.0366
g2	83.20	7.93	0.0953	0.1958	2009	15.95	0.0079	0.0085
g3	98.15	1.73	0.0176	0.0508	2031	12.02	0.0059	0.0174
g6	102.24	2.44	0.0239	0.0210	2010	12.98	0.0065	0.0078

As shown in Table 2-5, the coefficient of variation and also the estimation error of the parameter kj is larger than of three other parameters which suggest that the estimated kj values tend to differ significantly from the true value.

To observe an instance of poorly estimated k_j value, Figure 2-7 (a) shows an example of Van Aerde's model calibrated to a set of traffic data corresponding to Group 2 with 50 observations in the sample. Figure 2-7 (b) illustrates Van Aerde's model calibrated on a sample of observation points of the group 16 (i.e. the group in which points are equally distributed over all five bins) when the sample size is 900.

For both graphs, the blue circles are observed speed-density points aggregated at the density bins of 0.25 vpkpl. The red line shows the calibrated Van Aerde's model. The y-intercept of the calibrated model is the estimated free-flow speed and the x-intercept is the estimated jam density. As indicated in Figure 2-7 (a), the estimated jam density is 63 vpkpl which is significantly lower than the jam density of the comparison group (i.e. 100.7 vpkpl). This large error in estimating jam density results in large calibration error. We wish to avoid large errors in the estimates of the traffic stream characteristics

because these errors will undermine the credibility of the next step in the process, namely the identification of significant weather categorizations on the basis of differences between their associated traffic stream parameters values.

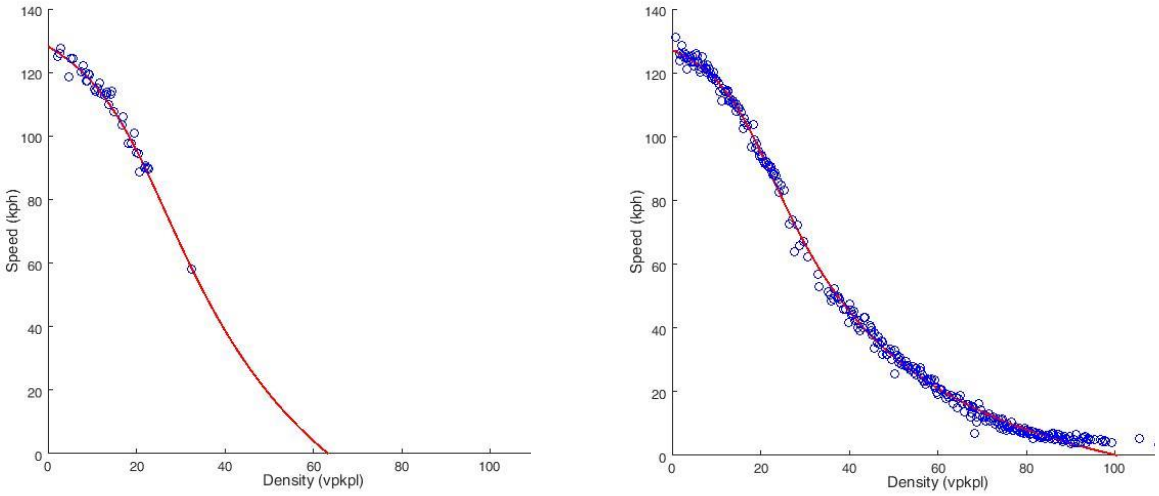

(a) (b)

Figure 2-7- Van Aerde's model calibrated to uncongested data (a) and the equally distributed data (b)

2.4.4. Improving the robustness of calibrating k_j

We hypothesize that we can make the calibration of Van Aerde's model more robust by constraining the value that k_j can assume and thereby reducing the calibration error (i.e. ε^c) as well as the parameter estimation errors. To examine this hypothesis, we propose a modified calibration technique compared to what has been suggested by Rakha et al. (2010), namely that the jam density is fixed at some value and the three other traffic stream parameters (i.e. u_f, u_c and q_c) are calibrated. The jam density for a typical freeway traffic stream is approximately 100 vpkpl (Dervisoglu et al., 2009) and therefore within the context of this study, we have fixed the jam density at 100 vpkpl. Then we repeated the method explained above by sampling from the same population as the one used above (the population with 23,370 data points). Since Figure 2-6 showed that the parameter estimation errors were less sensitive

to sample sizes when the sample size was larger than 100, this time we sampled at only 17 different sample size levels (i.e. 5, 10, 15, 20, 25, 30, 50, 100, 150, 200, 300, 400, 500, 600, 700, 800, 900) to reduce computational cost. Again, to maintain the randomness in the procedure, we carried out repetitions for each sample size; however, to reduce computational cost we carried out 25 repetitions rather than 50 repetitions. For each replication, we calibrated Van Aerde's model and estimated free-flow speed, speed-at-capacity, and capacity. Also, we calculated the calibration error (ε^{c}), and absolute relative error (ε^{u_f}, ε^{u_c}, and ε^{q_c}). To distinguish these two methods, we refer to the first method in which all four parameters are calibrated as "free k_j" and the second method, in which the value of k_j is fixed and only the other three parameters are calibrated as "fixed k_j".

Figure 2-8 compares the calibration errors from the free k_j and fixed k_j methods for the cases for which all the calibration data reflects uncongested traffic conditions (i.e. group 2).

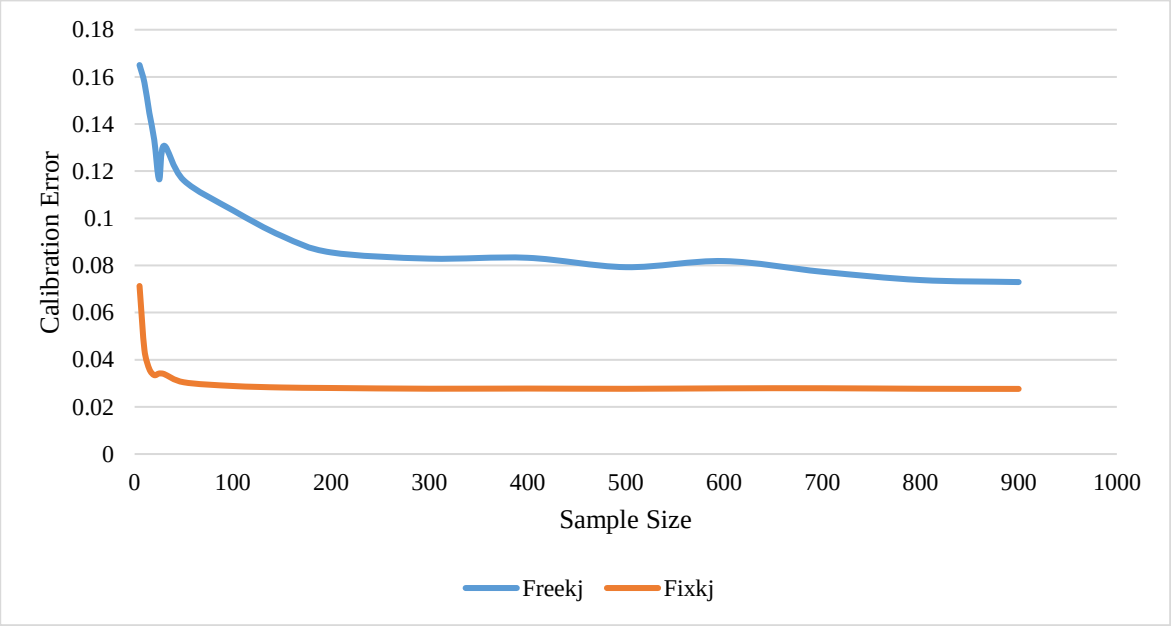

Figure 2-8- Calibration error for two calibration approaches: Freekj and Fixkj (calibration data from uncongested traffic regime only)

As shown in Figure 2-8 the calibration error when the k_j is fixed is much lower than when it is free and this is true for all sample sizes examined. This confirms our initial hypothesis that calibration errors

are reduced when k_j is fixed when calibrating Van Aerde's model to traffic data which does not contain observations from the congested regime.

Table 2-6 can be used to investigate the impact of fixing k_j. This table shows the difference of the calibration error ($\Delta\varepsilon^c$) for the two Fixkj and Freekj Van Aerde's model calibration approaches. The rows are the sample sizes and represent the number of observation points someone has in hand. The columns are the label of the groups introduced previously in Table 2-3. The pink cells identify the conditions in which the Fixkj has smaller calibration error and green cells show the conditions in which Freekj method results in smaller error.

Table 2-6- Comparing the Calibration Error for Freekj and Fixkj approaches (pink cells: less error for fixkj, Green cells: less error for freekj)

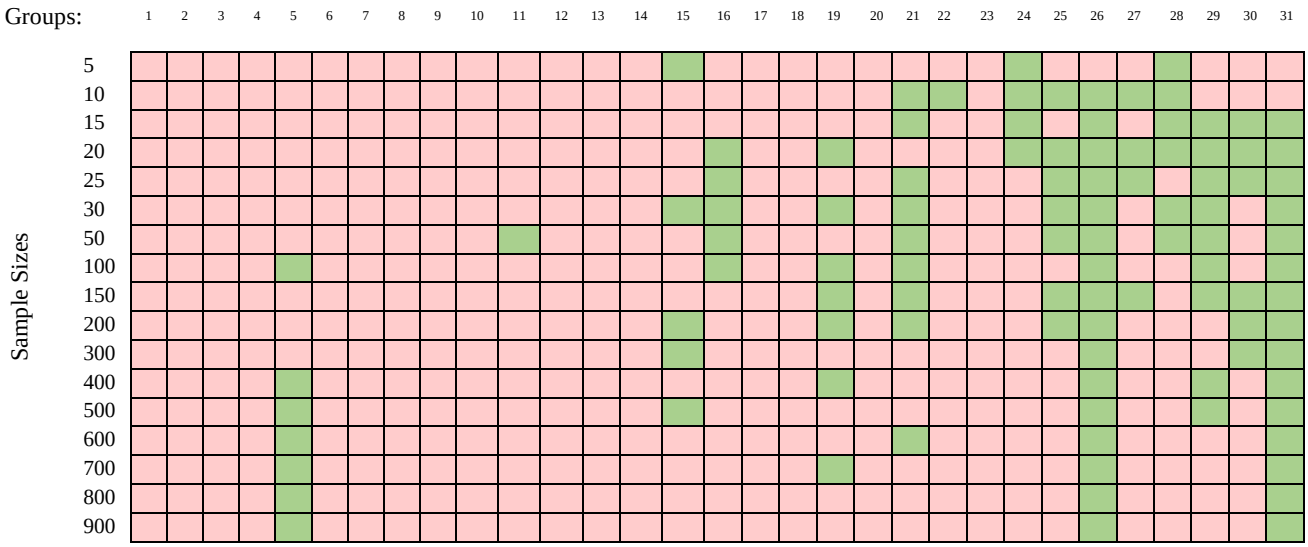

Table 2-6 helps the practitioners to choose between the two methods for calibration of the Van Aerde's model (i.e. fixkj or freekj) based on the number of observations and the distribution of the observations points along the density axis.

2.5. Model Generation

2.5.1. Develop models to predict the calibration error for Freekj and Fixkj calibration approaches

Though Table 2-6 can provide useful guidance for practitioners, its use is limited to the defined sample sizes and groups. To address this limitation, we develop a regression model to establish a relationship between the parameters shown in Table 2-7 (i.e. predictors) and the target variable (i.e. the calibration error).

Table 2-7- Model Input Parameters

Name	Description
N	Sample size
n_1 to n_5	Number of samples in bins 1 to 5
db_1 to db_5	Binary variable: (0 when there are no observation points in bin *i*, 1 otherwise)

The input parameters are highly correlated which results in redundancy and collinearity and avoids us using some techniques such as neural network to establish the relationship between the predictors and the target variables. Therefore, we apply a technique that includes the combination of Principal Component Analysis (PCA) and the Relevance Vector Machine (RVM) which is a nonlinear data-driven based regression technique. Using the PCA technique captures the maximum variability of the input variables. It transforms some highly correlated data points or observations to principal components which are some variables that are linearly uncorrelated. The number of principal components might be less than or equal to the initial variables; however, these newly generated variables are uncorrelated (Jolliffe, 2002). The RVM method was developed by Tipping (2001) as an improvement to the well-known Support Vector Machine (SVM) method. The important feature of RVM is that over-fitting is less of an issue.

In the modeling process we performed a cross-validation, so that 75% of the data points are used for training and the rest (25% of observations) employed for testing. The model calibration was carried out in R (script code is shown in Appendix 1).

To illustrate the use of the models, consider Table 2-8 which shows the observed calibration error and the calibration error estimated from the Fixkj and Freekj models for five sampling scenarios.

Table 2-8- Observed and Estimated Calibration Errors of both FixKj and Freekj Approaches for Some Sampling Instances

N	n1	n2	n3	n4	n5	db1	db2	db3	db4	db5	Fixkj error		Freekj error	
											Obs.	Est.	Obs.	Est.
25	0	5	0	15	5	0	1	0	1	1	0.1032	0.1028	0.1259	0.1285
50	10	20	0	0	20	1	1	0	0	1	0.0236	0.0233	0.0244	0.0247
100	0	20	20	20	40	0	1	1	1	1	0.0568	0.0562	0.0648	0.0700
500	0	0	200	300	0	0	0	1	1	0	0.4956	0.4747	0.2341	0.2097
900	180	540	180	0	0	1	1	1	0	0	0.0247	0.0381	0.0274	0.0354

In terms of the agreement between observed and predicted target variable for the testing dataset, some performance criteria, including Root Mean Square Error (RMSE), and R^2 are employed to evaluate the goodness of fit of the RVM model. Table 2-9 shows the values of these parameters for the both Freekj and Fixkj models. The results show excellent goodness of fit of the PCA + RVM model.

Table 2-9- Performance Measures for Developed Models

Performance measure	Freekj	Fixkj
RMSE	0.03	0.03
R^2	0.97	0.96

Figure 2-9 and Figure 2-10 illustrate the observed vs estimated calibration error for the tested data points for freekj and fixkj approaches respectively.

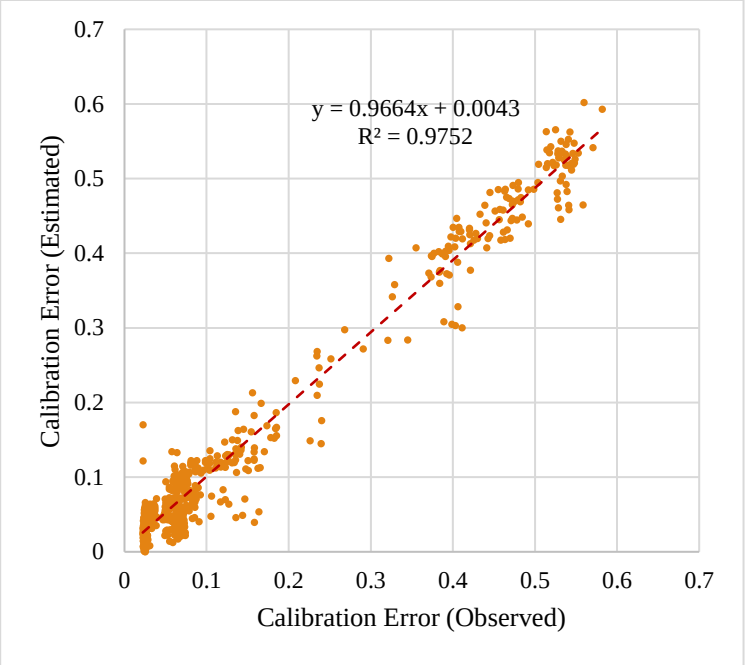

Figure 2-9- Observed vs. estimated calibration error for testing data (Freekj model)

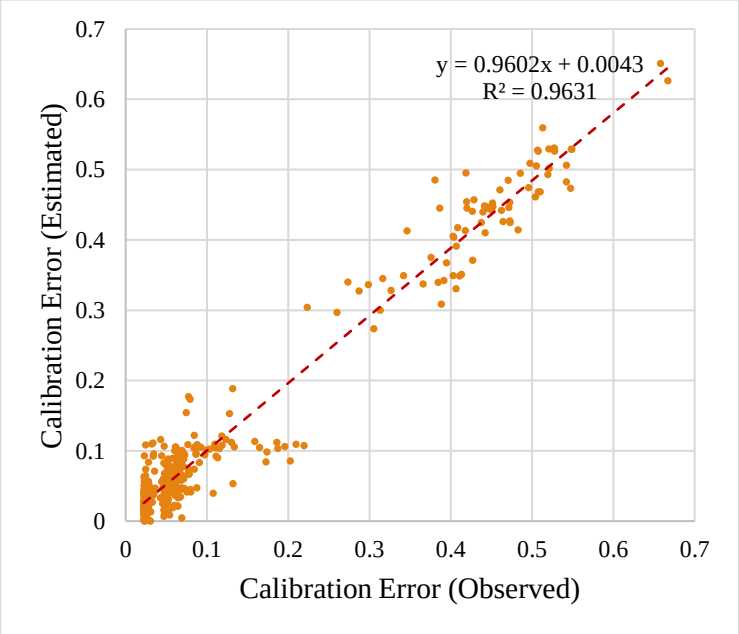

Figure 2-10- Observed vs. estimated calibration error for testing data (Fixkj model)

2.6. Conclusions

The distribution of the observations across density have an influence on the accuracy of the parameter value estimates; however, the number of observations –when exceeding a minimum of 100 observed points- does not have a considerable impact on the accuracy of parameter value estimates. It is common in practice that the congested regime is under-represented in the calibration data set. For these conditions, the estimation error for the jam density can be particularly large. For these cases, it is often beneficial to fix the jam density to some rational value in order to improve estimation accuracy.

In this chapter, we have demonstrated the influence that both the sample size and distribution have on the overall calibration error and on the parameter value estimation errors. We also developed models to estimate the calibration error as a function of the sample scheme and used these models to provide guidance on when to fix the jam density and when to calibrate a value for jam density.

Chapter 3

Determining Road Surface and Weather Conditions Which Have a Significant Impact on Traffic Stream Characteristics[1]

3.1. Introduction and Background

Microscopic simulation models are commonly used to evaluate the expected performance of candidate traffic improvement strategies. There is increasingly a desire to be able to use these models to capture travel time reliability as a component of the performance evaluation. Previous research has shown (FHWA, 2015) that weather conditions (e.g. rain, snow, wind, fog, etc.) and road surface conditions (e.g. wet, dry, icy, snow covered, etc.) are responsible for 15% of the non-recurrent congestion and therefore it is necessary to be able to reflect these different weather categorizations[2] within the simulation model. However, to do this we need to know which conditions to model, how to categorize them, and how these categories impact the traffic stream characteristics[3]. And given that the computation cost associated with microscopic traffic simulation modeling is relatively high, it is desirable to model the fewest categories necessary to still capture the required variations in the traffic stream characteristics.

[1] The contents of this chapter have been incorporated within an article published by Golshan & Hellinga in Transportation Research Board 95th Annual Meeting on Jan 12, 2016, available online: https://trid.trb.org/view.aspx?id=1394167 . R. Golshan., & B. Hellinga, "Determining Road Surface and Weather Conditions Which Have a Significant Impact on Traffic Stream Characteristics"

[2] We use the term "weather categorizations" to refer to a set of categories that includes both road surface conditions and weather conditions.

[3] Traffic stream characteristics are free speed, speed at capacity, jam density, and capacity flow rate.

The existing literature indicates that one of the characteristics of previous research efforts to study the impact of weather-related factors on traffic stream characteristics have established the weather categorizations *a priori*. Then, given these categorizations, an attempt is made to investigate the influence of these weather categories on the traffic stream characteristics of interest.

In this chapter, we are interested in identifying the set of weather categorizations which best describe the different weather regimes that have a statistically significant influence on the traffic stream characteristics. For example, instead of trying to determine the free speed associated with the condition of rain during the day and with the condition of rain during the night, we are interested in determining if we actually need to distinguish between these two categories. If there is no statistically significant difference between these two categories, we should aggregate them so that we have a model to estimate the free speed under rain, regardless of time of day (i.e. day or night).

3.2. Literature Review

A number of previous studies have confirmed the generally held perception that inclement weather impacts traffic stream operations.

A recent study by the 2nd Strategic Highway Research Program (SHRP2 L03) quantified the impact of weather (along with other factors) on travel time reliability (Cambridge Systematics, 2013). In this study, weather was categorized in terms of number of hours in the year with precipitation amounts greater or equal to 0.01, 0.05, 0.10, 0.25, and 0.5 inches, number of hours with measurable snow in the year, number of hours with frozen precipitation in the year, and number of hours of fog in the year. Regression models were developed to estimate different percentiles of the distribution of the travel time index (TTI). TTI is defined as the ratio of the actual travel time to the free-flow travel time (60 mph in the L03 project). For example, the model calibrated for the 80th percentile of the TTI in the peak period is:

$$80^{th}\ percentile\_TTI = e^{(0.139 \times dc_{crit} + 0.011 \times ILHL + 0.013 \times Rain05Hrs)} \quad (3\text{-}1)$$

where,

dc_{crit}: largest demand-to-capacity ratio for all links in the section

$ILHL$: annual lane hours lost because of road incidents within the peak period

$Rain05Hrs$: annual hours within peak period during which rainfall is ≥ 0.05 inches.

In the L03 project, after examining all possible interactions, no weather parameters were found to be significant except *Rain05Hrs*.

Most studies conducted to examine the impact of weather on traffic operations have quantified the impact on one or more of the traffic stream characteristics (i.e. speed, capacity, speed at capacity, or jam density). Ibrahim and Hall (1994) and Kyte et al. (2001) studied the impact of precipitation on speed-flow relationship and free flow speed respectively. Also, Kyte et al. (2001) and Brilon and Ponzlet (1996) showed the impact of diurnality (daylight and darkness) on the speed and capacity.

Stern et al. (2003) studied the impact of road surface condition (RSC) and weather conditions on delay. Data from both directions of 33 road segments in Washington D.C. were used to calibrate 66 linear regression models which predicted travel time as a function of RSC, precipitation, wind speed, and visibility. The results showed that RSC was statistically significant for most of the models, while precipitation was significant in many models and the wind speed and visibility were only significant for a few of the models.

Rakha et al. (2007) examined the impact of precipitation type (rain and snow), intensity (cm/h of liquid equivalent precipitation accumulation), and visibility (km) on traffic stream characteristics. Rainfall and snowfall intensities were divided into 3 categories each and visibility was divided into 4 categories. They characterized the traffic stream in terms of the four parameters that define Van Aerde's macroscopic speed-flow-density relationship (i.e. free-flow speed u_f, speed-at-capacity u_c, capacity q_c, and jam density k_j). They used 5-minute aggregated loop detector and weather data - including the combination of the precipitation and the visibility - from three different areas: Seattle, WA; Baltimore, MD; and Minneapolis-St. Paul, MN. They calibrated Van Aerde's model for each of the 24 precipitation-visibility combinations (plus the no precipitation - maximum visibility condition as the base condition) to find the associated four traffic stream parameters (u_f, u_c, k_j, q_c). Considering clear weather (no precipitation) as the base condition, the ratio of traffic stream parameters in each

category to the base category was computed. The T-test was used to identify whether or not the difference between each weather category and the base category is statistically significant. For each city, a regression model was developed for each traffic stream parameter separately for rain and snow. The general form of the regression model is:

$$WAF_{a,b} = c_1 + c_2 i + c_3 i^2 + c_4 v + c_5 v^2 + c_6 iv \quad (3\text{-}2)$$

where,

i: precipitation intensity (cm/h)

v: visibility (km)

c_i: model coefficient

$WAF_{a,b}$: weather adjustment factor of traffic parameter a for the city b.

Rakha et al. found that weather conditions had a statistically significant impact on free speed, speed at capacity, and capacity, but did not find a statistically significant impact on jam density.

One of the characteristics of the study by Rakha et al, and the other previous studies is that the weather categorizations are done *a priori*. No studies were found in the literature that attempt to identify the optimal set of categories in terms of their impact on the traffic stream characteristics.

The next section formulizes this problem and describes the methodology. Then the methodology is applied using field data.

3.3. Problem Formulation and Proposed Methodology

The problem formulation and proposed methodology is divided into the following three steps:

1. Create feasible schemes of categorization
2. Aggregate categories which are not statistically different
3. Select the preferred scheme

Each of these steps is described in the following subsections.

3.3.1. Categorization Schemes

Consider a set of environmental factors ($F_1,\ldots, F_n$) such as type of precipitation, wind speed, road surface condition, air temperature, etc. Each factor F_i is quantified in terms of m_i discrete levels ($L_{i,j}$; $j = 1,m_i$). Each unique environmental category is specified by the vector $\boldsymbol{C}$ having dimensions of $1 \times n$. The number of possible categories is the product of the number of levels for each factor (Equation (3-3)).

$$Total\ Categories = \prod_{i=1}^{n} m_i \tag{3-3}$$

We define a *categorization scheme* as the ordered sequence of the environmental factors in vector $\boldsymbol{C}$. To illustrate, consider three environmental factors, F_1, F_2, and F_3. The number of levels is $m_1 = 2$; $m_2 = 3$; $m_3 = 4$. Thus, there are $2 \times 3 \times 4 = 24$ unique categories. There are six categorization schemes, as follows:

$$\begin{aligned}
\boldsymbol{C_1} &= \{F_1, F_2, F_3\} \\
\boldsymbol{C_2} &= \{F_1, F_3, F_2\} \\
\boldsymbol{C_3} &= \{F_2, F_1, F_3\} \\
\boldsymbol{C_4} &= \{F_2, F_3, F_2\} \\
\boldsymbol{C_5} &= \{F_3, F_1, F_2\} \\
\boldsymbol{C_6} &= \{F_3, F_2, F_1\}
\end{aligned} \tag{3-4}$$

These categorization schemes are illustrated in Figure 3-1. Note that each categorization scheme contains the same number of unique categories. The only differences are in the order in which the environmental factors appear.

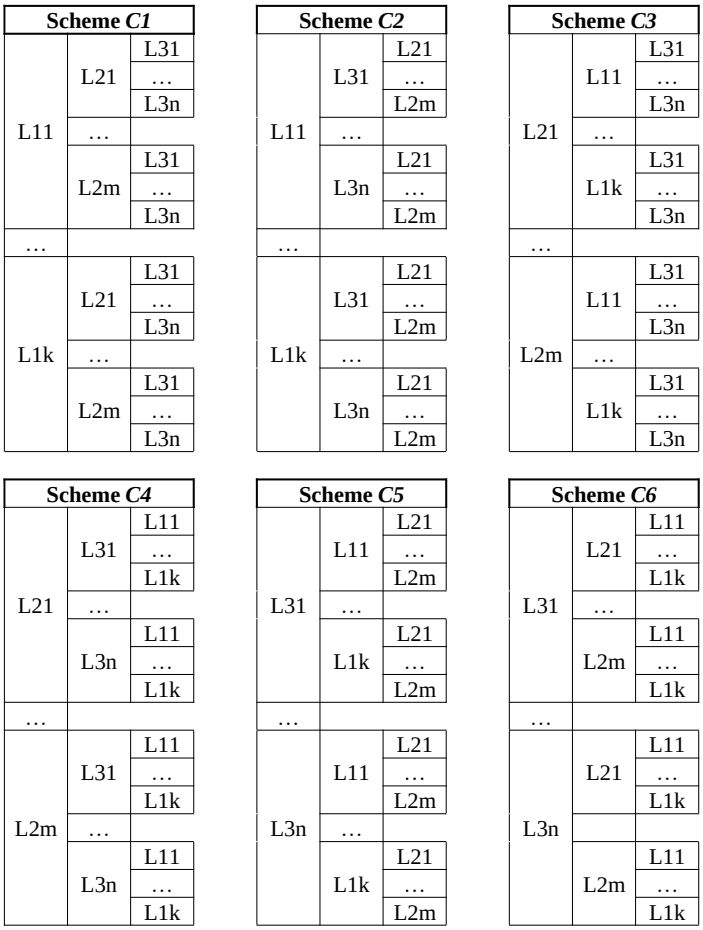

Figure 3-1- Illustration of categorization schemes.

Following the method adopted by Rakha et al *(2007)*, we parse a set of field data (consisting of traffic stream measurements and environmental measurements for the same location and aggregation time period) so that the entire set of field data is divided into the associated environmental categories. We then calibrate Van Aerde's macroscopic speed-flow-density relationship to the dataset associated with each category. The calibration procedure is selected using the methodology presented in the previous chapter. For different categories, we choose the method of calibration (i.e. Freekj vs Fixkj) based on the number of observation points in the category as well as the distribution of those points along the density axis.

3.3.2. Aggregate Categories

Rakha et al (2007) fit a linear regression to the results obtained from the calibration of Van Aerde's macroscopic model from all the categories. Thus, if they have 24 categories, as in the example above,

they had 24 observations for the linear regression calibration. And though their analysis determined whether or not the environmental factors were statistically significant, it does not provide evidence about which of the 24 categorizations provide statistically different parameter values.

In this work, our objective is to determine which categories can be aggregated. The calibration process results in a single estimate of the four parameters defining Van Aerde's model for each category. To compare two categories *A* and *B*, we assume that if the value estimated for one or more of the parameters associated with *A* is statistically different from the value estimated for category *B*, then those two categories are different from each other and should not be aggregated. To carry out this test, it is necessary to have an estimate of the variance of the estimated parameter values.

We propose to use the bootstrapping technique to obtain the standard error of the parameter values. Bootstrapping is a technique in which a large number of samples, *K*, are taken from the field data – with replacement. Each sample contains the same number of observations as in the original set of field data. For each sample, Van Aerde's model is calibrated -using the technique explained in Chapter 2- to obtain an estimate of the values of the four traffic stream parameters. As explained in Chapter 2, depending on the distribution of the calibration data and the number of observations in the calibration data set, we may use either the *Fixkj* or *Freekj* calibration approaches. When using the *Fixkj* approach, we estimate values for u_f, u_c, and q_c. When using the *Freekj* approach, we estimate the values of all four parameters (u_f, u_c, q_c, and k_j). In the application in this chapter, we find that the *Fixkj* approach is appropriate. The final estimate of each of the remaining three parameters is the mean of the estimated parameter values from the *K* samples and the standard error of the parameter is the standard deviation of the *K* estimated parameter values.

The next step is to compare the estimated parameters of different weather categories. Here, we follow the approach of using statistical methods. On the basis of the parameter estimates and the standard errors, categories can be compared using the analysis of variance (ANOVA) followed by Tukey's test (as post-hoc). This combination of these statistical tests enable us to determine:

1. Whether or not all categories are similar, and
2. If they are not all similar, how different each pair of the categories are from each other.

If the Tukey's test shows that all three estimated traffic flow parameters (i.e. u_f, u_c, and q_c) for the examined group of categories are not statistically different, then these categories are aggregated and the traffic stream parameters are estimated for the newly formed category.

Note that:

1. The aggregations can only occur for levels within the last environmental factor in the categorization vector ***C*** (i.e. factor in the right-most position in vector ***C***) and it is for this reason that different categorization schemes must be considered.
2. After aggregation of the last environmental factor level, new categories may be generated.
3. These newly generated categories will be checked to see if they can be aggregated with other categories at the second last environmental factor.
4. If no new categories can be generated by aggregating the categories in all vectors $\boldsymbol{C_i}$, remaining categories in each vector can be checked to see if they can be aggregated with remaining categories in other vectors.

This process continues until no more aggregations are warranted.

3.3.3. Select Preferred Categorization Scheme

The quality of the categorization scheme is quantified on the basis of the root mean squared error (RMSE) from all of the final categories:

$$RMSE_r = \frac{1}{N}\sum_{j=1}^{m_r}\sum_{i=1}^{n_j}\sqrt{\left(\frac{u_{obs_{ij}} - u_{est_{ij}}}{u_{\max_j}}\right)^2 + \left(\frac{q_{obs_{ij}} - q_{est_{ij}}}{q_{\max_j}}\right)^2 + \left(\frac{k_{obs_{ij}} - k_{est_{ij}}}{k_{\max_j}}\right)^2} \quad (3\text{-}5)$$

where,

$RMSE_r$: root mean square error of scheme r

u, q, k: speed (kph), flow (vphpl), and density (vpkpl) respectively

X_{obs}: observed value of traffic variable X

X_{est}: estimated value of traffic variable X (the closest point on Van Aerde's macroscopic speed-flow-density relationship)

X_{max}: maximum observed value of traffic variable X

m_r: number of categories in scheme r

n_j: number of observations in category j

N: number of observations in all categories

In this section, to have a consistent base to calculate the RMSE for all categories, we consider a constant value for X_{max}: 150 kph as $u_{\max_j}$, 150 vpkpl as $k_{\max_j}$, and 2500 vph as $q_{\max_j}$.

Finally, the scheme with the lowest RMSE is selected as the preferred categorization scheme.

3.4. Application to Field Data

We applied the proposed methodology to field data of the whole year 2014 obtained from the Minneapolis-St. Paul (Twin Cities) in Minnesota, U.S. This area is located in northern U.S. so more extreme weather conditions including snowfall, icy road, etc. are experienced. Moreover, traffic data, road surface data, and weather data were available publicly in this area. Traffic data was obtained through a database which included the traffic data retrieved from induction loop detector throughout the Twin Cities. This database was accessible to the public via Minnesota Department of Transportation (MnDOT) website *(Minnesota department of transportation (MnDOT).)*. The RSC and weather data were obtained through the Road Weather Information System (RWIS) database accessible from the same website. Traffic data were available at a temporal resolution of one observation every 30 seconds while RSC and weather data were available at a resolution of 5 minutes.

The study section is the westbound direction of I-694 between Rice Street and Victoria N Street (Figure 3-2). This section is a basic freeway section (i.e. not impacted by weaving or on or off ramps) consisting of 2 lanes and it experiences recurrent congestion during both the morning and afternoon peak hour. The posted speed is 60 mph (96 kph). Traffic data were aggregated across lanes at 5-minute resolution. Figure 3-3 shows the station five-minute-aggregated speed values as a function of time of day for two randomly selected weekdays in 2014. The figure shows that the study section experiences a wide range of traffic conditions (i.e. both congested and uncongested traffic states), which is advantageous for calibrating Van Aerde's macroscopic speed-flow-density model.

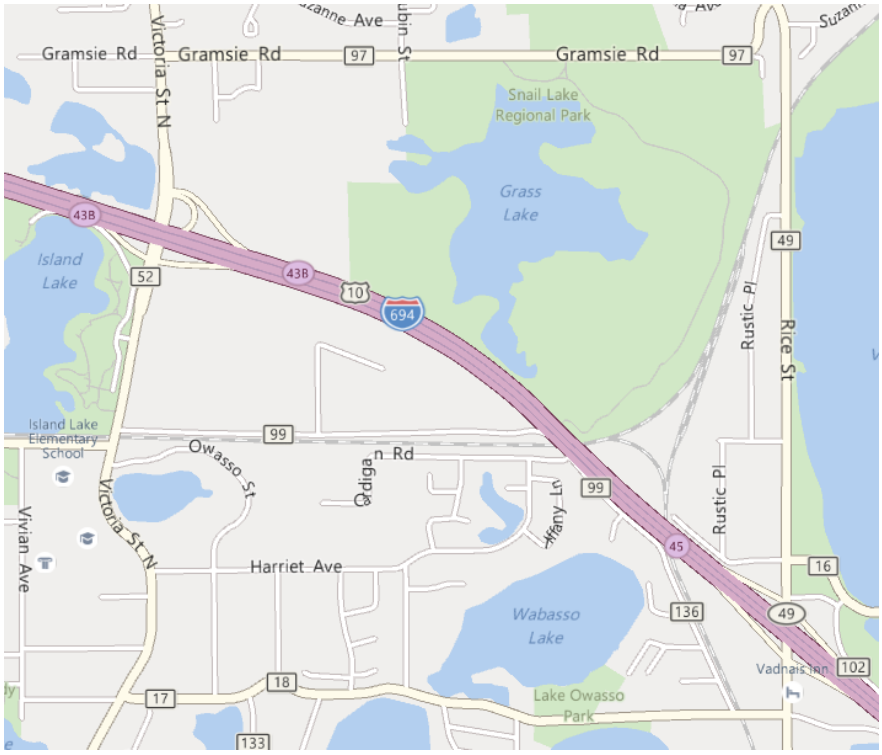

Figure 3-2-Study area (source: HERE Map, Microsoft Corporation, 2016)

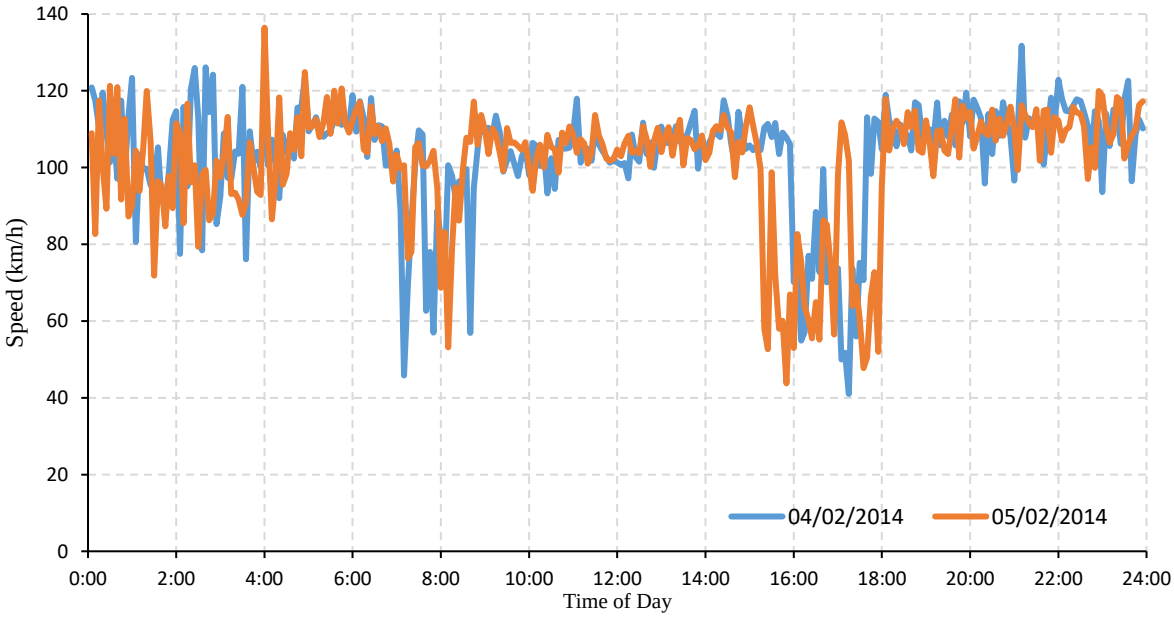

Figure 3-3- Five-minute-aggregated station speed data for two randomly selected weekdays.

Examination of the field traffic data revealed anomalies under very low flow conditions and therefore data from 11 pm to 5 am were excluded from the analysis. After synchronization of traffic and weather data 61,012 observation points (each associated with a 5-minute interval between 5 am and 11 pm) were used for the analysis.

As a starting point to illustrate the methodology three environmental factors were considered in the analysis.

1. Road surface condition (3 levels: dry, wet, ice);
2. Type of precipitation (4 levels: no precipitation, rain, frozen, snow); and
3. Diurnality (2 levels: day (sunrise to sunset), night (after sunset and before sunrise; excluding 11 pm to 5 am)).

The proposed method can be applied with a larger number of factors and larger number of levels for each factor.

Road surface conditions are defined as below:

Wet = of moisture on the pavement sensor with a surface temperature above freezing (0°C).

Ice = ice and water mixture at or below freezing (0°C) with insufficient chemical to keep the mixture from freezing.

We note that road surface conditions are impacted by numerous factors including winter road maintenance activities, weather conditions, traffic volumes, local topography, etc. However, our analysis does not make assumptions about the relative frequency with which categorizations will be observed in the future and therefore changes to, for example, winter road maintenance standards or practices, are not detrimental to the application of our model.

The number of categories resulting from the interaction of these factors is 24 (3×4×2). As per the proposed methodology described in the previous section, the data set was parsed into 24 sub-sets – one for each categorization. The number of observations in each of the 24 categories is shown in Table 3-1.

We can observe that for some of the categories there are no observations (e.g. *Rain, Ice, Day*) and therefore for these categories it is not possible to calibrate Van Aerde's model. Also, it is not possible to calibrate Van Aerde's model when there are less than 5 observation points available since four parameters are being estimated. Therefore, a minimum of 5 observations are required to calibrate Van Aerde's model. This results in 17 categories for which Van Aerde's model can be calibrated. It should be noted that some categories happen rarely and have a very low frequency. For instance, the combination of a dry surface condition and the raining weather only happens when a very light rain starts during the time interval but the film of the water on the surface is not enough to be detected by the road surface sensors.

Table 3-1- Possible Categories

ID	Precipitation	Surface	Day/Night	No. of Points	ID	Precipitation	Surface	Day/Night	No. of Points
1	NoPrecip	Dry	Day	34531	13	Snow	Dry	Day	95
2	NoPrecip	Dry	Night	9811	14	Snow	Dry	Night	58
3	NoPrecip	Wet	Day	7157	15	Snow	Wet	Day	558
4	NoPrecip	Wet	Night	5210	16	Snow	Wet	Night	291
5	NoPrecip	Ice	Day	651	17	Snow	Ice	Day	17
6	NoPrecip	Ice	Night	393	18	Snow	Ice	Night	0
7	Rain	Dry	Day	161	19	Frozen	Dry	Day	2
8	Rain	Dry	Night	35	20	Frozen	Dry	Night	0
9	Rain	Wet	Day	1007	21	Frozen	Wet	Day	669
10	Rain	Wet	Night	142	22	Frozen	Wet	Night	220
11	Rain	Ice	Day	0	23	Frozen	Ice	Day	4
12	Rain	Ice	Night	0	24	Frozen	Ice	Night	0

As per the findings from Chapter 2, we investigated the distribution of the points over the five density bins. Then, we used the models we developed in the previous chapter to estimate the calibration error of each category for the freekj and the fixkj approaches. The one with the lower error was selected as the preferred calibration approach for that category. The distribution of the observation points and the estimated error for both calibration approaches are listed in Table 3-2.

The first column is the ID of the category which is consistent with Table 3-1. Column 2 is the number of observation points in each category. Columns 3 to 7 contain the number of observation points in each of the five density bins. Columns 8 to 12 are the corresponding values of the binary variables *db1* to *db5* (these were defined in Chapter 2). Columns 13 and 14 are estimated calibration errors obtained from the PCA+RVM models developed in Chapter 2 for the Freekj and Fixedkj models respectively. Column 15 is the difference of the calibration error of Freekj and Fixkj. Positive value in any rows of column 15 mean that the Freekj approach results in the higher calibration error compared to the Fixkj approach for that category.

Table 3-2-Selected Calibration Approach

ID	N	n1	n2	n3	n4	n5	db1	db2	db3	db4	db5	Freekj Error	Fixkj Error	Error Difference	Selected Approach
1	34531	28313	6076	141	1	0	1	1	1	1	0	0.0000	0.0000	0.0000	Fixkj
2	9811	9581	221	9	0	0	1	1	1	0	0	0.0000	0.0000	0.0000	Fixkj
3	7157	5573	1564	20	0	0	1	1	1	0	0	0.0000	0.0000	0.0000	Fixkj
4	5210	4850	354	6	0	0	1	1	1	0	0	0.0000	0.0000	0.0000	Fixkj
5	651	550	101	0	0	0	1	1	0	0	0	0.0803	0.0088	0.0715	Fixkj
6	393	356	37	0	0	0	1	1	0	0	0	0.0879	0.0049	0.0830	Fixkj
7	161	147	12	2	0	0	1	1	1	0	0	0.0336	0.0120	0.0215	Fixkj
8	35	33	1	1	0	0	1	1	1	0	0	0.0480	0.0199	0.0280	Fixkj
9	1007	740	267	0	0	0	1	1	0	0	0	0.0250	0.0233	0.0018	Fixkj
10	142	133	9	0	0	0	1	1	0	0	0	0.1307	0.0506	0.0801	Fixkj
13	95	78	17	0	0	0	1	1	0	0	0	0.1187	0.0444	0.0743	Fixkj
14	58	58	0	0	0	0	1	0	0	0	0	0.1297	0.0368	0.0930	Fixkj
15	558	375	182	1	0	0	1	1	1	0	0	0.0251	0.0140	0.0111	Fixkj
16	291	251	40	0	0	0	1	1	0	0	0	0.1196	0.0353	0.0842	Fixkj
17	17	9	7	1	0	0	1	1	1	0	0	0.0622	0.0294	0.0328	Fixkj
21	669	528	140	1	0	0	1	1	1	0	0	0.0202	0.0197	0.0005	Fixkj
22	220	219	1	0	0	0	1	1	0	0	0	0.1418	0.0546	0.0872	Fixkj

As shown in Table 3-2, the difference of the calibration error is zero for the categories 1 to 4; therefore, we arbitrarily elected to use the Fixkj model for calibrating Van Aerde's model. For all other categories, the Fixkj model is preferred as it is estimated to provide lower calibration errors.

Then we implemented the bootstrapping technique to obtain the standard error of each estimated parameter. The number of replications in the bootstrapping procedure was set at 100, meaning that Van Aerde's model was calibrated to find values of u_f, u_c, and q_c 100 times for each of the 17 categories. Six categorization schemes were possible as shown in Table 3-3.

Table 3-3- Possible Categorization Schemes

Scheme 1

Precipitation	Road Surface	Diurnality
NoPrecip	Dry	Day
NoPrecip	Dry	Night
NoPrecip	Wet	Day
NoPrecip	Wet	Night
NoPrecip	Ice	Day
NoPrecip	Ice	Night
Rain	Dry	Day
Rain	Dry	Night
Rain	Wet	Day
Rain	Wet	Night
Rain	Ice	Day
Rain	Ice	Night
Snow	Dry	Day
Snow	Dry	Night
Snow	Wet	Day
Snow	Wet	Night
Snow	Ice	Day
Snow	Ice	Night
Frozen	Dry	Day
Frozen	Dry	Night
Frozen	Wet	Day
Frozen	Wet	Night
Frozen	Ice	Day
Frozen	Ice	Night

Scheme 2

Road Surface	Precipitation	Diurnality
Dry	Frozen	Day
Dry	Frozen	Night
Dry	NoPrecip	Day
Dry	NoPrecip	Night
Dry	Rain	Day
Dry	Rain	Night
Dry	Snow	Day
Dry	Snow	Night
Ice	Frozen	Day
Ice	Frozen	Night
Ice	NoPrecip	Day
Ice	NoPrecip	Night
Ice	Rain	Day
Ice	Rain	Night
Ice	Snow	Day
Ice	Snow	Night
Wet	Frozen	Day
Wet	Frozen	Night
Wet	NoPrecip	Day
Wet	NoPrecip	Night
Wet	Rain	Day
Wet	Rain	Night
Wet	Snow	Day
Wet	Snow	Night

Scheme 3

Road Surface	Diurnality	Precipitation
Dry	Day	NoPrecip
Dry	Day	Rain
Dry	Day	Snow
Dry	Day	Frozen
Dry	Night	NoPrecip
Dry	Night	Rain
Dry	Night	Snow
Dry	Night	Frozen
Ice	Day	NoPrecip
Ice	Day	Rain
Ice	Day	Snow
Ice	Day	Frozen
Ice	Night	NoPrecip
Ice	Night	Rain
Ice	Night	Snow
Ice	Night	Frozen
Wet	Day	NoPrecip
Wet	Day	Rain
Wet	Day	Snow
Wet	Day	Frozen
Wet	Night	NoPrecip
Wet	Night	Rain
Wet	Night	Snow
Wet	Night	Frozen

Scheme 4

Precipitation	Diurnality	Road Surface
Day	Dry	Frozen
Day	Dry	NoPrecip
Day	Dry	Rain
Day	Dry	Snow
Day	Ice	Frozen
Day	Ice	NoPrecip
Day	Ice	Rain
Day	Ice	Snow
Day	Wet	Frozen
Day	Wet	NoPrecip
Day	Wet	Rain
Day	Wet	Snow
Night	Dry	Frozen
Night	Dry	NoPrecip
Night	Dry	Rain
Night	Dry	Snow
Night	Ice	Frozen
Night	Ice	NoPrecip
Night	Ice	Rain
Night	Ice	Snow
Night	Wet	Frozen
Night	Wet	NoPrecip
Night	Wet	Rain
Night	Wet	Snow

Scheme 5		
Precipitation	**Diurnality**	**Road Surface**
NoPrecip	Day	Dry
NoPrecip	Day	Wet
NoPrecip	Day	Ice
NoPrecip	Night	Dry
NoPrecip	Night	Wet
NoPrecip	Night	Ice
Rain	Day	Dry
Rain	Day	Wet
Rain	Day	Ice
Rain	Night	Dry
Rain	Night	Wet
Rain	Night	Ice
Snow	Day	Dry
Snow	Day	Wet
Snow	Day	Ice
Snow	Night	Dry
Snow	Night	Wet
Snow	Night	Ice
Frozen	Day	Dry
Frozen	Day	Wet
Frozen	Day	Ice
Frozen	Night	Dry
Frozen	Night	Wet
Frozen	Night	Ice

Scheme 6		
Diurnality	**Precipitation**	**Road Surface**
Day	NoPrecip	Dry
Day	NoPrecip	Wet
Day	NoPrecip	Ice
Day	Rain	Dry
Day	Rain	Wet
Day	Rain	Ice
Day	Snow	Dry
Day	Snow	Wet
Day	Snow	Ice
Day	Frozen	Dry
Day	Frozen	Wet
Day	Frozen	Ice
Night	NoPrecip	Dry
Night	NoPrecip	Wet
Night	NoPrecip	Ice
Night	Rain	Dry
Night	Rain	Wet
Night	Rain	Ice
Night	Snow	Dry
Night	Snow	Wet
Night	Snow	Ice
Night	Frozen	Dry
Night	Frozen	Wet
Night	Frozen	Ice

The first iteration of the category aggregation process is illustrated in **Figure** 3-4 for Scheme 4. Grey cells are associated with the categories that were excluded from the analysis because of insufficient observations. Traffic flow parameter values resulting from the calibration of Van Aerde's model are shown for each category. ANOVA has been conducted separately for each parameter (i.e. u_f, u_c and q_c) in each category. The null hypothesis is that all categories have the same population (are similar) while the alternative analysis is that at least one category is different. The significance level is set to 5% and any P-value smaller than 0.05 results in rejecting the null hypothesis and confirming that at least one category is significantly different from others.

There are two possible outcomes from the ANOVA analysis:

1. If the P-values for all four traffic flow parameters are larger than 0.05, it can be concluded that there is no difference between the traffic parameters from each category and therefore there is no need to consider them as separate categories. Consequently, these categories can be aggregated into a single category.
2. If the P-value for at least one of the four traffic flow parameters is less than or equal 0.05, it can be concluded that there is a difference between the traffic parameters from the examined categories and therefore there is a need to consider them as separate categories. When there are only two categories being compared, then no addition analysis is required. However, when three or more categories are examined, then additional analysis is needed to determine if the parameter values are different across all the categories or only a subset of the categories. We use Tukey's test to carry out this evaluation.

To illustrate, consider the ANOVA results for the impact of weather (i.e. precipitation) during the day when the road surface is dry (i.e. comparison of the Day/Dry/NoPrecip, Day/Dry/Rain, and Day/Dry/Snow categories at top of **Figure** 3-4). The P-values indicate there is insufficient evidence to conclude that the weather impacts speed-at-capacity (P-value is greater than 0.05). However, there is evidence to conclude that weather impacts free flow speed and capacity (P-value $\leq$ 0.05).

In this case there are more than two categories so Tukey's test is conducted to provide pairwise category comparisons between the three categories. The results of the three pairwise comparisons indicate that the value of the free flow speed is not statistically different between the Day/Dry/NoPrecip and the Day/Dry/Rain conditions and is statistically different between Day/Dry/NoPrecip and Day/Dry/Snow and between Day/Dry/Rain and Day/Dry/Snow. This suggests that we are concerned only with free speed then the Day/Dry/NoPrecip and Day/Dry/Rain categories can be combined. However, we are also interested in the other traffic stream parameters, namely speed at capacity and capacity. Examining the results from these parameters we observe that (i) the speed at capacity is statistically different for each of three categories and (ii) the capacity flow is different between Dry/Day/NoPrecip and Dry/Day/Snow and between Dry/Day/Rain and Dry/Day/Snow condition; suggesting that the Day/Dry/NoPrecip and Day/Dry/Rain categories should not be combined.

This process is continued for each of the initial categories. As indicated in Figure 3-4 by the solid blue arrows, the analysis suggests that some of the initial categories should be combined.

Figure 3-4- Category aggregation for scheme 4 - first iteration

The next step is to examine if the categories newly formed in iteration 1 are significantly different from their neighbors (if any) in the same group. For instance, all three initial categories in Night/Dry/* group were aggregated and reduced to only one larger category; therefore, no category remained at that group other than the newly formed category of Night/Dry/(NoPrecip+Rain+Snow). But, in the group of Night/Wet/*, the four initial categories were decreased to three categories. It is necessary to examine if the remaining three categories in this group are significantly different. Table 3-4 illustrates the P-values obtained from performing ANOVA on these three categories. The results show that the newly formed category Night/Wet/(NoPrecip+Rain) is significantly different from its neighboring categories Night/Wet/Snow and Night/Wet/Frozen and therefore they should not be aggregated.

Table 3-4- Instance of Examining the Differences between Newly Formed Categories (Iteration 1 for Scheme 4)

ID	Compared Categories			u_f (kph)	u_c(kph)	q_c(vph)	Pairwise	Tukey's Test		
								P-u_f	P-u_c	P-qc
C26	Night	Wet	NoPrecip+Rain	109.6	97.4	1769	C26/C16	0.00	0.00	0.00
C16	Night	Wet	Snow	86.5	62.2	1206	C26/C22	0.17	0.06	0.00
C22	Night	Wet	Frozen	104.4	82.4	785	-	-	-	-
	ANOVA P-value			0.00	0.00	0.00				

This process is applied to other newly formed categories to complete iteration 1 for Scheme 4. As shown at the right hand side of

Figure 3-4, iteration 1 has resulted in a reduction in the number of categories from 17 to 13 for Scheme 4. Iterations are continued until no more changes to the categorizations are warranted. The same method was applied to the other categorization schemes. The final categories for schemes 1 to 6 are shown in Table 3-5.

Table 3-5- Final categories in each categorization scheme

Scheme 1 & 2

	Road Surface	Dry		Wet		Ice	
	Diurnality	Day	Night	Day	Night	Day	Night
Precipitation	NoPrecip	X	X	X	X	X	X
	Rain	X		X			
	Snow	X		X	X	X	
	Frozen			X	X		

Scheme 3 & 4

	Road Surface	Dry		Wet		Ice	
	Diurnality	Day	Night	Day	Night	Day	Night
Precipitation	NoPrecip	X	X	X	X	X	X
	Rain	X					
	Snow	X		X	X	X	
	Frozen			X	X		

Scheme 5 & 6

	Road Surface	Day			Night		
	Diurnality	Dry	Wet	Ice	Dry	Wet	Ice
Precipitation	NoPrecip	X	X	X	X	X	X
	Rain	X	X		X		
	Snow	X	X	X	X	X	
	Frozen		X			X	

As shown in Table 3-5 the schemes with the same highest-level factor (i.e. F_m in the vector of $\boldsymbol{C}$= {F_m, F_n, F_k}), have the same set of final categories (i.e. schemes 1 and 2, 3 and 4, 5 and 6). The final categories as well as estimated traffic parameters for all schemes are provided in Table 3-6.

Table 3-6- Traffic Parameters of Final Categories in All Schemes

	Diurnality	Road Surface	Precipitation	u_f (kph)	u_c (kph)	k_j (vphpl)	q_c (vph)
Schemes 1 & 2	Day	Dry	No Precip	115.7	101.1	100	1847
	Night	Dry	No Precip	113.1	97.3	100	1784
	(Day+Night)	Dry	Rain	112.8	102.6	100	1687
	(Day+Night)	Dry	Snow	107.5	93.5	100	1743
	Day	Ice	No Precip	118.0	74.1	100	1674
	Night	Ice	No Precip	107.6	96.1	100	1737
	Day	Ice	Snow	111.6	102.3	100	1338
	Day	Wet	Frozen	103.8	97.5	100	1689
	Night	Wet	Frozen	104.4	82.4	100	785
	Day	Wet	No Precip	109.3	96.9	100	1732
	Night	Wet	No Precip	109.7	95.4	100	1775
	(Day+Night)	Wet	Rain	111.1	90.7	100	1658
	Day	Wet	Snow	94.5	89.9	100	1303
	Night	Wet	Snow	86.5	62.2	100	1206
Schemes 3 & 4	Day	Dry	No Precip	115.7	101.1	100	1847
	Day	Dry	Rain	112.3	102.2	100	1688
	Day	Dry	Snow	107.6	97.6	100	1759
	Day	Wet	(NoPrecip+Rain)	111.6	98.7	100	1730
	Day	Wet	Snow	94.5	89.9	100	1303
	Day	Wet	Frozen	103.8	97.5	100	1689
	Day	Ice	NoPrecip	118.0	74.1	100	1674
	Day	Ice	Snow	111.6	102.3	100	1338
	Night	Dry	All	112.9	97.9	100	1789
	Night	Wet	(NoPrecip+Rain)	109.6	97.4	100	1769
	Night	Wet	Snow	86.5	62.2	100	1206
	Night	Wet	Frozen	104.4	82.4	100	785
	Night	Ice	NoPrecip	107.6	96.1	100	1737
Schemes 5 & 6	Day	Dry	No Precip	115.7	101.1	100	1847
	Day	Wet	No Precip	109.3	96.9	100	1732
	Day	Ice	No Precip	118.0	74.1	100	1674
	Day	Dry	Rain	112.3	102.2	100	1688
	Day	Wet	Rain	110.2	92.0	100	1668
	Day	Dry	Snow	107.6	97.6	100	1759
	Day	Wet	Snow	94.5	89.9	100	1303
	Day	Ice	Snow	111.6	102.3	100	1338
	Day	Wet	Frozen	103.8	97.5	100	1689
	Night	Dry	No Precip	113.1	97.3	100	1784
	Night	Wet	No Precip	109.7	95.4	100	1775
	Night	Ice	No Precip	107.6	96.1	100	1737
	Night	(Dry+Wet)	Rain	110.2	94.8	100	1658
	Night	Dry	Snow	111.2	61.3	100	2198
	Night	Wet	Snow	86.5	62.2	100	1206
	Night	Wet	Frozen	104.4	82.4	100	785

The RMSE values were computed for all schemes (Table 3-7) and it is observed that Schemes 5 and 6 have the lowest RMSE values and therefore are preferred over the other categorization schemes.

Table 3-7- Specifications and RMSE of the Categorization Schemes

Schemes	Factor Order	Number of final categories	RMSE
Scheme 1	Precipitation---->Road Surface---> Diurnality	14	0.0464
Scheme 2	Road Surface---->Precipitation----->Diurnality	14	0.0464
Scheme 3	Road Surface---->Diurnality---> Precipitation	13	0.0463
Scheme 4	Diurnality---->Road Surface---> Precipitation	13	0.0463
Scheme 5	Precipitation---->Diurnality---> Road Surface	16	0.0456
Scheme 6	Diurnality---->Precipitation---> Road Surface	16	0.0456

3.5. Conclusions

This chapter has proposed a method to objectively determine the optimal weather and road surface condition categorizations in terms of their impact on traffic stream characteristics. The method was illustrated through the application to a set of traffic, weather, and road surface condition data from Minnesota. The results demonstrate that:

1. The proposed method can be practically applied using field data to determine the optimal categorization of weather, road surface, and environmental conditions and the associated traffic stream characteristics.
2. It is not necessary to represent all possible combinations of the weather, road surface condition, or environmental factors in the categorization because some of these combinations are associated with traffic stream characteristics that are not statistically different from the characteristics associated with one or more other categories.
3. The aggregation of categories is a function of the order in which the weather, road surface condition, and environmental factors are considered within the categorization scheme. Consequently, it is necessary to consider all possible schemes and to have an objective means of selecting the optimal scheme.
4. In the example application, the number of categories is reduced from 17 to 16 as a result of aggregation of categories which are not statistically different.

Chapter 4

Identifying Parameters to Model Traffic During Inclement Weather using Microsimulation[4]

4.1. Introduction

Traffic microsimulation models are widely used to evaluate the impact of transportation improvement alternatives. Recently, there is increased interest in evaluating the impact that different improvement alternatives have on travel time reliability. Travel time reliability considers the day-to-day variations of travel times that result from variations in demand and variations in capacity. The inclusion of demand variation in traffic microsimulation models is straightforward because demand is a direct input parameter to the model. However, variations in capacity result from a variety of sources including incidents, construction, and weather and these are typically not captured directly as inputs to the model.

The focus of this chapter is on developing a method by which microsimulation model uses can determine appropriate model input parameter values that reflect the influence of inclement weather on traffic stream characteristics.

[4] The contents of this chapter have been incorporated within a paper that has been submitted for publication. R. Golshan; B. Hellinga and A. Zarinbal, "Modeling Weather Conditions Using Microsimulation" Submitted to the Journal of Transportation Research Record. Submission date Aug. 1, 2016.

4.2. Literature Review

The existing body of literature can be divided into two categories as follows:

(1) The first category consists of studies that have examined the influence of weather conditions on one or more traffic stream characteristics. Edward (1999) studied the impact of three weather categories (i.e. dry, rainy, and foggy) on traffic flow characteristics such as mean speed. Caro et al. (2007) and Boer et al. (2007) studied the impact that fog has on vehicle time headways. Broughton et al. (2007) studied the impact of three visibility levels on car-following characteristics using the car-following model developed by Van Winsum (1999). Rakha et al. (2007) used weather data and loop detector data to quantify the impact of precipitation type and intensity and visibility on traffic stream characteristics. They also developed "weather adjustment factors" which could be used to estimate traffic stream characteristics under adverse weather conditions as a function of the type and intensity of precipitation and visibility level.

(2) The second category consists of studies that have examined methods for selecting microsimulation input parameter values that correspond to specific weather conditions. Rakha et al. (2008) derived analytically the relationship between two parameters of the VISSIM Wiedemann 99 car-following model (CC0 and CC1) and traffic flow parameters. Rakha et al. (2009) incorporated weather adjustment factors into microscopic traffic simulation models including VISSIM. For example, using field data they determined the maximum deceleration as a function of rainfall intensity and then suggested that this could be used as a means of specifying the value for the VISSIM input parameter "maximum deceleration". They also proposed weather adjustment factors for several other model input parameters including safety distance, visibility distance, front gap, and rear gap.

There are two main challenges associated with modelling the impacts of weather:

The first is that the same adverse weather condition can have very different impacts depending on the geographic location. For example, the impact of a snow storm event on traffic stream characteristics in a location for which snow storms are common will be very different from the same weather event in a location that rarely experiences snow. As a result, we are left with a choice of defining parameters which capture the average impact across a range of geographical areas or defining

a set of model input parameter for each geographical area separately. Rakha et al (2007) developed weather adjustment factors using traffic and weather data from three sites in USA. Thus their method reflects some average of the impact across these three sites as well as each individual geographic area. However, it is not clear that this will adequately capture the impact of a given weather condition at some other location.

The second challenge relates to which microsimulation input parameters should be adjusted for adverse weather. Most of the commonly used microsimulation models have a very large number of input parameter values and it is not clear which ones are important for capturing the impacts of adverse weather.

In this chapter we propose an approach that addresses both of the above two challenges. More specifically, we propose a method which (1) can be used to determine the weather impacts for a given local geographical area; and (2) systematically identifies the set of microsimulation model input parameters (in this chapter we have used the VISSIM model) that are most important for capturing these weather impacts.

Users specify the desired macroscopic traffic stream parameters associated with the weather category of interest and the proposed model provides recommended VISSIM model input parameter values.

4.3. Problem Formulation

Consider the road environmental categories $w_1, \ldots, w_n$. Each environmental category is defined in terms of a set of characteristics which can include precipitation (type and intensity), road surface condition, wind speed and direction, visibility, etc. If the environmental category is defined on the basis of only weather characteristics, then this is a weather category. For simplicity, throughout the remainder of this chapter we use the term environmental category and weather category interchangeably.

We are interested in simulating the traffic flow under a given weather category using traffic microsimulation models. For that, we are looking for a specific set of model input parameters such that

when we use those input parameters, the simulation produces traffic stream characteristics which are consistent with those that are observed in the field under those weather conditions.

As described in previous chapters, the characteristics of the traffic stream can be defined in terms of four macroscopic parameters, namely free-flow speed (u_f), speed-at-capacity (u_c), jam density (k_j) and capacity (q_c). We define $\hat{X}$ as the set of observed (or desired) traffic flow parameters) and $\tilde{X}$ as the set of simulated traffic flow parameters.

The observed (or desired) traffic flow parameters are influenced by the weather category and therefore $\hat{X}_i = f(w_i)$.

The traffic flow parameters associated with the simulated traffic stream are impacted by the model input parameter values and therefore $\tilde{X}_i = f(p_i)$ where p_i is the set of model input parameters of the traffic microsimulation model which corresponds to the weather category w_i.

In this chapter we propose a method to map w_i to the microsimulation model input parameters and generate p_i to satisfy $\hat{X} = \tilde{X}_i$.

4.4. Methodology

The development of the proposed model consists of the following four steps:

1- Identify the microsimulation model input parameters which have the greatest impact on the output of the traffic microsimulation model.
2- Generate a large sample from the input parameter distributions.
3- Find the corresponding traffic flow parameters for each sample of input parameters.
4- Develop a relationship between traffic flow parameters and input parameters.

We note that in this chapter we elected to use the VISSIM microsimulation software as the simulation tool; however, the proposed method is applicable for all other traffic microsimulation models.

4.4.1. Selecting Input Parameters

Each traffic microsimulation model typically has a large number of input parameters. To know which parameters should be considered in the analysis, we follow the following steps:

1- Make a short list of input parameters
2- Perform sensitivity analysis

4.4.1.1. Shortlisted Parameters

Many previous studies have examined the calibration and validation of traffic microsimulation models. Several of these studies have examined the relative importance of the model input parameters. In creating a shortlist of candidate input parameters, we make use of the findings from these previous studies to determine good candidates to be placed in the list of viable input parameters. Also, common sense and applicability are other considerations when choosing candidate parameters. For instance, if the study network is part of a freeway, then the parameters related to riding a bicycle would not be part of the shortlisted parameters.

There are more than 190 parameters in the VISSIM software (Ge and Menendez, 2012), many of which are related to driver behavior. The input parameters and their range were investigated in previous research (Gomes et al., 2004; B. Park and Qi, 2006; Lownes and Machemehl, 2006; Ge and Menendez, 2012). The parameters listed in Table 4-1 are those which were identified most frequently in these previous studies as having an important influence on the traffic stream behavior.

Table 4-1-Important VISSIM Input Parameters Specified in Previous Research

Parameter code	Parameter Name	Description
p1	MaxDecelOwn	Maximum deceleration (own)
p2	MaxDecelTrail	Maximum deceleration (trailing vehicle)
p3	AccDecelOwn	Accepted deceleration (own)
p4	AccDecelTrail	Accepted deceleration (trailing vehicle)
p5	DecelRedDistOwn	Deceleration reduction distance (own)
p6	DecelRedDistTrail	Deceleration reduction distance (trailing vehicle)
p7	CoopDecel	Maximum cooperative deceleration
p8	SafDistFactLnChg	Safety distance reduction factor
p9	LookAheadDistMax	Look ahead distance (maximum)
p10	W99cc0	Standstill distance
p11	W99cc1	Headway time
p12	W99cc2	'Following' variation
p13	W99cc3	Threshold for entering 'Following'
p14	W99cc4	Negative 'Following' threshold
p15	W99cc5	Positive 'Following' threshold
p16	W99cc6	Speed dependency of oscillation
p17	W99cc7	Oscillation acceleration
p18	W99cc8	Standstill acceleration
p19	W99cc9	Acceleration at 80 km/h
p20	LnChgDist	Lane change distance
p21	EmergStopDist	Emergency stop distance

4.4.1.2. Sensitivity Analysis

Having established an initial set of 21 candidate input parameters, a sensitivity analysis was conducted to determine the relative importance of these parameters. We used the *Elementary Effect* technique with the *Trajectory Sampling* approach developed by Morris (1991) and implemented by Ge and Menendez (2012) to quantify the sensitivity of the model output to the input parameters. Equation (4-1) computes the *Elementary Effect* for each parameter:

$$EE_i = \frac{Y(X_1, \dots, X_{i-1}, X_i + \Delta, X_{i+1}, \dots, X_k) - Y(X_1, \dots, X_{i-1}, X_i, X_{i+1}, \dots, X_k)}{\Delta} \quad (4\text{-}1)$$

where,

EE_i: "Elementary Effect" of parameter i,

X_i: input parameter i,

$Y(X)$: the model output

Δ: the amount of change in input parameters

The magnitude and acceptable range for the input parameters are usually very different. For instance, one parameter may change between 0.1 and 0.5 while the other may change from 50 to 100. Consequently, rather than using the same value of Δ for all parameters, we define Δ for each parameter as:

$$\Delta_i = d \cdot r_i \tag{4-2}$$

where,

Δ_i: the change step value of parameter i

d: constant multiplier for all parameters

r_i: range of parameter i

Consequently, the elementary effect is calculated as:

$$EE_i = \frac{Y(X_1, \dots, X_{i-1}, X_i + \Delta_i, X_{i+1}, \dots, X_k) - Y(X_1, \dots, X_{i-1}, X_i, X_{i+1}, \dots, X_k)}{\Delta_i} \tag{4-3}$$

The use of *Trajectory Sampling* lets us evaluate the elementary effect of each input parameter n times where n is the number of trajectories. Each trajectory consists of $p + 1$ nodes (p is the number of parameters), and the model output (i.e. $Y(X)$) is calculated at each node. Every node of P_i consists of a set of input parameters $X_1,\dots,X_k$, and the value of only one parameter changes by Δ_i from P_{i-1} to P_i and only "one" other parameter changes by Δ_{i+1} from node P_i to P_{i+1}. Therefore, the EE of each parameter is calculated according to Equation (4-4):

$$EE_1 = \frac{Y(X_1^0 + \Delta_1, X_2^0) - Y(X_1^0, X_2^0)}{\Delta_1}$$

$$EE_2 = \frac{Y(X_1^0 + \Delta_1, X_2^0 + \Delta_2) - Y(X_1^0 + \Delta_1, X_2^0)}{\Delta_2} \quad (4\text{-}4)$$

Figure 4-1 illustrates a sampling trajectory for a two-parameter model (n=1, p=2). In Figure 4-1, the two input parameters are X_1 and X_2, and the nodes are P_0, P_1, and P_2 (the trajectory is P_0-P_1-P_2).

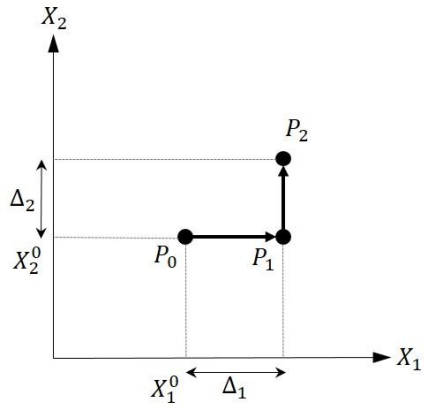

Figure 4-1- One trajectory for a two-parameter model

In most cases, several trajectories are used to enable several evaluations of the *Elementary Effect* of each parameter. The literature advises that the number of trajectories be between 10 and 50 (Campolongo et al., 2007). When there is more than one trajectory, it is suggested that the trajectories be located at the maximum Euclidian distance from each other (Ge and Menendez, 2012). Therefore, choosing the starting point of the trajectory (P_0) is important. We suggest the use of Latin Hypercube Sampling (LHS) to choose the trajectory starting points in order to maintain the furthest distance between the starting points (P_0).

The procedure to choose the microsimulation input parameters is illustrated in Figure 4-2.

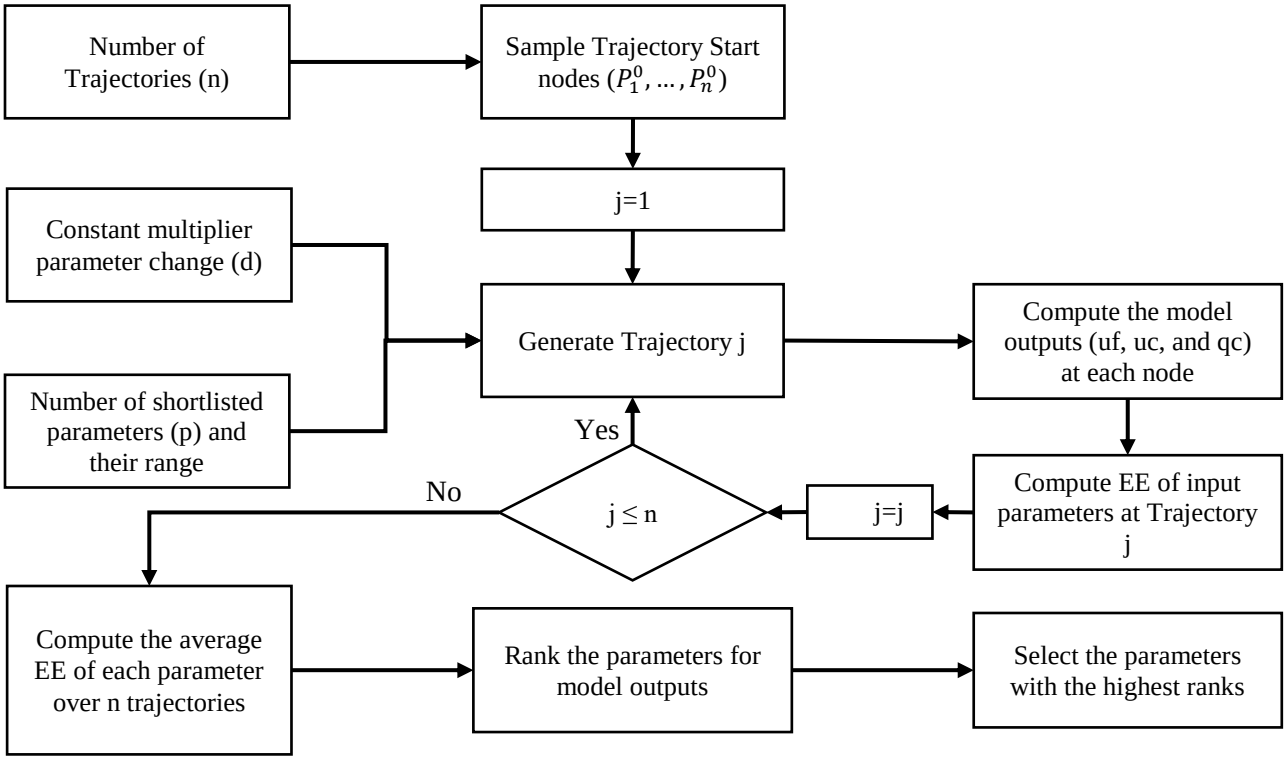

Figure 4-2-Sensitivity Analysis Procedure

The model outputs considered here are free-flow speed (u_f), speed-at-capacity (u_c) and capacity (q_c). The jam density (k_j) was considered constraint. For each node P_i in each trajectory, these model outputs are estimated, and eventually, the average EE of each parameter is calculated for each model output. To estimate the model outputs, we calibrate Van Aerde's single regime macroscopic speed-flow-density relationship (Van Aerde and Rakha, 1995) to the simulation output. We used the calibration method described by Rakha and Arefeh (2010) and discussed in previous chapters of this thesis.

We set the constant multiplier for all parameters (i.e. d) to be 0.1. Therefore, for input parameters $X_1,\dots,X_{21}$, the parameter change steps $\Delta_1, \dots, \Delta_{21}$ were computed by multiplying each parameter range (r_i) by the constant multiplier d. We decided to have 50 sampling trajectories (n = 50) and used Latin Hypercube Sampling technique to generate the starting points (i.e. P_i^0) for each of the n trajectories. Since we had 21 shortlisted parameters (p = 21) listed in Table 4-1, we had 50 × (21 + 1) = 1100 nodes. Each node has a set of model input parameters.

A hypothetical section of freeway was used as the test network (Figure 4-3). Each freeway link consisted of two lanes except the first 1150 m of the horizontal link which has three lanes. A lane drop from three to two was located at the horizontal lane before the measurement point. A temporally varying traffic demand pattern was used to generate both uncongested and congested traffic conditions at the measurement point. Each simulation run consisted of 3900 seconds; the first 300 seconds of which were used for warm-up and data were not collected. Traffic flow and speed was captured during the remaining 3600 seconds and aggregated at five-minute intervals. Therefore, each simulation run produced 12 aggregated five-minute speed-flow observations. We repeated each simulation run 10 times with different random seeds to obtain 120 observations. Then we calibrated Van Aerde's model to these 120 observations to obtain an estimate of u_f, u_c and q_c.

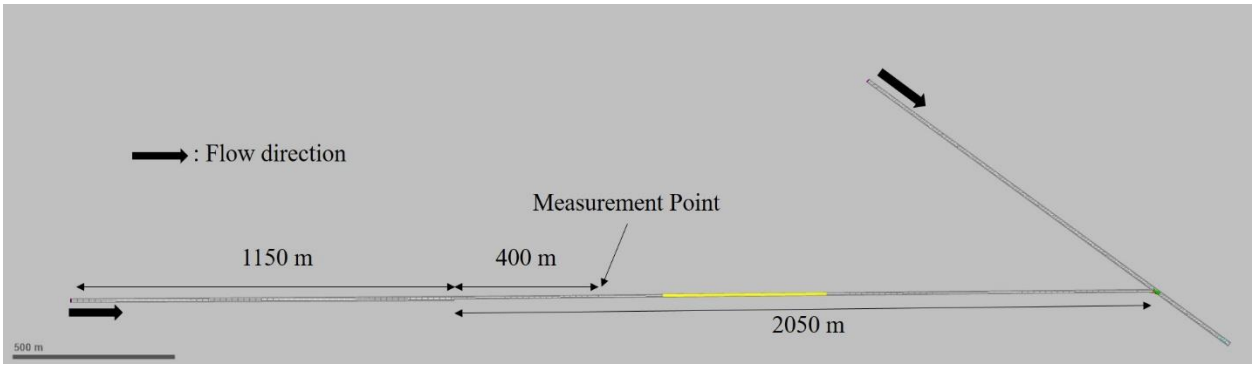

Figure 4-3- Simulation Network Used for Sensitivity Analysis

The final ranking of the parameters based on their impact on each model output is listed in Table 4-2. These rankings are based on the *Elementary Effect* of each parameter averaged over 50 trajectories. In other word, the elementary effect was estimated 50 times and the reported elementary effect is the average over the 50 trajectories.

Table 4-2- Rankings of VISSIM input parameters (impact on each model output)

Rank	u_f	u_c	q_c
1	p17	p19	p11
2	p14	p14	p19
3	p8	p17	p15
4	p15	p15	p14
5	p19	p8	p8
6	p10	p10	p10
7	p11	p3	p17
8	p3	p4	p3
9	p21	p11	p21
10	p4	p7	p4
11	p1	p21	p7
12	p7	p1	p1
13	p2	p2	p2
14	p18	p18	p12
15	p12	p12	p18
16	p16	p16	p5
17	p13	p13	p16
18	p5	p5	p13
19	p9	p9	p9
20	p20	p20	p6
21	p6	p6	p20

The change of the elementary effect values for each model output (i.e. u_f, u_c and q_c) is shown in Figure 4-4. The horizontal axis consists of parameters based on their rank in Table 4-2. The vertical axis is the value of the elementary effect of each parameter regarding the model output.

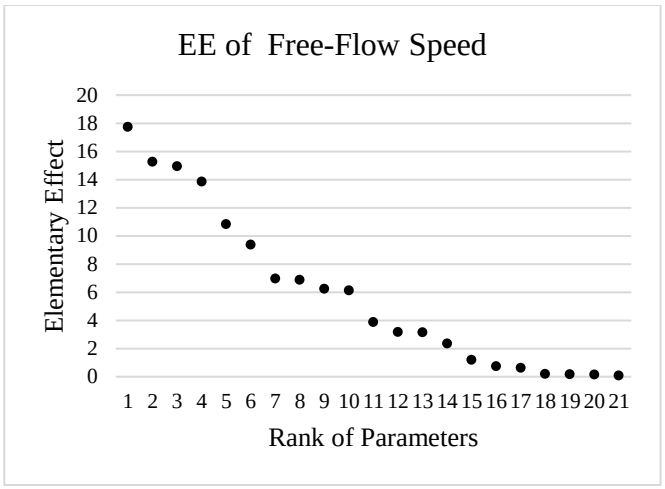

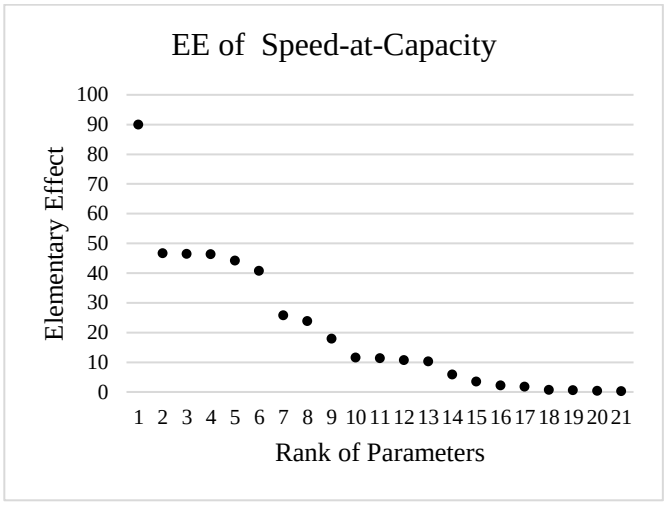

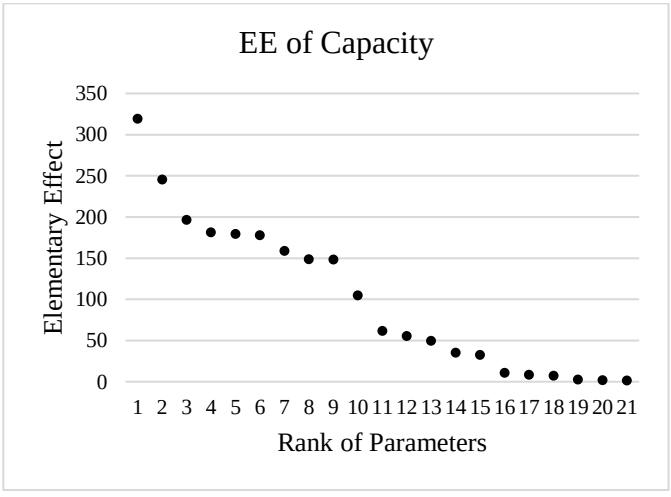

Figure 4-4- Elementary Effect of Parameters

To determine the global rank of each parameter we normalized the computed elementary effects with the maximum computed EE for each u_f, u_c, and q_c. Then we took an average of normalized u_f, u_c, and q_c elementary effect of each parameter. The global ranking of the parameters is provided in Table 4-3 and illustrated in Figure 4-5 .

Table 4-3- Global ranking of VISSIM input parameters

Rank	Parameter	Average Normalized EE
1	p19	0.79
2	p17	0.67
3	p14	0.65
4	p15	0.64
5	p8	0.63
6	p11	0.53
7	p10	0.51
8	p3	0.38
9	p21	0.31
10	p4	0.31
11	p1	0.17
12	p7	0.17
13	p2	0.15
14	p18	0.10
15	p12	0.07
16	p16	0.03
17	p13	0.03
18	p5	0.02
19	p9	0.01
20	p20	0.01
21	p6	0.00

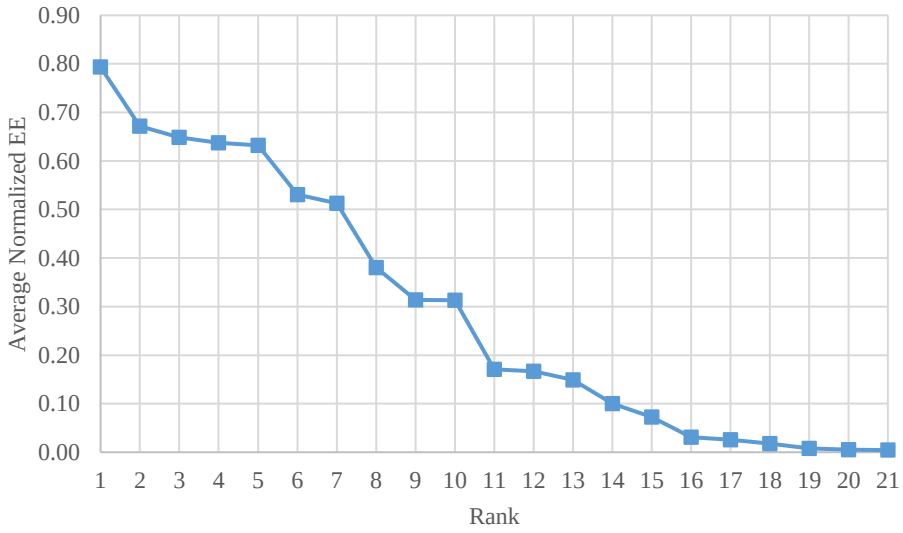

Figure 4-5- Average Normalized Elementary Effect of VISSIM Parameters

The following step in the approach requires the generation of simulation runs to cover the range of values for each of the considered VISSIM parameters. Consequently, we desire to minimize the number of parameters considered while at the same time including those parameters which have a substantive impact on the simulation outputs. Considering the average normalized elementary effect values, we selected the first ten parameters with the highest ranks as the ones that we consider in next steps. We note that parameter ranked 9th (p21) is the "Emergency Stop Distance" which is the distance before a lane drop or merging section at which a vehicle will stop and wait for a gap to merge. Since this parameter is specific to the networks with lane drops or merging sections, we removed it from the set of selected parameters and considered the remaining nine parameters in the next step. We also considered two additional model inputs:

1. The fraction of heavy vehicles in the traffic stream
2. The desired speed distribution.

The final parameters are listed in Table 4-4.

Table 4-4- Final input parameters

#	Parameter code	Parameter Name
1	p3	AccDecelOwn
2	p4	AccDecelTrail
3	p8	SafDistFactLnChg
4	p10	W99cc0
5	p11	W99cc1
6	p14	W99cc4
7	p15	W99cc5
8	p17	W99cc7
9	p19	W99cc9
10		RelFlow
11		DesSpeedDistr

4.4.2. Generate the Samples

Now that we have established the microsimulation model input parameters to consider, it is necessary to develop a relationship between these input parameters and the traffic stream characteristics. To do this we carry out simulation runs using different combinations of values for the input parameters. To generate these combinations, we must:

- Define the feasible range of values for each parameter; and
- Select a method for determining the combination of parameter values to simulation (i.e. a sampling method)

We determined the range of the input parameters listed in Table 4-4 by considering the upper and lower bounds of those parameters in VISSIM, taking into account the ranges mentioned in other studies, and by using engineering judgment. Parameters 1 to 10 were considered continuous while parameter 11 (i.e. Desired Speed Distribution) was considered categorical. We assumed desired speed distribution to vary from 80 kph to 130 kph. The range of the parameters is shown in Table 4-5.

Table 4-5- VISSIM input parameter range

#	Parameter Name	Lower bound	Upper bound	Unit
1	AccDecelOwn	-3	-0.5	m/s^2
2	AccDecelTrail	-3	-0.5	m/s^2
3	SafDistFactLnChg	0	1	-
4	W99cc0	1	5	m
5	W99cc1	0.5	3	s
6	W99cc4	-1	0	-
7	W99cc5	0	1	-
8	W99cc7	0	1	m/s^2
9	W99cc9	0.5	3	m/s^2
10	RelFlow	0.01	0.2	-
11	DesSpeedDistr	80	130	km/h

We select Latin Hypercube Sampling (LHS) for sampling from the distributions of the input parameter distributions. Using LHS avoids over sampling or under sampling from different parts of the distribution by taking equal number of samples from the same-probability sections of the distribution. For instance, if 100 samples are to be taken, LHS divides the distribution to same probability zones (e.g. 20 zones with 5% probability of occurrence each) and takes 5 samples randomly within each zone.

4.4.3. Generating Desired Speed Distributions

VISSIM microsimulation software samples from a user specified Desired Speed Distribution (DSD) to assign speeds to vehicles in the network when there is no other speed limitation such as reduced speed zones, etc. This impacts road capacity and also the maximum speed in the network (B. Park and Schneeberger, 2003).

There are two challenges to determining DSDs from field data. One is obtaining speed data from individual vehicles. The second is determining if the measured speed represents the desired speed or a constrained speed. We addressed these two challenges as follows.

We used 20-second resolution loop detector data obtained from three dual-loop stations on the QEW highway (posted speed limit of 100 kph) located in Ontario, Canada. We identified individual vehicle speeds by extracting the measured speeds from only those 20-second intervals for which only a single

vehicle passed the detector. We attempted to avoid including constrained speeds by using only observations between 12 am (midnight) and 5 am; when traffic demands and densities are very low. Data was taken from all three lanes and speeds less than 60 kph and greater than 170 kph were excluded. The distribution of the remaining speed observations show that the DSD follows a normal distribution (Figure 4-6).

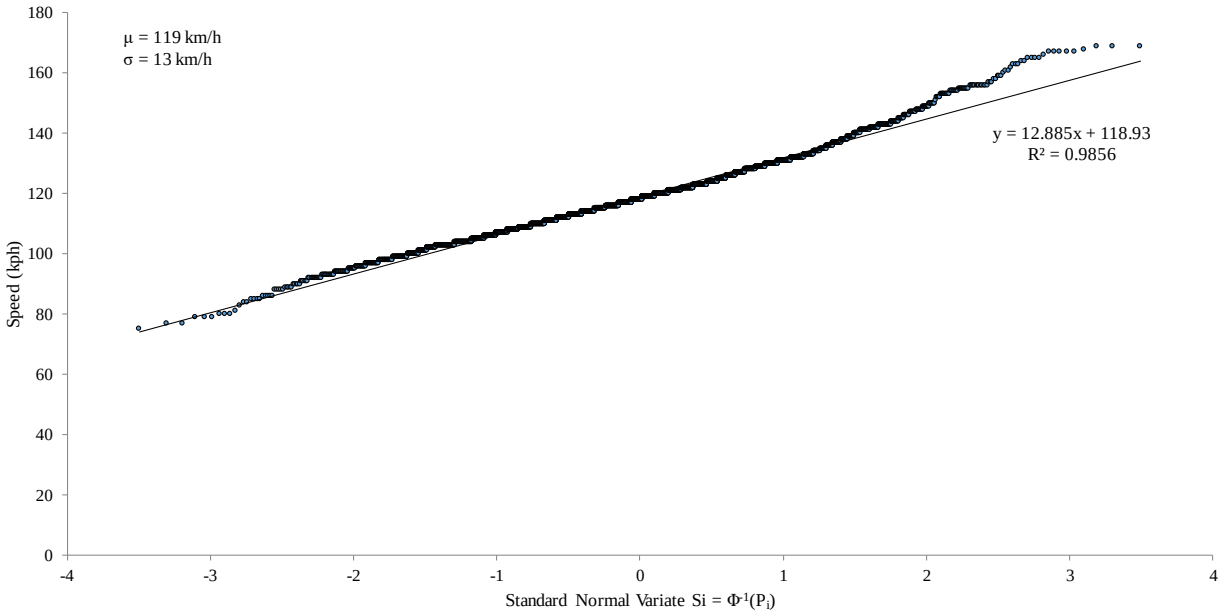

Figure 4-6- Normal Probability Plot of QEW DSD Speed Data Points

The mean value of the observed speed data was 119 kph and the standard deviation was 13 kph which results in a coefficient of variation of 0.109.

We require the ability to specify additional DSDs having higher and lower mean speeds. We assumed that all DSDs (for passenger cars) follow the Normal distribution with the same coefficient of variation as the QEW dataset (i.e. COV =0.109).

We defined 26 DSDs starting from 80 kph and ending in 130 kph (i.e. 80kph, 82 kph, 84 kph, …, 130 kph). The DSD label denotes the mean of the distribution.

4.4.4. Heavy Vehicle Desired Speed Distributions

Heavy vehicles have operational characteristics that are different from passenger cars. These differences arise from different acceleration and deceleration rates as well as regulations (e.g. there

may be a different speed limit for heavy vehicles). Consequently, it is also necessary to have different DSDs for heavy vehicles.

Only a few studies have investigated the characteristics of free speed distributions for heavy vehicles. Hoogendorn (2005) reported that the coefficient of variation of trucks in unconstrained traffic flow on a freeway with a posted speed limit of 100 kph is 0.077.

In many jurisdictions in North America, speed limiters are mandatory on large trucks and a common maximum speed is 105 kph (65 mph). Thus we generated the heavy vehicle DSDs using the same method used for passenger car DSDs, except COV = 0.077 and all generated speed values higher than 105 kph, were reduced to 105 kph. As an example, the desired speed distribution of 94 kph is illustrated in Figure 4-7.

Heavy vehicle DSDs of 80 kph, 82 kph, …,104 kph, 105 kph were generated (14 DSDs in total). For each simulation, the passenger car DSD was selected through Latin Hypercube sampling and the heavy vehicle DSD was determined as a function of the passenger car DSD using Equation (4-5).

$$\overline{DSD}_i^{hv} = \begin{cases} \overline{DSD}_i^{pc} & ,if\ \overline{DSD}_i^{pc} < 105\ kph \\ 105\ kph & ,if\ \overline{DSD}_i^{pc} > 105\ kph \end{cases} \quad (4\text{-}5)$$

where,

$\overline{DSD}_i^{hv}$: mean of the desired speed distribution for heavy vehicles in simulation *i*

$\overline{DSD}_i^{pc}$: mean of the desired speed distribution for passenger cars in simulation *i*

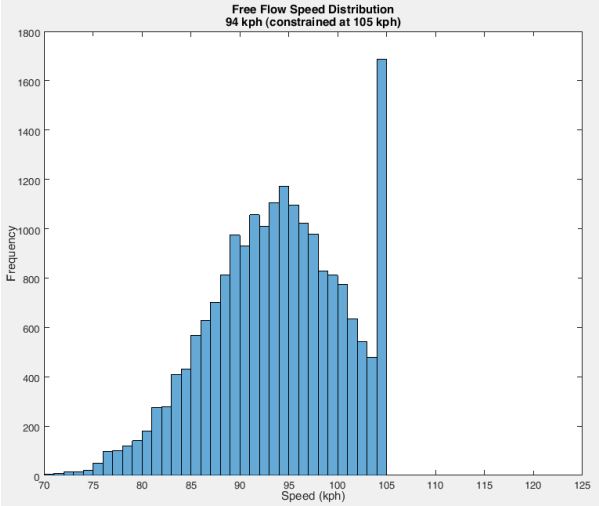

Figure 4-7- Heavy Vehicle Desired Speed Distribution (DSD^{hv} of 94 kph)

4.4.5. Taking Samples from Input Distributions

Having determined which VISSIM input parameters and their respective ranges of values to consider, we took 300,000 samples using Latin Hypercube Sampling (LHS). Each sample consisted of values for the 11 parameters listed in Table 4-4.

4.4.6. Microsimulation Modeling

A hypothetical freeway network (Figure 4-8) was coded in VISSIM. The lane width is 3.5 m throughout the network. The network was designed to enable the generation of congested and uncongested traffic conditions. The first 660 m from Entry point 1 consists of 3 lanes. The remainder of the network consists of 2 lanes. Flow and speed measurements are extracted from VISSIM at an aggregation interval of 5 minutes. Density was estimated as flow/speed.

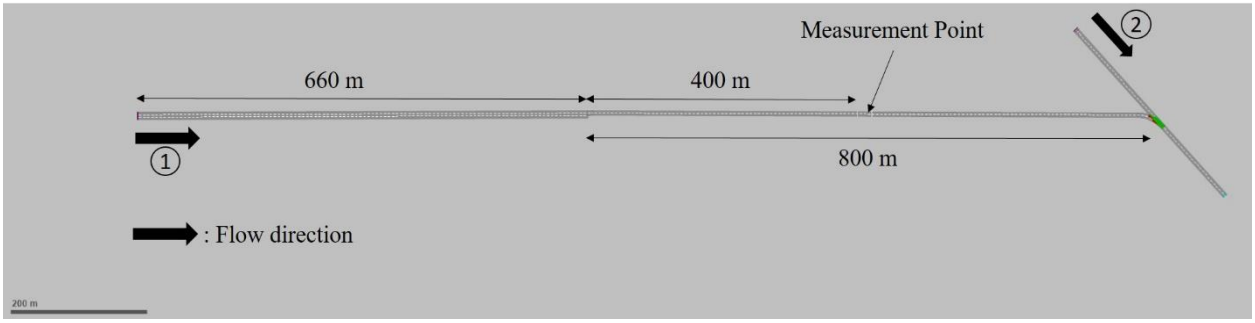

Figure 4-8- Simulation Network Coded in VISSIM

The time-varying traffic demands entering the network at origins 1 and 2 are provided in Table 4-6:

Table 4-6- Traffic demand at origins 1 and 2

Origin 1		Origin 2	
Time Interval	**Flow Rate (vph)**	**Time Interval**	**Flow Rate (vph)**
0-300	500	0-300	0
300-600	500	300-600	0
600-900	1500	600-900	0
900-1200	2500	900-1200	0
1200-1500	3500	1200-1500	0
1500-1800	5000	1500-1800	0
1800-2100	6000	1800-2100	0
2100-2400	6000	2100-2400	0
2400-2700	5000	2400-2700	250
2700-3000	4000	2700-3000	2000
3000-3300	3000	3000-3300	2000
3300-3600	2000	3300-3600	1000
3600-3900	1000	3600-3900	500

The interval 0-300 seconds was used for warm-up. No output was captured during the warm-up interval. From 300 to 1500 seconds, the uncongested traffic condition was simulated. From 1500 to 2400 seconds we simulated capacity flow at the measurement point and from 2400 to 3600 seconds we simulated traffic congestion, ranging from moderate to severe congestion. From 3600 to 3900 seconds we let the network discharge any queued vehicles.

In each simulation run 12 speed-flow-density points were generated and for each sample of input parameters values, we run the simulation 10 times with 10 different random seeds to obtain 120 speed-flow-density points.

4.4.7. Estimating Traffic Flow Characteristics

For each set of input parameter values we determine the resulting traffic flow characteristics (i.e. free-flow speed (u_f), speed-at-capacity (u_c), jam density (k_j), and the capacity (q_c)) by fitting Van Aerde's traffic flow model to the 120 simulation data points.

A custom fitting algorithm was developed within Matlab software to calibrate Van Aerde's model. This code calibrates Van Aerde's model in a three-dimension (speed-density-flow) space. As per the method used by Rakha and Arafeh (2010) the 120 observations were parsed and then aggregated over density range into a number of bins to reduce the computational cost. All observations within each density bin were aggregated to create a single representative point. The speed, density and flow of this single point was computed as the mean of speed, density, and flow values of all points in that bin. To solve the optimization problem when fitting Van Aerde's curve, we used the Matlab *multi-start* algorithm which applies *fmincon* (i.e. a function in Matlab that finds the minimum of constrained nonlinear multi-variable functions) from several uniformly distributed starting points. Since *fmincon* is a gradient –based technique, it may fall in local optimums; therefore, the use of *multi-start* algorithm reduces the chance of a false global optimum. (Mathworks Inc., 2016)

After estimating traffic flow characteristics for all samples, we had a set of traffic parameters Y_i (i.e. $u_{f,i}$, $u_{c,i}$, $k_{j,i}$, and $q_{c,i}$) for each sample of input parameters X_i (i.e. $X_i^1, \dots, X_i^{11}$).

4.4.8. Develop Relationship Between Traffic Flow Parameters and Microsimulation Input Parameters

The final step in our approach is specifying and calibrating a model to reflect the relationship between traffic flow parameters and microsimulation input parameters.

Given the highly non-linear nature of the relationship, we elected to use a neural network to establish the relationship. A neural network is a complex system in which a number of simple processing elements –called *neurons*- are working parallel to each other. This complex system attains

the knowledge from the experience, and stores the knowledge as the strength or weight in its inter-neuron connections (Haykin, 1999). A neural network has three layers: input layer, output layer, and hidden layer. The number of neurons in the hidden layer impacts the flexibility of the neural network to develop the relationship between input and output layers. More neurons in the hidden layer result in a more flexible neural network; however, the increase in the number of neurons in the hidden layer is constrained by the computational cost which increases by adding more neurons.

Heaton (2008) suggests that the number of neurons be between the size of the input and output layers and recommends that the number of hidden neurons be less than twice the size of the input layer. In this research we considered five parameters at the input layer and ten parameters at the output layer (shown in Figure 4-9). Therefore, we built the neural network with eight neurons in the hidden layer.

We used Matlab to train the neural network. We used 75% of the whole data set (225,000 samples randomly chosen) for training, and 15% (45,000 samples) for validation. We also used 10% (30,000 samples) for testing the network performance by Matlab software.

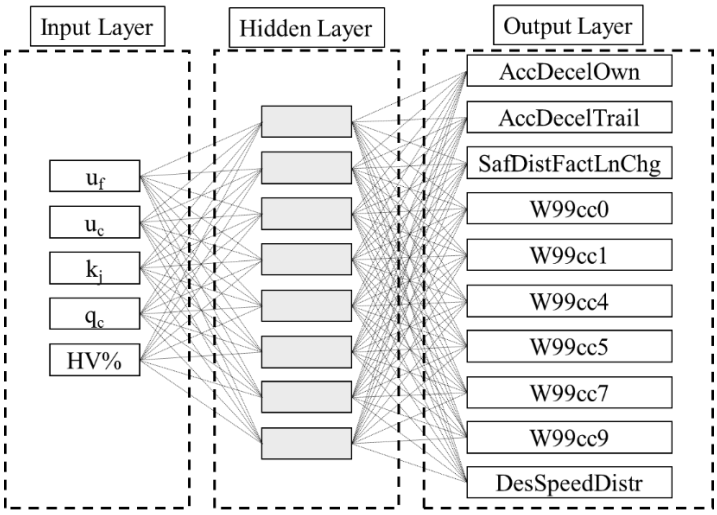

Figure 4-9- Neural Network Diagram

There are different training algorithms that can be implemented when a neural network is built. Matlab software recommends *Bayesian Regularization* algorithm for large networks. We also tested Levenberg-Marquardt algorithm; however, the result of the *Bayesian Regularization* algorithm was

more promising. The characteristics of the built neural network, in terms of the mean squared error (MSE) and R^2 are shown in Table 4-7.

Table 4-7-Neural Network Characteristics

	MSE	R^2
Training	0.54	0.98
Testing	0.53	0.98

The neural network provides a function that if the traffic flow characteristics are given as an input, then the neural network outputs the values that are to be used for the VISSIM input parameters:

$$Y = NN(X) \tag{4-6}$$

Where: Y is the traffic microsimulation input parameters; X is the traffic flow parameters shown in Figure 4-9 at output and input layers respectively; and NN is the built neural network.

It should be noted that there might be more than one unique set of microsimulation input parameters that can simulate a traffic flow with some specific characteristics, but the developed NN model gives only one set of input parameters. The users should be aware this notion when they implement the NN model developed in this work for some works like safety analysis where the value of some microsimulation input parameters have a considerable impact on the safety surrogates.

4.5. Model Validation

Validation of the developed model is carried out by selecting a set of desired traffic stream parameters; providing these as inputs to the developed neural network model which estimates the values to be used for the VISSIM model input parameters. These parameters are used within the simulation model to simulate a variety of traffic conditions. Then Van Aerde's macroscopic speed-flow-density relationship is calibrated to the simulated data to determine the associated traffic stream parameters. Finally, these traffic flow parameters are compared back to the original set of desired traffic stream parameters. We repeat this process for a large sample of desired traffic stream parameters. This entire procedure is shown in Figure 4-10.

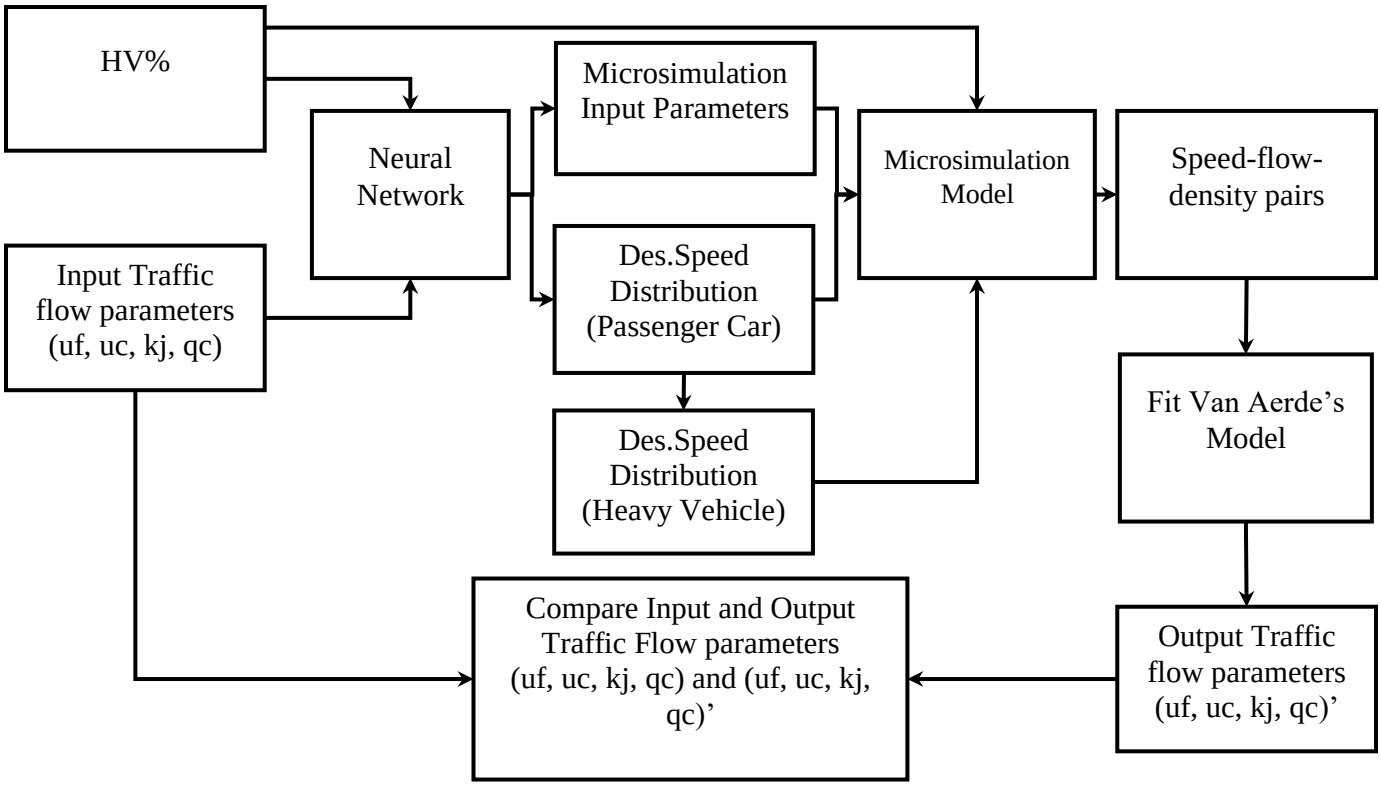

Figure 4-10- Validation Process

To generate random samples of traffic flow parameters, first we checked whether or not these parameters are correlated. We calculated the coefficient of correlation between the traffic flow parameters obtained from fitting Van Aerde's model on the 300,000 samples used in building the neural network. We noticed that the free-flow speed and speed-at-capacity values were correlated; however, significant correlations between other parameters were not found. The coefficients of correlation values are shown in Table 4-8.

Table 4-8-Coefficient of Correlation of Traffic Flow Parameters

	u_f	u_c	k_j	q_c	hv%
u_f	1.00	0.51	-0.02	0.04	-0.01
u_c	0.51	1.00	-0.01	0.20	-0.16
k_j	-0.02	-0.01	1.00	-0.06	-0.18
q_c	0.04	0.20	-0.06	1.00	-0.10
hv%	-0.01	-0.16	-0.18	-0.10	1.00

Therefore, 5000 random samples were generated for u_f, k_j, q_c, and the ratio of heavy vehicles (hv%) based on their range in the outputs of 300,000 simulation runs. We used LHS technique to generate random samples. Given the correlations that exists, the values for u_c were computed as a function of u_f. We calibrated the linear regression model shown in Equation (4-7) using the outputs of the 300,000 simulation runs.

$$u_c = 38.2 + 0.31u_f \quad (4\text{-}7)$$

We applied 5,000 samples of the desired traffic flow parameters (u_f, u_c, k_j, q_c) as input into our neural network. The output of the neural network was the microsimulation input parameters as well as the desired speed distributions of passenger cars.

The heavy vehicle DSD's were computed based on Equation (4-5). We performed the simulation runs using the following input parameters for each of the 5000 random samples:

1- VISSIM input parameters (outputs of the neural network)
2- Passenger car DSD's (output of the neural network)
3- Heavy vehicle DSD's (computed using Equation (4-5))
4- Heavy vehicle ratio (hv%) (sampled randomly along with 5000 samples of u_f, u_c, k_j, and q_c)

Van Aerde's model was calibrated to the 5-minute aggregated speed-flow-density points obtained from the simulations to obtain the output traffic flow parameters (u_f, u_c, k_j, q_c)'. We call this set of traffic stream parameters the "simulated" values. To assess the quality of the proposed neural network model we calibrated a linear regression model as

$$X_{sim} = A \cdot X_{des} + B \quad (4\text{-}8)$$

where X_{des} is the desired value of parameter X , and X_{sim} is its simulated value. The A and B values as well as R-square and root-mean-square errors (RMSE) of the fitted curve are shown in Table 4-9 for all four traffic flow parameters.

Table 4-9- Regression Model Specifications of Input and Output Traffic Flow Parameters

Traffic Flow Parameter	A	B	R^2	RMSE
u_f (kph)	0.93	6.74	0.98	2.13
u_c (kph)	1.08	-5.88	0.66	3.91
k_j (veh/lane-km)	0.77	28.05	0.89	6.84
q_c (vphpl)	0.88	199.1	0.94	113.40

Also, the fitted curves are shown in Figure 4-11(a) to Figure 4-11(d). The results shown in Table 4-9 and Figure 4-11 confirm that the neural network performs well for free flow speed and speed-at-capacity, but performs less well for higher values of the jam density and the capacity. As a result, we decided to consider upper bounds for the jam density and capacity parameters. Based on Figure 4-11(c) and Figure 4-11(d) the upper bound of the jam density was considered to be 150 vehicles/lane-km and the upper bound of the capacity was set to 2400 vphpl. Consequently, the model would not be valid beyond these upper bounds. Applying these limits resulted in removing 2,088 points out of the 5,000 samples that we generated for the validation process. We again developed the relationship between desired and simulated values of traffic flow parameters using the Equation (4-8). The characteristics of the newly calibrated regression models (shown in Table 4-10) confirm the improvements in estimating all traffic flow parameters.

Table 4-10- Regression Model Specifications of Input and Output Traffic flow Parameters (Bounded Model)

Traffic Flow Parameter	A	B	R^2	RMSE
u_f (kph)	0.93	6.56	0.98	2.07
u_c (kph)	1.04	-3.61	0.69	3.51
k_j (veh/lane-km)	0.90	12.91	0.94	4.04
q_c (vphpl)	1.01	-4.51	0.97	65.42

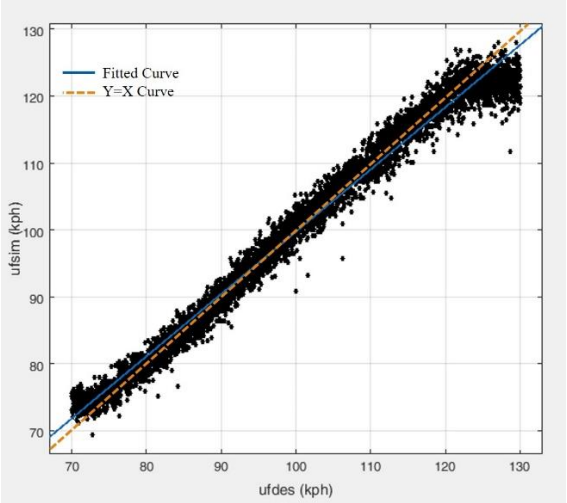

(a)

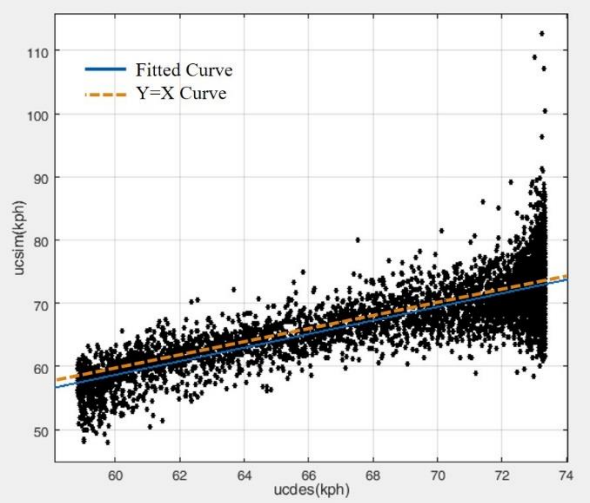

(b)

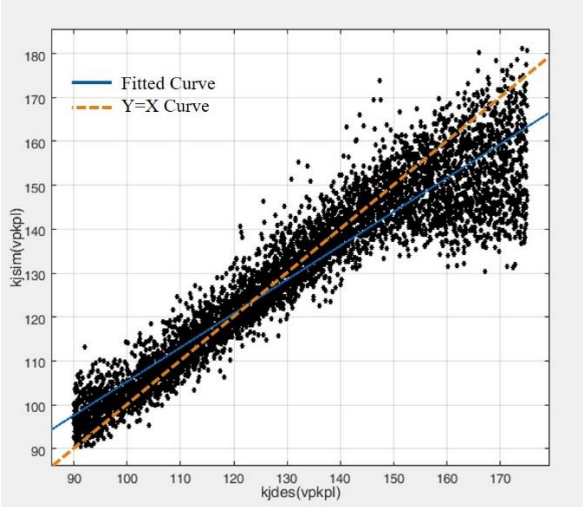

(c)

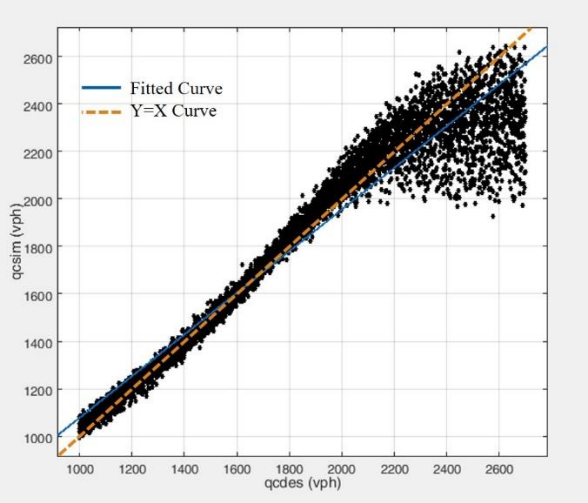

(d)

Figure 4-11-Desired vs. Simulated values of traffic flow parameters

The bounded model shows significant improvements in some parameters. The slope of the fitted line for jam density changed from 0.77 to 0.90, R-squared increased from 0.89 to 0.94, and the root-mean-square error decreased by 40%. The fitted line of the capacity also shows significant improvements. The slope changed from 0.88 to 1.01, the intercept changed from 199.10 to -4.5, and the root-mean-square error decreased by 42%. The bounded model also shows some improvement for the free-flow speed and the speed-at-capacity; however, these improvements are not very significant.

Figure 4-12 (a) to (d) illustrates the fitted curve of the regression model for the bounded model in which we limited the upper bound of the jam density and capacity to 150 vehicles/lane-km and 2400 vph respectively.

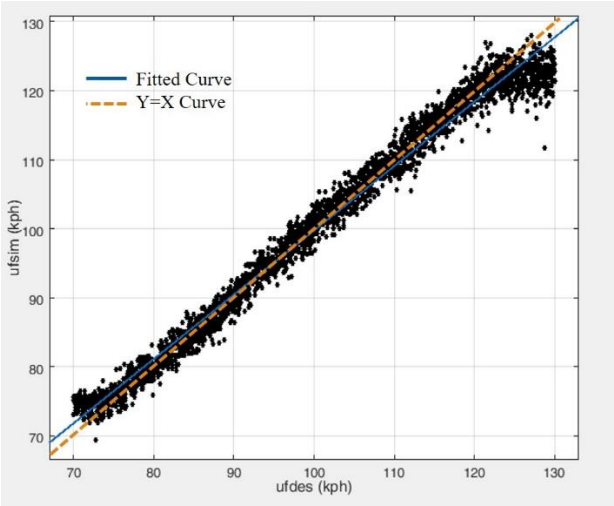

(a)

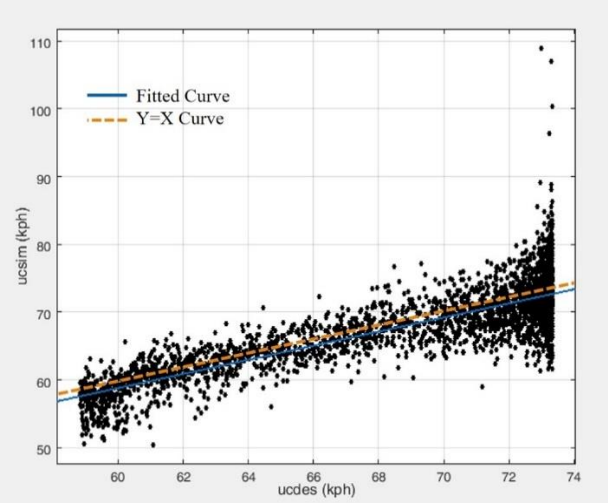

(b)

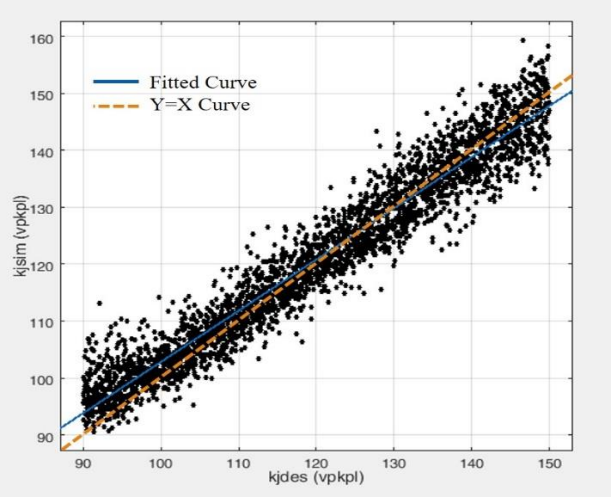

(c)

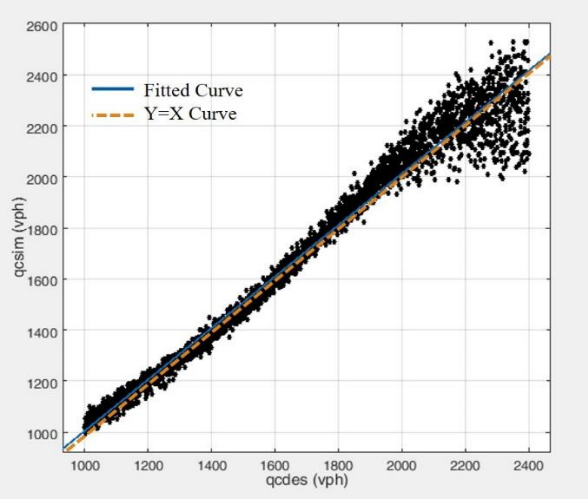

(d)

Figure 4-12- Desired vs. Simulated values of traffic flow parameters (bounded model)

To make the result of this research more applicable for practitioners, a web-based software has been developed for implementation of the models described in this chapter. The traffic flow parameters (u_f, u_c, k_j, q_c) are the inputs to the software program. The program estimates the VISSIM parameter values

using the neural network model developed in this work. These VISSIM parameters can be used to simulate a traffic stream having the characteristics defined by the traffic flow parameters which were the input to this program. The software will be accessible at *http://VISSIM.waterlootraffic.com*.

4.6. Application

We obtained loop detector and weather data from the Minnesota Department of Transportation (Minnesota department of transportation (MnDOT).) for the year 2014 for a section of I-694 in Twin Cities, Minnesota (detector station located between Rice street and Victoria St. N.)

We selected three weather categories (listed in Table 4-11) and assuming the jam density is 100 vpkpl we calibrated Van Aerde's model to estimate the three remaining traffic flow parameters (i.e. u_f, u_c, and q_c). The estimated traffic flow parameters are shown in Table 4-11.

Table 4-11-Selected Weather Categories and Estimating Traffic Stream Characteristics (Field data)

ID	Road Surface	Precipitation Type	Diurnality	u_f (kph)	u_c (kph)	q_c (vphpl)
1	Ice	None	Day	118	74.1	1674
2	Dry	Snow	Night	111.2	61.3	2198
3	Wet	Snow	Night	86.5	62.2	1206

Then, we used the neural network model developed in this chapter to estimate the values for the input parameters of the VISSIM microsimulation model. We assumed 10% heavy vehicles in the traffic stream. The estimated values of the VISSIM input parameters are shown in Table 4-12. These are the parameters that should be used to simulate each of the three weather categories for the two-lane freeway section. The parameters P1 to P9 were introduced in Table 4-4.

Table 4-12-VISSIM Input Parameters Estimated by the Neural Network

ID	P1	P2	P3	P4	P5	P6	P7	P8	P9	DSD (pc)	DSD (hv)
1	-1.752	-1.746	0.503	4.366	1.406	-0.51	0.47	0.47	1.74	PC126	HV105
2	-1.748	-1.737	0.774	3.905	0.693	-0.49	0.53	0.60	1.71	PC112	HV105
3	-1.748	-1.751	0.513	4.639	2.345	-0.50	0.47	0.47	1.75	PC92	Hv92

To check if our neural network model has provided appropriate values for the VISSIM input parameters, we simulated the study area under each of the three weather conditions in the VISSIM software using the input parameters shown in Table 4-12.

Finally, we calibrated Van Aerde's model to the output obtained from each simulated weather category (Table 4-13). We have also shown the absolute relative error (ARE) of the simulated traffic parameters in the same table. These results show that the differences between the traffic

stream characteristics estimated from the field data and from the simulation are very small and confirms that the developed neural network model performs well.

Table 4-13-Simulated Traffic Parameters and Their Absolute Relative error (%)

Road Surface	Precipitation Type	Diurnality	u_f (kph)		u_c (kph)		q_c (vphpl)	
			Est.	ARE (%)	Est.	ARE (%)	Est.	ARE (%)
Icy	None	Day	115.9	1.8%	72.3	2.4%	1688	0.8%
Dry	Snow	Night	107.6	3.2%	65.3	6.5%	2055	6.5%
Wet	Snow	Night	82.3	4.9%	61.3	1.4%	1198	0.7%

4.7. Conclusions

This chapter presents a method by which VISSIM input parameter values can be determined to achieve a freeway traffic stream with any (realistic) characteristics. This ability has many applications for microsimulation model applications, including the modeling of inclement weather. Using local meteorological and traffic data, it is possible to determine the traffic stream characteristics associated with specific weather conditions. Then the model proposed in this chapter can be used to determine the VISSIM input parameters that are best able to produce a traffic stream with the characteristics associated with weather category.

The model was validated using 5000 randomly generated samples. Those samples were different from the ones used for training the neural network. In validation process we noticed our model did perform well in most of the range of parameters but not in very high jam density and capacity values. Considering that those high values are not usually achievable in reality, we revised the upper boundaries for the capacity and jam density range of the developed model (essentially restricting the model to realistic traffic stream characteristics). The finalized model is shown to perform well for the range of realistic traffic flow parameters of freeways with two lanes at each directions and is simple to use.

Chapter 5

Estimating the Cost of Travel Time (Un)Reliability

5.1. Introduction

Traditionally, most evaluations of road improvements quantify benefits on the basis of the changes in the average travel time (on some "average" day) and the value of time. However, increasingly, there is interest not only in the change in the average travel time, but also about the day-to-day variability of the route travel time. This interest stems from the belief that there is a cost associated with unreliability (i.e. the experienced travel time differs from the anticipated travel time) that is an addition to the actual travel time cost (i.e. travel time multiplied by the value of time) (Warffemius, 2013). This cost is associated with either the wasted time when people arrive earlier than desired or possible penalties when they are late.

In the context of public transit systems, the cost of travel time (un)reliability is generally determined as a function of the deviation between the experienced travel time and the scheduled travel time (Kittelson & Associates et al., 2013). In this context, the transit schedule informs travelers and determines the time that they should expect the trip to take. For personal auto modes, a relatively large body of work has appeared in the literature over the past few years focused on travel time reliability in which the travel time reliability has been quantified as the deviation between the experienced travel time and some expected travel time. In this work, the expected travel time is typically determined as some measure of central tendency of the travel time distribution. In this thesis, we use the analogy to

the public transit, and we hypothesize that the travel time reliability cost for auto users is a function of the deviation of the experienced travel time and the *anticipated* travel time. We use the term *anticipated* rather than *expected* because in mathematical terms, *expected* is equivalent to the average or mean of the distribution. We do not wish to restrict the value of the anticipated travel time to be equal to the mean of the distribution.There is a lack of knowledge about how travelers determine their anticipated travel time and there remains a lack of consensus about how to define the anticipated travel time for determining the monetary impact of unreliability.

This research examines these two issues. In particular, we are interested in (1) determining if/how the anticipated travel time is related to the distribution of travel times experienced during previous days; and (2) the extent to which unusually long travel times influence anticipated travel times.

5.2. Literature Review

Mahmassani and Chang (1985) investigated the process by which travelers' form their "anticipated" travel time using a simulation approach. They modeled home-to-work trips on a nine-mile hypothetical four-lane highway (two lanes at each direction) and asked 100 participants with a restricted work starting time to submit their preferred arrival time once at the beginning of the survey, and then their preferred departure time every "day" during the survey. These departure times were the input to a simulation model in which every participant was assumed to represent 20 drivers in the simulated traffic stream. With the variation of the departure times, the traffic flow was different at a specific time from "day" to "day" during the simulation and thereby, the simulated travel time by each traveler was different. As an output of the simulation model, the participants' arrival time (considered as actual arrival times) were reported to the attendees at the end of each day. Then participants were asked to submit the departure time of day $i+1$ given they were aware of the actual arrival time of day i. This process continued for 24 days.

The study showed that the reported departure time of each respondent did not change except during the first few days suggesting that drivers require only a small sample of experience to form their anticipation for future trips. However, the study did not show how the anticipated travel time is related to the distribution of experienced travel time. Furthermore, the day-to-day variations in travel time were relatively small so the impact of unusually long travel times was not examined.

In another study, Fujii and Kitamura (2000) investigated the impact of information and actual travel time of real drivers and real trips on the anticipated travel time using stated preference survey during a freeway closure event in Osaka, Japan in which participants submitted their anticipated travel time for the next day after they performed their travel each day. The route was new to travelers since they previously used to take the closed freeway to reach to their destination. Contrary to the work by Mahmassani and Chang (1985) which assumed that the travelers were exposed to no source of information except their driving experience, Fujii and Kitamura considered different media as the sources of information including mass media, word of mouth, traffic information systems based on telephone, and the actual experienced travel times by the travelers. Similar to the work of Mahmassani and Chang (1985), Fujii and Kitamura computed the anticipated travel time based on the departure time and anticipated arrival time of the respondents. Their study focused on examining the influence that sources of travel time information have on anticipated travel times, particularly for drivers who were unfamiliar with the route (i.e. limited experience from previous trips). The sample size of this study was relatively small (complete data were available from 41 respondents) and similar to like the previous study the relationship between the anticipated travel time and experienced travel time distribution was not discussed.

Avineri and Prashker (2006) studied the impact of travel time information on route choice. They investigated whether or not the existence of travel time information results in better route choice decisions by drivers. They concluded that contrary to common believe, the availability of travel time information does not result in better route choices. They did not study the relationship between the anticipated travel time and the distribution of the experienced travel times.

Do and Kobayashi (2000) statistically examined the Rational Expectations (RE) hypothesis proposed by Muth (1961). The RE hypothesis states that the subjective probability distribution of events coincides with the objective probability distribution as a consequence of people's long-term learning behavior. Do and Kobayashi tested whether the travelers' long-term expected travel time coincides with the mathematical expected value of the 'true' travel times. They performed an in-house experiment with sixty participants who provided anticipated travel time and route choice for the next day over a period of 30 consecutive days. They concluded that the RE hypothesis cannot be rejected

suggesting that anticipated travel times are equivalent to the mean of the travel times experienced on previous trips.

There has been very little work conducted to understand the relationship between the distribution of experienced travel times and anticipated travel time for a future trip and the work that has been done suggests that anticipated travel times are equivalent to the mean of the experienced travel times.

The limitation of this former work is that the influence of unusually long travel times was not explicitly studied. Unusually long travel times may occur as a result of inclement weather, special events, incidents, or temporary lane closures. The mean is highly sensitive to these extreme values. We hypothesize that drivers discount the impact of unusually long travel time with respect to determining their anticipated travel time and therefore do not form their anticipated travel time as the mean of all previously experienced travel times. This distinction is important when attempting to quantify the impact of travel time reliability (e.g. the cost of unreliability). It is generally accepted that travel time reliability is quantified in terms of the distribution of travel times (or some point estimates from this distribution). If the cost of travel time is related to the difference between the experienced travel time and the anticipated travel time, then the manner in which the anticipated travel time is determined is important. Furthermore, if the anticipated travel time is considered to be equivalent to the mean of the experienced travel times, then unusually long travel times have the potential to dramatically increase the cost associated with unreliability.

Thus this research attempts to determine:

1. The relationship between the distribution of experienced travel times and anticipated travel time for a future trip; and
2. The influence that unusually long travel times have on the anticipated travel time.

5.3. Problem Formulation

Assume that a commuter i drives from origin o to destination d using route r. Then $t_{o,d,r,k,j,i}$ is the travel time experienced on day j when departing the origin during time interval k. We define τ_{odr} as the distribution of travel times experienced by a number of drivers across different days making trips between origin o and destination d using route r and departing in the same time interval. We define the

"anticipated" travel time as the time a traveler forecasts for their next trip (i.e. for the next day) and assume that this anticipation is based on travel times that have been experienced in the past for the same trip (i.e. same origin, destination, route, and departure time). Then $\tilde{\tau}_{odr}$ is the average of the anticipated travel times from a number of drivers (for the same trip origin, destination, route and departure time).

We make two hypotheses:

1. $\tilde{\tau}_{odr}$is some function of the distribution of experienced travel times (i.e. $\tilde{\tau}_{odr} = f_1(\tau_{odr})$)
2. Unusually long travel times may occur as a result of unscheduled or unexpected events (e.g. adverse weather, collisions, etc.). It is hypothesized that travelers discount the influence of these travel times when forming their anticipated travel times because they believe that these travel times are unusual (e.g. rare). We define $\hat{\tau}_{odr}$ as a travel time threshold. Experienced travel times greater than $\hat{\tau}_{odr}$ are discounted (or ignored) in terms of their influence on the anticipated travel time.

Table 5-1 illustrates $\tilde{\tau}_{odr}$and $\hat{\tau}_{odr}$on a hypothetical travel time distribution. The objective of this research is to determine if there is evidence to support these hypotheses and if so, to calibrate values for $\tilde{\tau}_{odr}$ and $\hat{\tau}_{odr}$.

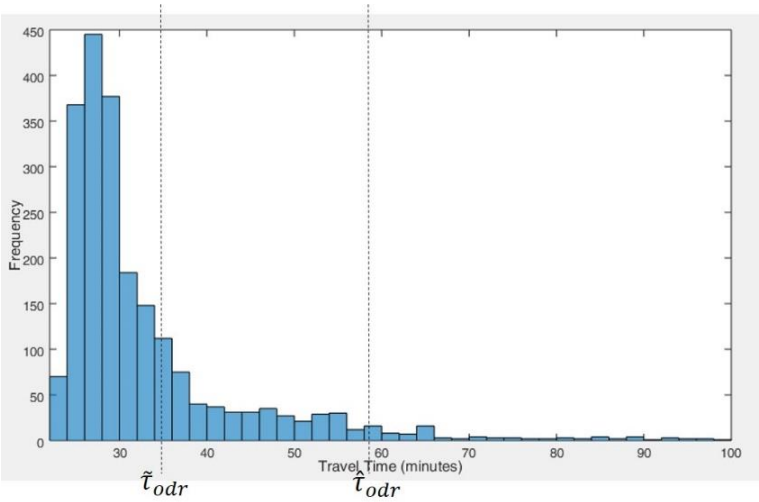

Figure 5-1- Illustrative $\tilde{\tau}_{odr}$ and $\hat{\tau}_{odr}$ on a travel time distribution

5.4. Methodology

A web-based stated preference survey was constructed to address the formulated problem.

Generally, travelers obtain their information of the travel time from different sources including media and previous driving experience. The precision, penetration rate, and the level of access to the traffic information likely varies widely across different media types and different travelers. To avoid the heterogeneity caused by drivers with access to different traveler information, we assume the travel time information is solely available from previous experience travelling the same trip.

We divide the methodology into two parts. First we characterize the relationship between the anticipated travel time and travel time distribution when we assume that drivers consider all experienced travel times (i.e. we do not assume that they discount the impact of unusually long travel time). Then we describe the method we followed to explore the influence that unusually long travel times have on the anticipated travel time. The survey was distributed through Canadian Institute of Transportation Engineers (CITE) mailing list and also through another mailing list of people with post-secondary education. The survey was distributed to approximately 3000 people and obtained a response rate of just over 10%. Most of the respondents had more than 5 years of driving experience as illustrated in Figure 5-2.

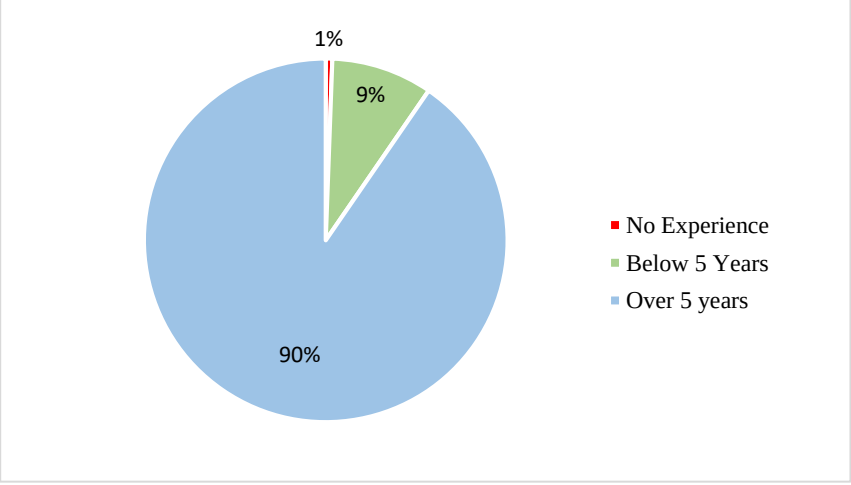

Figure 5-2 - Respondents' driving experience

5.4.1. Model 1: Anticipated Travel Time

The first portion of the survey consisted of a hypothetical scenario in which respondents were presented with a set of trip travel times experienced over the past 6 weeks and then the respondent was asked to forecast the travel time for the same trip in the future.

There were a number of issues that we attempted to avoid when we designed the survey.

The first is the *bias of personality*. Construal-level theory suggests that when there is a temporal, social, spatial, and/or hypothetical distance between people and the object or event they are thinking about, then the thinking becomes less concrete and more abstract (Trope and Liberman, 2010). In our survey there was a probability that if we framed our question in a context and asked respondents about a decision about themselves in that context, they would answer the question considering other contexts arising from their personal experiences, emotions, constraints, etc. (i.e. influences external to the scenario presented in the survey question). Therefore, to avoid this bias, we asked the respondents to make a decision which would impact a third person, not themselves.

The second is *Gambler's fallacy*. There is a misconception when people try to decide between some independent events. They believe that when an event occurs, the chance of the same event occurring in the future decreases even though the events are independent (Hahn, 2014). To avoid this problem, instead of asking survey respondents to indicate their anticipated travel time multiple times (e.g. after each simulated day) we elected to present the respondents with a set of historical (experienced) travel times and then ask them to provide a single anticipated travel time.

The part of the survey that aims to find the relationship between the anticipated travel time and the experienced travel time distribution consisted of two sections:

1. First, the respondents were presented with a hypothetical scenario
2. Then, they were asked to answer a question based on the story that was just narrated

The scenario, which was the same for all respondents, described a 50km home-to-work commuter trip (traversing mainly a freeway) and introduced a hypothetical distribution of experienced travel times. We generated the individual travel times from a Beta distribution (Weifeng et al., 2013) and

assumed a minimum travel time of 30 minutes. The parameters of the hypothetical travel time distribution are shown in Table 5-1.

Table 5-1-Travel Time Distribution Parameters

Parameter	Value
$\boldsymbol{\alpha_1}$	1.3
$\boldsymbol{\alpha_2}$	4.95
$\boldsymbol{a}$	30
$\boldsymbol{b}$	89

The frequency diagram of the distribution (10,000 samples) is illustrated in Figure 5-3.

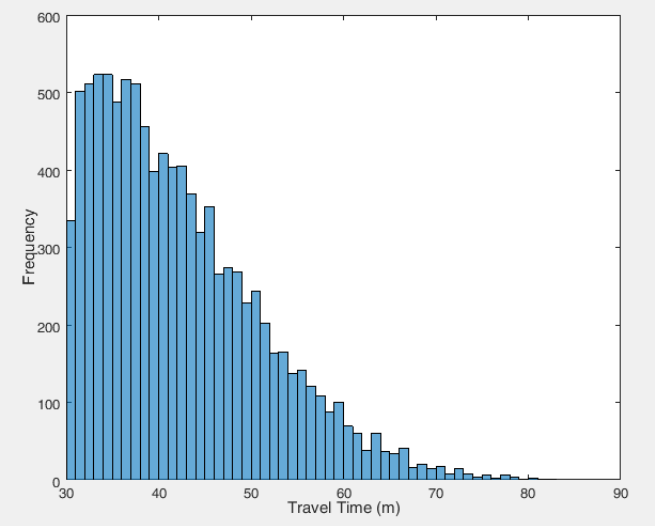

Figure 5-3- Underlying travel time distribution

Then we sampled from the distribution using Latin Hypercube Sampling to obtain travel times for 30 trips (corresponding to 6 weeks of weekday commuting home to work trips) from the generated distribution. The travel times are shown in Figure 5-4. The scenario narrative presented in the survey is as follows:

> *"Six weeks ago you and your partner moved to a large city to start new jobs. Each weekday you have to drop your partner off at their place of work at 8:00 AM and then drive to your work. The distance from your partner's place of work to your place of work is 50 km. There is only one practical route to take and it is mostly on a*

freeway. If there are no delays, then the fastest you can make the trip is 30 minutes. However, travel times can be longer because of traffic congestion, construction, severe weather, special events, or collisions.

One of your work colleagues has just moved into a house near your partner's work and will be driving the same route that you take and will also be departing at 8:00 AM. They have asked you how long they should plan for the drive to take given that they don't want to be too early or too late at work."

After reading this narrative, the survey respondent was presented with each week of travel times on a separate (sequential) webpage. There was no restriction on how long respondents could view each graph and respondents could move to previous or following pages in the survey at will. The mean travel time of the samples was 42.53 with the 95% confidence limits of ±3.37 minutes. The minimum and maximum travel time were 30 minutes and 71 minutes respectively.

Then, we proposed the following question to the respondents:

"Now that you have had a chance to review the travel times you experienced driving to work over the past 6 weeks, let me remind you of the question.

One of your work colleagues has just moved into a house near your partner's work and will be driving the same route that you take and will also be starting their trip at the same time of day as you do. They have asked you how long they should plan for the drive to take (in minutes) given that they don't want to be too early or too late at work.

Based on your experience over these past 6 weeks of driving this route, what is your estimate of the trip travel time (in minutes)?"

The respondents could choose an integer value between 30 and 71 minutes for their response from a dropdown menu.

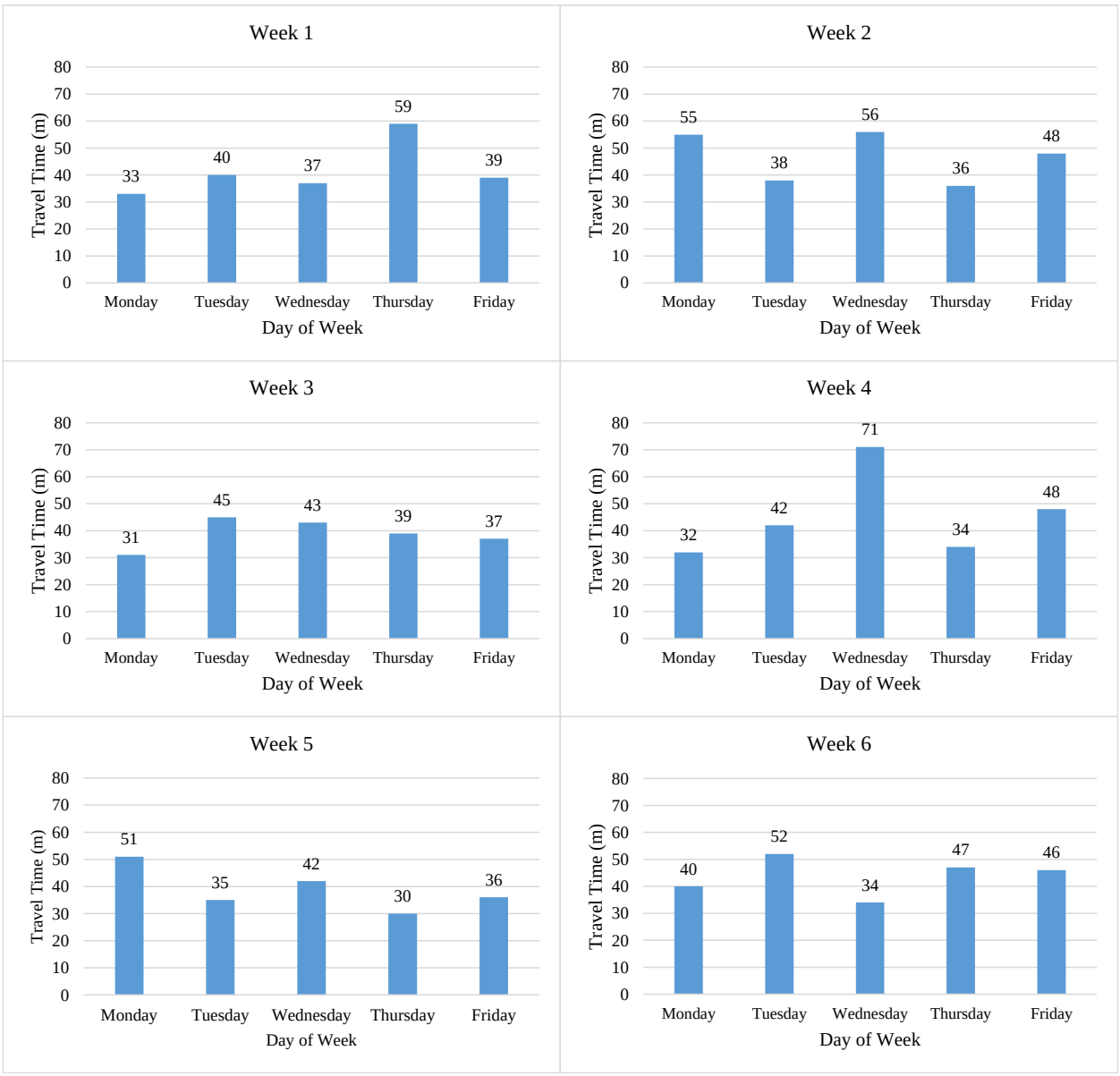

Figure 5-4- Weekday hypothetical travel times

5.4.2. Responses

The survey was distributed to more than three thousand potential respondents – most of them with post-secondary degrees, driving experience, and associated with the transportation engineering profession. 303 responses were received, cleared, and analyzed.

The average anticipated travel time was 46.2 minutes and the standard deviation was 5.6 minutes. Also, the confidence interval of the anticipated travel time was (45.6, 46.8) at the 95% confidence level.

As a first step, we examined whether or not the anticipated travel time corresponds to the mean of the distribution of experienced travel times (i.e. supports the Rational Expectations hypothesis). A statistical comparison (T-test) between the mean of the 30 experienced travel times and the mean anticipated travel time at the 95% of confidence level shows that the p-value of the means difference is 0.02 which is smaller than 0.05; therefore, the difference between the means is significant at the 95% confidence level. This suggests that the respondent's anticipated travel time is <u>not</u> equal to the average experienced travel time and therefore does not support the Rational Expectations hypothesis.

We then explored if the anticipated travel time corresponds to some percentile of the distribution of experienced travel times. Figure 5-5 shows the CDF of the population of the trip travel times and the CDF of the sample of 30 trip travel times provided to the survey respondents. The solid black vertical line is the average anticipated travel time obtained from the 303 respondents. The dashed black vertical lines represent the 95% confidence interval for the mean anticipated travel time. From this figure, we can observe that the mean anticipated travel time corresponds to the 70th percentile of the experienced travel times. Furthermore, using the 95 percent confidence limits of the anticipated travel time we can observe that the corresponding 95 percent confidence limits of the percentile of the experienced travel time distribution ranges from 67th to 72nd percentile which corresponds to 45.8 minutes and 47.3 minutes respectively. Therefore:

$$\tilde{\tau}_{odr} = 70th\ percentile\ of\ (\tau_{odr}) \quad \textbf{(5-1)}$$

where, $\tilde{\tau}_{odr}$ and τ_{odr} were defined earlier.

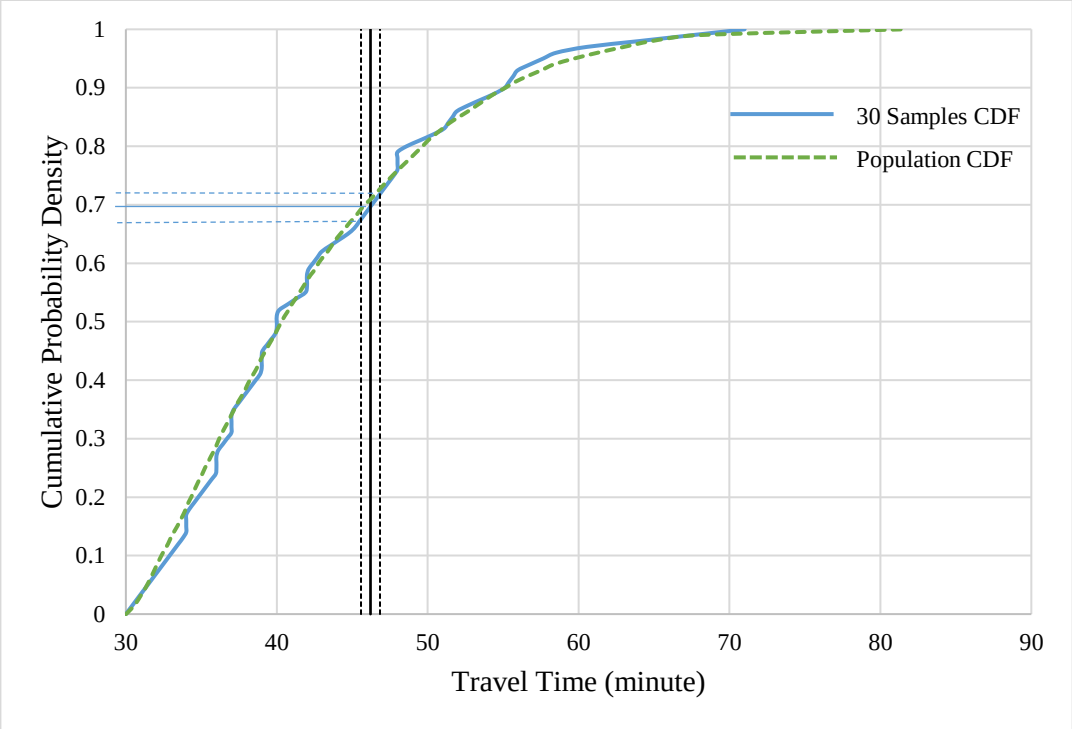

Figure 5-5- Cumulative probability distribution of experienced travel times

5.4.3. Model 2: Anticipated Travel Time considering an Extreme Travel Time Threshold

The second objective was to discover whether or not travelers discount the impact of unusually long travel times. Again we used the stated preference survey method and combined the questions for this part of the survey with the questionnaire that we used in the anticipated travel time survey.

Unusually long trips are considered as an indicator of unreliability of travel. Therefore, the related body of the literature can be found in the research associated with measures of travel time reliability. Several metrics have been proposed to measure travel time reliability (TTR). NCHRP project 3-68 "*Guide to freeway performance measurement*" introduced four measures of TTR including: buffer index, planning time index, percent of trips with space mean speed ≤ 50 mph and percent of trips with space mean speed ≤ 30 mph (Margiotta et al., 2006).

Van Lint et al. categorized TTR metrics in 5 groups: 1) statistical range methods; 2) buffer time methods; 3) tardy trip measures; 4) probabilistic measures; and 5) skew-width methods (Van Lint et al., 2008).

SHRP2 L08 project "I*ncorporating travel time reliability into the highway capacity manual"* has categorized TTR indices into two groups: 1) core measures; and 2) supplemental measures. Core measures include planning time index, 80th percentile travel time index, semi-standard deviation, and failure/on-time measures while standard deviation and misery index are categorized as supplemental measures (Kittelson and Associates, 2012).

The SHRP2 L03 project recommends several reliability metrics as well. Comparing to SHRP2 L08, it confirms using planning time index, 80th percentile travel time index, failure/on-time measures and misery index. It excludes standard deviation and semi-standard deviation while including buffer time index and skew statistics (Cambridge Systematics, 2013).

Jin and McLeod (2013) recommend using 90th percentile travel time index and using 40 mph as threshold for on-time arrival measure. Table 5-2 indicates a list of TTR metrics with their definitions.

Table 5-2- Travel Time Reliability Metrics (Jin and McLeod, 2013)

Reliability Performance Metrics	**Definition**	**Units**
Buffer Index (BI)	The difference between the 95th percentile travel time and the average travel time, normalized by the average travel time	Percent
Failure/on-time measures	Percent of trips with travel times <: $(1.1 \times Median\ travel\ time)$; and $(1.25 \times Median\ travel\ time)$ Percent of trips with space mean speed <: (50 mph, 45 mph, 40 mph, 30 mph)	Percent
Planning time index	95th percentile travel time	None
80th percentile travel time index	Self-explanatory	None
90th percentile travel time index	Self-explanatory	None
Skew statistics	The ratio of (90th percentile travel time minus the median) divided by (the median minus the 10th percentile)	None
Misery index	The average of the highest five percent of travel times divided by the free-flow travel time	None
Semi standard deviation	The standard deviation of travel time pegged to the free flow rather than the mean travel time	None

Based on the measures suggested for the travel time reliability in the literature, we considered two methods for mapping $\hat{\tau}_{odr}$ to the travel time distribution:

a) Threshold as a multiple of free flow travel time
b) Threshold as a percentile of the travel time distribution

Therefore, we proposed two questions each of which was associated with one of these two methods.

5.4.4. Threshold as a multiple of free flow travel time

This survey question was:

> *"In the previous question you were asked to tell your work colleague how long they should expect the drive to work to take based on your experience driving that same route.*
>
> *As you observed in the previous question, trip travel times can vary from one day to the next as a result of collisions, construction, temporary road or lane closures, special events, severe weather, etc.*
>
> *When determining the time that the trip should be expected to take, some people might ignore some of the longest travel times that were experienced because those long travel times were caused by unusual events.*
>
> *Assume that you identify unusually long travel times as some multiplier of the fastest travel time. For example, if the fastest travel time is 30 minutes, and you identify the multiplier as 1.4, then any travel time greater than 30 × 1.4 = 42 minutes would be considered unusually long and you would ignore this trip experience when making your estimate of how long your colleague should plan for the trip to take.*
>
> *Select from the list below the multiplier that best represents the travel times which you would consider as unusually long and would ignore when estimating the travel time for a future trip. For each multiplier, the travel time listed in parentheses is relative to a fastest travel time of 30 minutes."*

Respondents had a variety of choices ranging from 1.4 to 3.0 (with the steps of 0.2). We collected 302 responses to this question. The response mean was 1.83±0.03 at the confidence level of 95%. Also, the standard deviation was 0.30.

5.4.5. Threshold as a percentile of the travel time distribution

Through some pilot survey question testing, we determined that asking the respondent to identify a specific percentile of the experienced travel time was not well understood. Instead we asked the respondents to report the number of longest experienced trips they would ignore when they plan their day-to-day trips. Following, is the question from the survey:

> *"In the previous question, you identified unusually long travel times (i.e. those that you ignored when estimating the expected travel time for a next trip) as those which exceeded some multiple of the fastest travel time. For example, you may have indicated that you ignore the trips that take at least 1.8 times longer than the fastest trip.*
>
> *Another approach is to simply ignore some number of the longest travel times experienced. Using this approach, and assuming 20 work days in the month, select from the list below the number of the longest travel times you would ignore when estimating the amount of time your colleague should plan for the trip to take."*

Respondents could select one of the choices listed in the second column of Table 5-3. Each choice corresponds to a specific percentile of the travel time distribution shown in the third column

Table 5-3- Choices in Question Regarding Extreme TT Threshold Based on DTT Percentile

Choice#	Description	DTT Percentile
1	I would consider all of the travel times that I experienced	100%
2	I would ignore the one longest trip out of the past 20 trips	95%
3	I would ignore the two longest trips out of the past 20 trips	90%
4	I would ignore the three longest trips out of the past 20 trips	85%
5	I would ignore the four longest trips out of the past 20 trips	80%
6	I would ignore the five longest trips out of the past 20 trips	75%
7	I would ignore the six longest trips out of the past 20 trips	70%
8	I would ignore the seven longest trips out of the past 20 trips	65%
9	I would ignore the eight longest trips out of the past 20 trips	60%

We received 292 answers to this question. The average response was 2.73±0.17 at the 95% confidence level and the standard deviation of the responses was 1.50.

5.4.6. Choosing the Extreme Travel Time Threshold

The responses to these two methods (*a* and *b*) were examined against the sample of 6 weeks of trip travel times provided to the survey respondents in the first part of the questionnaire. From method *a* we multiple 1.83 (the average obtained from the survey) by the free flow travel time of 30 minutes to obtain a travel time threshold of 54.9 minutes. From method *b* respondents indicated they ignored 2.7 of their 20 longest experienced travel times when they plan their future trips. This corresponds to the 87^{th} percentile of the travel time distribution which corresponds to 52.7 minutes in the considered distribution. Though the two models use different approaches to define unusually long travel times, when applied to the sample distribution of travel times, they provide essentially the same results (Table 5-4).

Table 5-4-Comparison of the Methods *a* and *b*

	Average Response	**Percentile of the given DTT**	**Extreme Travel Time Threshold (minute)**	**Difference**
Method *a*	1.83 (multiplier to the free speed)	89.5%	54.9	4%
Method *b*	2.7 (ignored longest trips)	87%	52.7	

We were also interested in whether or not respondents had a preference for the way in which they considered unusually long travel times. Consequently, a final survey question, as follows, was included in the survey.

> *"The previous two questions considered different ways of defining "unusually" long trip travel times (i.e. those past trips which you ignore when considering how long the same trip would take in the future):*
>
> Question a *identified these unusually long trips as ones for which the travel time exceeded some multiple of the fastest travel time.*

Question b *identified these unusually long trips as a number of the longest trips in the past month.*

Which question (a or b) best describes the way that you consider the impact that unusually long trip travel times have on your estimate of how long the same trip will take in the future?"

298 respondents answered to this question. The results indicate that a small majority (56%) of respondents prefer to define unusually long travel times in terms of some multiple of the free speed travel time (choice *a*) and 44% prefer to define unusually long travel times in terms a percentile of the experienced travel time distribution (choice *b*).

These results suggest that drivers ignore unusually long travel times when computing the anticipated travel time. Consequently, we propose a two stage model for estimating the anticipated travel time. The first stage consists of eliminating unusually long travel times using either model *a* or model *b* to produce a *truncated* distribution of experienced travel time. The second stage consists of selecting the anticipated travel time as a percentile of the truncated experience travel time distribution.

We calibrate the percentile in the same manner as was done for Model 1, but in this case using the truncated distribution. This is shown in Figure 5-6. We can observe that the mean anticipated travel time reported by the survey respondents corresponds to the 80^{th} percentile of the truncated distribution of experienced travel times.

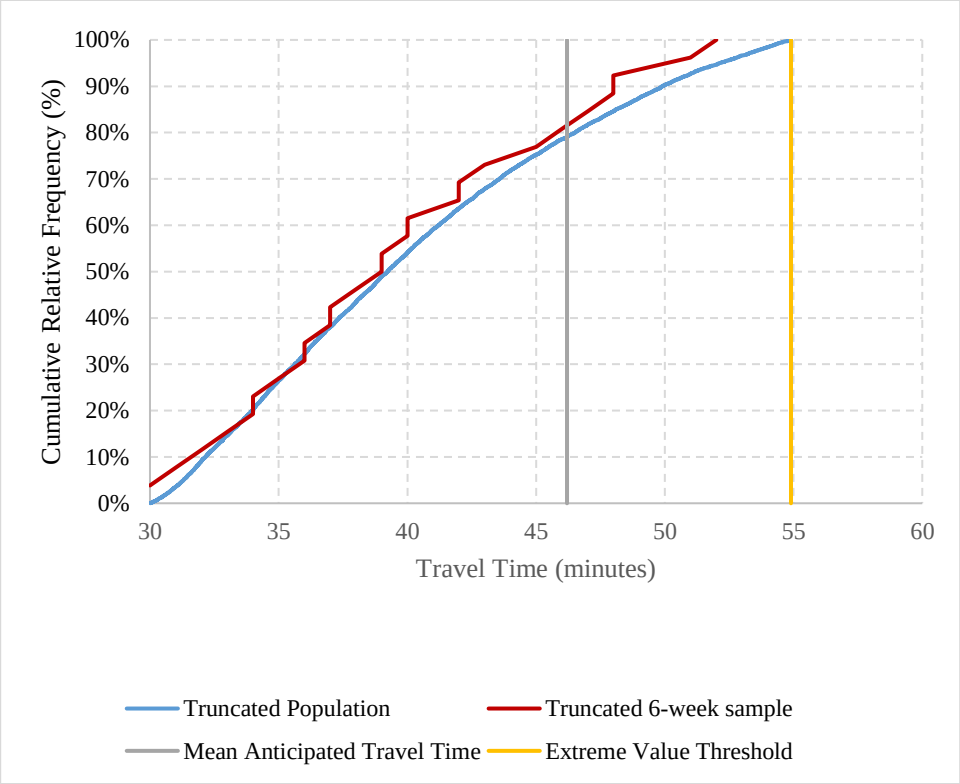

Figure 5-6- Cumulative probability distribution of truncated experienced travel times

5.5. Cost of Travel Time (Un)Reliability

To apply the findings of this chapter to compute the associate cost of travel time (un)reliability, we follow the following steps:

1- We use the above findings to compute: *i*) the anticipated travel time, and *ii*) extreme travel time threshold, based on the travel time distribution.

2- Most of the cost functions developed in the literature to monetize the schedule delay costs, use the concept of "preferred arrival time". Travelers reaching the destination before this time are considered early and travelers reaching their destination after this time would be considered late. In this work, to map the travel time distribution –which defines the aggregate characteristics of trip time of a group of travelers - to the existing cost functions, we assume the preferred arrival time in the existing cost functions as the anticipated travel time in our research, and we label the travel time values:

   a. smaller than the anticipated travel time as "early".

b. between the anticipated travel time and the extreme value threshold as “late”.

c. Larger than the extreme value threshold as “extremely late”.

3- Compute the schedule cost of early trips (i.e. schedule delay early) and late trips (i.e. schedule delay late) using the existing cost functions. VSDE is the value of the schedule delay early and VSDL is the value of schedule delay late. Several research works such as Lam and Small (2001) and Tseng et al.(2005) has estimated values for VSDE and VSDL. The sum of schedule cost of early and late trips is considered as cost of travel time reliability.

4- Note that based on the work done by Tseng et al. (2008) which is supported by the outcomes of the survey performed in this research, we assume that the cost of schedule delay has a maximum value which is equivalent to the schedule delay cost of the extreme threshold travel time. In other words, the schedule delay cost increases while the travel time increases up to the point that the travel time reaches to the extreme travel time threshold. After that the schedule delay cost will not increase anymore. Therefore, the schedule delay cost of the trips which are labeled as “extremely late” will be constant and equivalent to the schedule delay cost at the extreme threshold travel time.

The travel time reliability cost is computed using the following equation:

$$TTR_{cost} = \left[n_1 \cdot \int_{\tau_f}^{\hat{\tau}} |\tau - \tilde{\tau}| \cdot c(\tau) \cdot P(\tau) d\tau \right] + \left[n_2 \cdot \int_{\hat{\tau}}^{\tau_{max}} (\hat{\tau} - \tilde{\tau}) \cdot VSDL \cdot P(\tau) d\tau \right] \qquad (5\text{-}2)$$

where: n_1 is the number of vehicles which travel times are shorter than the extreme travel time threshold and n_2 is the number of vehicles which travel times are longer than the extreme travel time threshold P is the probability density of travel time, and $c(\tau)$ is the cost function defined below. Other parameters were defined previously.

$$c(\tau) = \begin{cases} VSDE\,, & \tau < \tilde{\tau}_{odr} \\ VSDL, & \tilde{\tau}_{odr} < \tau \end{cases} \qquad (5\text{-}3)$$

5.6. Conclusion

In this chapter we have proposed and calibrated two models for estimating the anticipated travel time.

Model 1 assumes that drivers consider all previous trip travel times and suggests that the anticipated travel time is equal to the 70^{th} percentile of the travel time distribution.

Model 2 reflects the hypothesis that drivers ignore unusually long travel times when determining their anticipated travel time. The survey results support this hypothesis. It was found that on average, respondents defined the extreme value threshold as (a) 1.83 times the free speed or (b) the 87^{th} percentile of the travel time distribution. A small majority of the respondents indicated that they found method *a* more intuitive. However, when applied to the 6 weeks of travel time data, both methods provide essentially the same travel time threshold.

We then found that the anticipated travel time corresponds to the 80^{th} percentile of the truncated travel time distribution.

The proposed model is attractive as it is consistent with intuition and the model is less susceptible to extreme values than the Rational Expectation model. It is also as simple to apply as the Rational Expectation model.

The proposed model has been calibrated using stated preference data. Using the existing data set it is not possible to validate the proposed model by confirming that the model also holds true for other distributions of experienced travel times. Consequently, additional validation of this model is needed. One method is that an additional stated preference survey be conducted to ask respondents to indicate their anticipated travel time but to provide the respondents with a set of travel times which reflect a distribution which is different from the one used in this work, but still realistic.

The model can be used along with any existing cost functions to compute the cost of travel time reliability which is an input to the alternative analysis project. As a recommendation for further research we suggest that research be done specifically to investigate the schedule delay costs associated with travel times that exceed the extreme value threshold.

Chapter 6

Demonstrating the methodology: Alternative Analysis

6.1. Introduction

To demonstrate the application of the methods proposed in this research we applied them to a hypothetical problem in which two road improvement alternatives are being compared. The goal is to compute the travel time reliability cost of both alternatives. This cost is an essential part of choosing the preferred alternative. In common practice, the preferred alternative is usually selected taking into account all benefits and costs of a project including the infrastructure cost, environmental cost, user cost, etc. Travel time reliability cost is categorized under the user cost; therefore, it is necessary to evaluate it and to include it within the evaluation of the competing alternatives.

For the purposes of illustrating the methods proposed in this thesis, the alternative analysis in this chapter is done solely on the basis of the travel time and travel time reliability costs; other benefits and costs are not considered in choosing the preferred alternative. Moreover, although the study area is modelled after an actual freeway interchange within the real world, the problem and the alternatives being evaluated are hypothetical.

The evaluation of the two alternatives is conducted carrying out the steps shown in Figure 6-1.

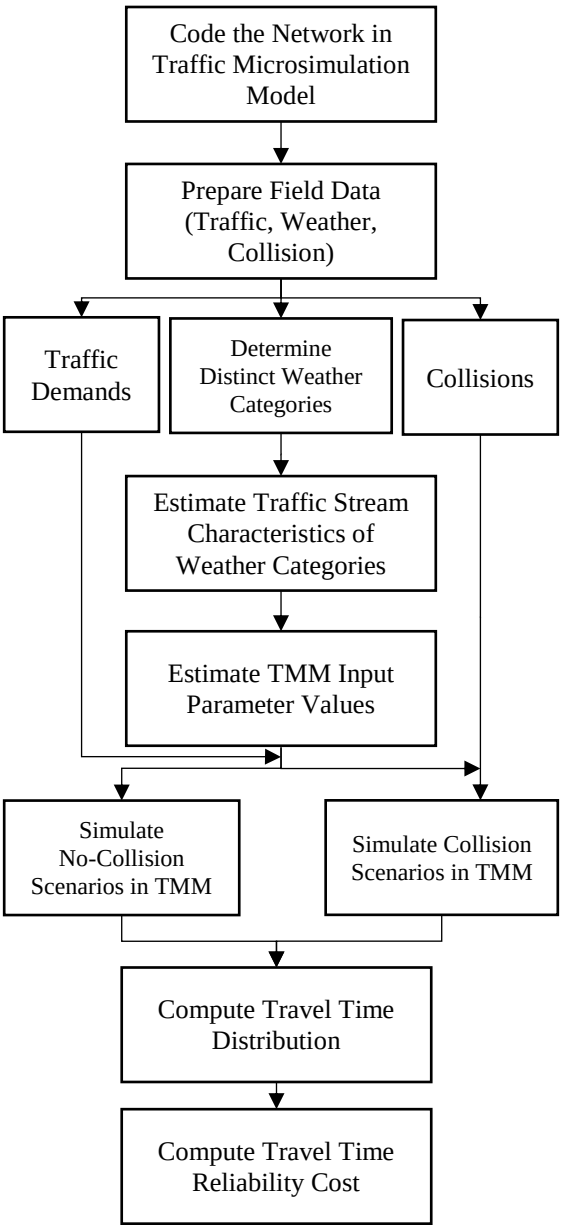

Figure 6-1- Steps within the analysis of the alternatives

6.2. Study Area

The study area is an existing freeway interchange on I-694 in Twin Cities (Minneapolis-St. Paul) region in Minnesota, U.S. The interchange connects the freeway to a two-way two-lane urban roadway Victoria Street North. The freeway is a divided four-lane (two lanes at each direction) oriented in an east-west direction. The study area is shown in Figure 6-2. Also, the interchange geometry is shown in Figure 6-3.

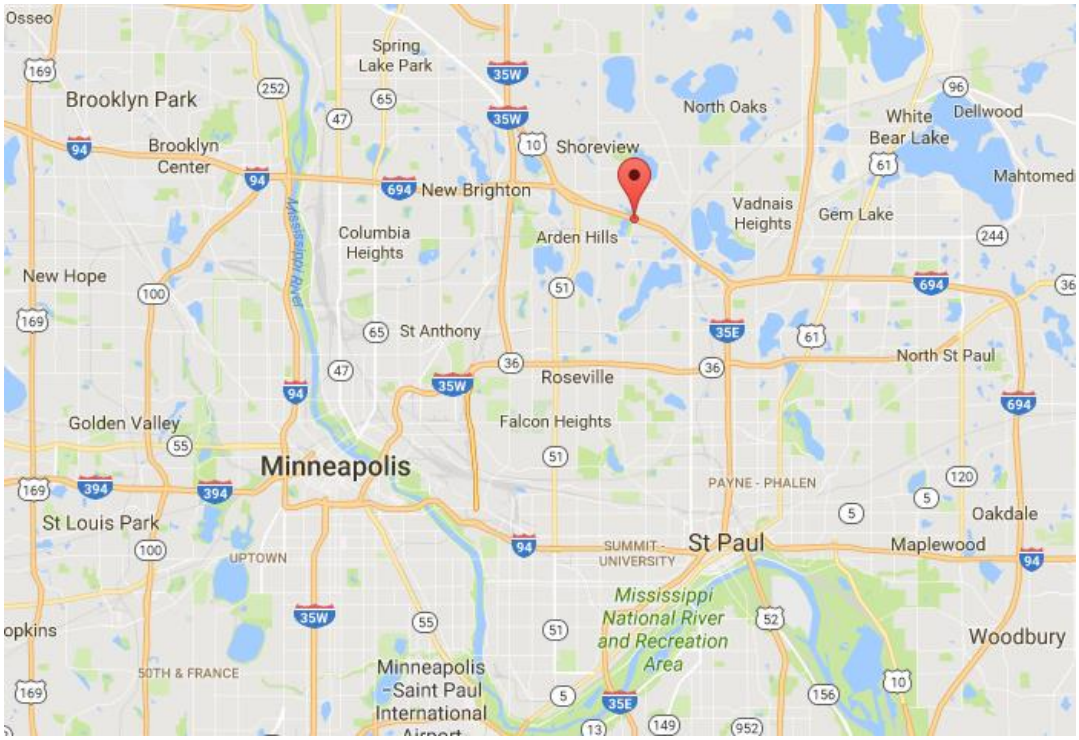

Figure 6-2-Study area and the surrounding road network (Google Maps, 2016)

Figure 6-3-Existing interchange geometry (Google Maps, 2016)

Loop detector data obtained from this section of freeway indicates that roadway experiences recurrent congestion during the morning and afternoon peak hours. A sample of loop detector data for this freeway section was shown in Figure 3-2 in Chapter 3.

6.3. Code the network and preparing field data

All the field data are for the year 2014. The traffic data and weather data came from the Minnesota department of Transportation (MnDot) as described in Chapter 3. Collision data and annual crash facts were obtained from the Office of traffic safety in the Minnesota Department of Public Safety.(MnDPS, 2015)

In our hypothetical problem, we assume that the traffic demand will increase in the near future and there are concerns about the adequacy of the existing interchange design. Two alternative roadway improvements are being considered.

Alternative 1 consists of maintaining the existing interchange geometry, but adding one lane in each direction to Victoria Street. The intersections of Victoria Street and the on/off ramps to/from I-694 would be controlled by traffic signals.

Alternative 2 consists of replacing the existing interchange with a full cloverleaf interchange while keeping the lane increase suggested in the Alternative 1. With the full cloverleaf interchange design, there is no need for traffic signals at the intersections between the on/off ramps and Victoria Street.

We used the VISSIM model as the traffic microsimulation software to code the alternatives. The coded network for Alternative 1 and Alternative 2 are shown in Figure 6-4 and Figure 6-5 respectively.

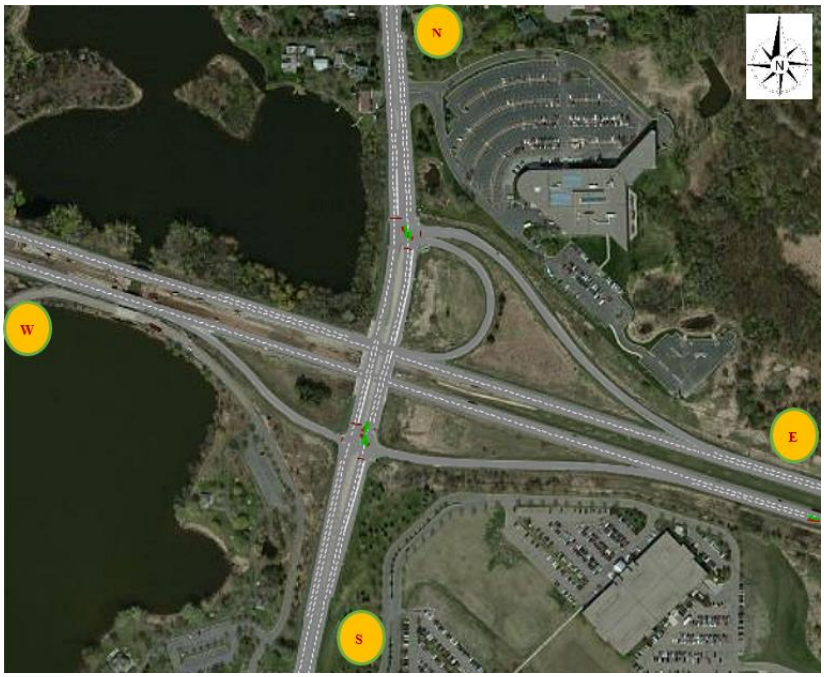

Figure 6-4- Geometry for Alternative 1

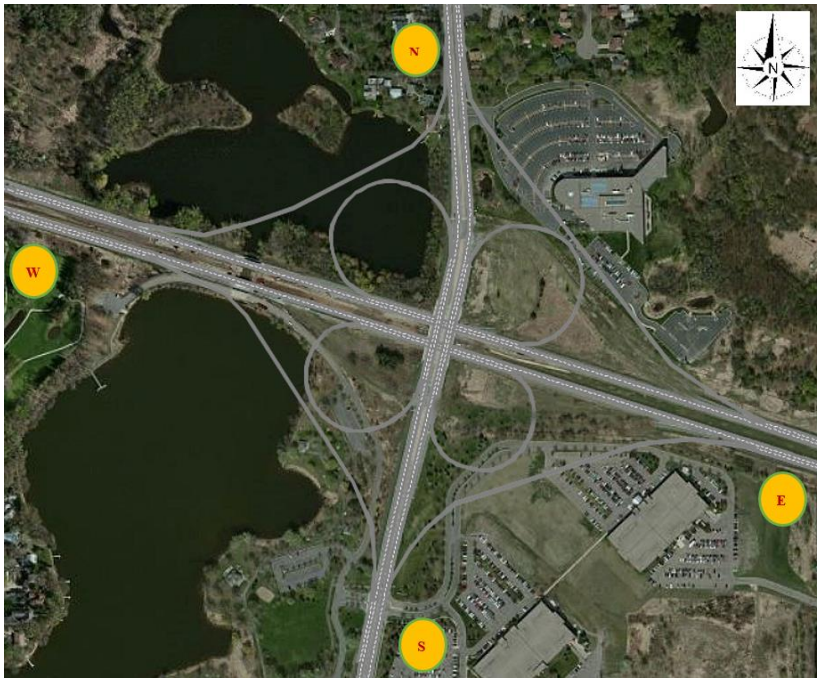

Figure 6-5- Geometry for Alternative 2

6.4. Determine distinct weather categories and their traffic stream parameters

We used the output categories from Chapter 3 of this thesis since we used the same facility and same geographical area as used in the case study in chapter 3. There were 16 distinct weather categories at the end of chapter 3. The traffic flow parameters of the weather categories were also estimated using the technique introduced in chapter 2. The finalized weather categories are listed below in Table 6-1 along with their traffic flow parameter values.

Table 6-1- Weather Categories with Their Traffic Flow Parameter Values

No	Road Surface	Precipitation	Diurnality	u_f	u_c	k_j	q_c
1	Dry	NoPrecip	Day	115.7	101.1	100	1847
2	Wet	NoPrecip	Day	109.3	96.9	100	1732
3	Ice	NoPrecip	Day	118.0	74.1	100	1674
4	Dry	Rain	Day	112.3	102.2	100	1688
5	Wet	Rain	Day	110.2	92.0	100	1668
6	Dry	Snow	Day	107.6	97.6	100	1759
7	Wet	Snow	Day	94.5	89.9	100	1303
8	Ice	Snow	Day	111.6	102.3	100	1338
9	Wet	Frozen	Day	103.8	97.5	100	1689
10	Dry	NoPrecip	Night	113.1	97.3	100	1784
11	Wet	NoPrecip	Night	109.7	95.4	100	1775
12	Ice	NoPrecip	Night	107.6	96.1	100	1737
13	(Dry+Wet)	Rain	Night	110.2	94.8	100	1658
14	Dry	Snow	Night	111.2	61.3	100	2198
15	Wet	Snow	Night	86.5	62.2	100	1206
16	Wet	Frozen	Night	104.4	82.4	100	785

6.5. Estimate VISSIM input parameters

The next step is to estimate the VISSIM input parameters required to model each of these 16 weather categories. We applied the model developed in Chapter 4 to estimate the VISSIM input parameters for each of the 16 categories. For each weather category, we provided as input to the neural network model the associated traffic flow parameters from Table 6-1 as well as the heavy vehicle ratio (which we assumed to be 10%). For each weather category, the neural network model provided the recommended value to be used for the 11 VISSIM input parameters. The estimated VISSIM input parameters are

listed in Table 6-2. The last two columns are the desired speed distributions for passenger cars and heavy vehicles respectively.

6.6. Prepare input demand

The eastbound and westbound traffic demand in the freeway was obtained from the induction loop detectors. The northbound and southbound traffic flow at the arterial road was assumed as a fraction (i.e. 60%) of the eastbound and westbound freeway flow respectively. We decided to perform the simulation from 6:00 AM to 10:00 PM. We started the simulation from 5:55 AM to let the network load the demand for five minutes. The interval of 5:55 AM to 6:00 AM was considered as the warm-up period and no results were captured during that time. To determine the traffic assignment ratios, we selected the static traffic assignment technique that assigns fixed proportions of traffic flow at each approach to the diverging roadways. The assignment ratios are shown in Table 6-3. Also, the route numbers are shown in Table 6-4.

The loop detectors data was aggregated at five-minute intervals and the year of data was 2014 (the whole year). To generate demand scenarios, we only considered weekday traffic data. Also, to include day-to-day demand variation: first we investigated the traffic volume distribution of the field detector data, and then we defined some demand levels. The average coefficient of variation (COV) of the whole five-minute intervals from 6:00 Am to 10:00 PM was 0.15.

Table 6-2- Estimated VISSIM Input parameters

No	AccDecel Own	AccDecel Trail	SafDistFact LnChg	W99cc0	W99cc1	W99cc4	W99cc5	W99cc7	W99cc9	PC DSD	HV DSD
1	-1.765	-1.753	0.171	5.102	1.239	-0.519	0.385	0.332	1.801	PC128	PC105
2	-1.755	-1.754	0.177	5.037	1.375	-0.519	0.391	0.320	1.789	PC122	PC105
3	-1.752	-1.746	0.502	4.367	1.405	-0.507	0.473	0.469	1.743	PC126	PC105
4	-1.758	-1.750	0.178	5.114	1.474	-0.523	0.391	0.320	1.788	PC124	PC105
5	-1.756	-1.757	0.200	4.938	1.437	-0.517	0.397	0.337	1.791	PC122	PC105
6	-1.752	-1.752	0.183	5.051	1.353	-0.520	0.393	0.317	1.784	PC120	PC105
7	-1.733	-1.739	0.293	5.019	2.132	-0.528	0.433	0.321	1.736	PC108	PC105
8	-1.754	-1.744	0.217	5.167	2.064	-0.531	0.407	0.321	1.773	PC124	PC105
9	-1.746	-1.747	0.212	5.039	1.471	-0.522	0.404	0.315	1.768	PC118	PC105
10	-1.760	-1.756	0.175	5.034	1.296	-0.518	0.388	0.329	1.797	PC124	PC105
11	-1.756	-1.756	0.179	5.010	1.304	-0.517	0.390	0.325	1.792	PC122	PC105
12	-1.753	-1.754	0.183	5.024	1.368	-0.519	0.393	0.320	1.786	PC120	PC105
13	-1.756	-1.756	0.183	4.999	1.466	-0.519	0.393	0.326	1.791	PC122	PC105
14	-1.748	-1.737	0.774	3.904	0.693	-0.492	0.532	0.595	1.706	PC112	PC105
15	-1.748	-1.751	0.513	4.639	2.345	-0.505	0.470	0.472	1.748	PC92	PC92
16	-1.749	-1.755	0.330	5.417	3.318	-0.490	0.402	0.383	1.777	PC116	PC105

Table 6-3-Traffic assignment ratios

O/D	E	W	N	S
E	-	0.80	0.08	0.12
W	0.80	-	0.08	0.12
N	0.20	0.20	-	0.60
S	0.50	0.40	0.10	-

Table 6-4-Route Numbers

O/D	E	W	N	S
E	-	2	1	3
W	5	-	4	6
N	7	9	-	8
S	10	12	11	-

We assume that the distribution of day-to-day traffic demands (for the same time of day) follow a normal distribution. We define five demand levels: 1) lowest; 2) low; 3) average; 4) high; and 5) highest and assigned a probability to each demand level. These levels were generated by multiplying the base demand by the values of -2 COV, -1 COV, 1, +1 COV, and +2 COV. The reason is that we

considered that each demand level included 1 standard deviation of the probability density function. An instance of the probability density function for the base demand of 1000 vph divided into 5 levels is illustrated in Figure 6-6. As shown, the probability of the demand levels 1 to 5 are 6%, 25%, 38%, 25%, and 6% respectively. These probabilities are used when we take multiple samples from demand distributions for simulation. Samples are taken proportionate to their probability.

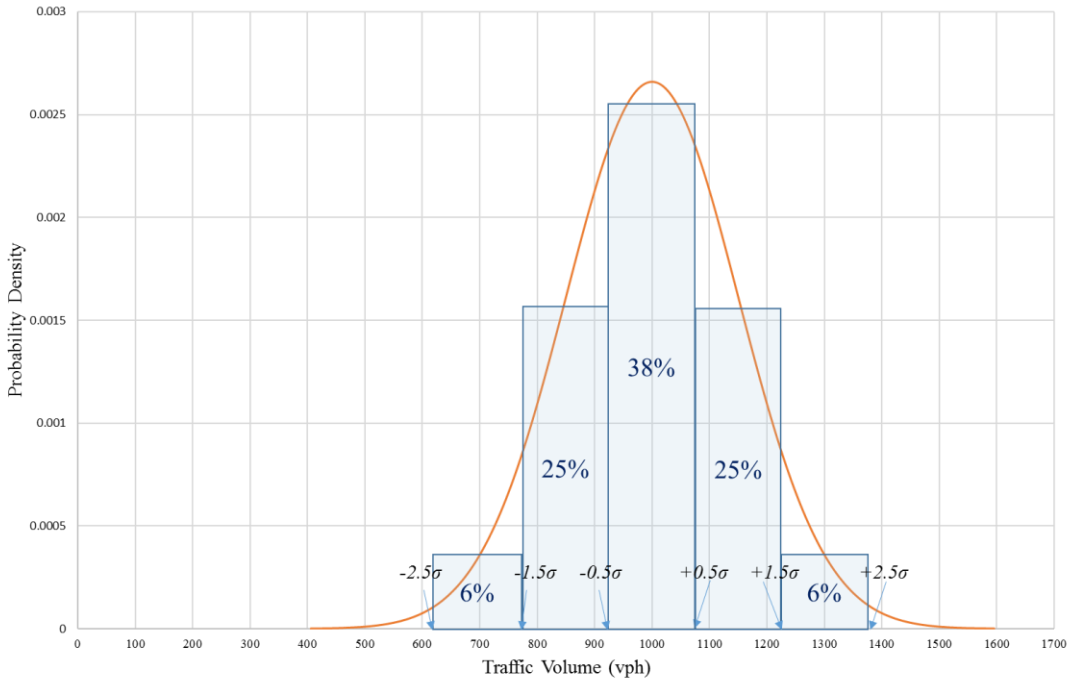

Figure 6-6-Demand probability density function

6.7. Collision Scenarios

Another important source of travel time variation is the occurrence of incidents. We incorporate the impact of collisions on travel times by modelling a representative sample of collisions. For each collision, we must define the location, duration, time of occurrence, and severity (i.e. capacity reduction). We assumed that the collisions were independent from the weather. Also, we assumed that all collisions occur only on the freeway and not on the crossing arterial (i.e. Victoria Street) and that at most a single collision event occurs on a single day.

The frequency of collisions during the year 2014 was estimated from the annual vehicle collision report of the department of public safety of the state of Minnesota. We estimated that 52 collisions happened during that year in the study area.

The duration of collisions was assumed to follow a Weibull distribution according to Nam and Mannering (2000). Also, a study on the collision duration on freeways by Smith and Smith (2002) provided empirical distributions for collision duration using an extensive field data. We decided to not model collisions with very short durations (i.e. 10 minutes and shorter) within our simulation. Therefore, we estimated the parameters of the Weibull distribution as (α=1.17, β=32.36, and γ=5).

We assumed that the duration of the collision is correlated with the collision severity (i.e. the magnitude of the capacity reduction associated with the collision). Since, the freeway section in our simulation network has two lanes at each direction, we assumed that collisions will block either one or two lanes. Furthermore, more arbitrarily, we assumed that 2 out of 52 collisions blocked both freeway lanes while other collisions just blocked one lane.

The location and the start time of the collisions were assumed to be purely random in the network and simulation period respectively. Also, the dominant weather category was assigned to each collision randomly but proportionate to the category frequency. We also assigned the demand level to each collision randomly. The resulting set of collisions was applied to evaluate both Alternative 1 and Alternative 2. Table 6-5 identifies the characteristics of all 52 simulated collisions.

Table 6-5-Characteristics of the Collision Scenarios

Scenario #	Severity	Time			Longitudinal Position		Latitudinal Position		
	No of Blocked Lanes	Duration (s)	Start Time	End Time	Direction	Location from start (m)	Lane (Shoulder=1, Median=2)	Demand Level	Weather category
1	1	6120	10:54 AM	12:36 PM	EW	2872	1	4	1
2	1	5880	2:29 PM	4:07 PM	EW	601	2	5	1
3	1	5400	1:17 PM	2:47 PM	EW	587	1	4	4
4	1	5100	5:20 PM	6:45 PM	WE	2684	2	2	1
5	2	4500	1:55 PM	3:10 PM	WE	1582	1,2	3	1
6	1	3900	7:08 AM	8:13 AM	WE	2387	1	3	1
7	1	3780	4:00 PM	5:03 PM	WE	390	1	3	1
8	1	3660	10:59 AM	12:00 PM	WE	378	2	3	1
9	1	3600	12:36 PM	1:36 PM	WE	583	2	3	1
10	1	3420	8:38 PM	9:35 PM	WE	70	1	3	1
11	2	3300	8:37 AM	9:32 AM	EW	830	1,2	3	2
12	1	3240	7:04 AM	7:58 AM	EW	1643	1	3	2
13	1	3240	8:26 AM	9:20 AM	WE	1583	2	3	4
14	1	3000	9:54 AM	10:44 AM	WE	2363	1	3	3
15	1	2940	11:19 AM	12:08 PM	EW	2513	1	2	2
16	1	2700	7:19 PM	8:04 PM	EW	982	1	2	1
17	1	2520	6:25 PM	7:07 PM	EW	1584	2	3	4
18	1	2520	8:30 PM	9:12 PM	WE	1614	1	3	2
19	1	2400	6:58 AM	7:38 AM	WE	451	2	2	13
20	1	2400	2:17 PM	2:57 PM	EW	872	2	2	1
21	1	2280	12:45 PM	1:23 PM	EW	2026	1	1	3
22	1	2100	3:30 PM	4:05 PM	WE	2100	1	3	3
23	1	2100	4:12 PM	4:47 PM	WE	1960	2	4	1
24	1	2040	11:41 AM	12:15 PM	EW	289	2	5	1
25	1	1920	9:50 AM	10:22 AM	EW	1941	1	2	1
26	1	1860	7:21 PM	7:52 PM	EW	2456	2	4	1
27	1	1800	12:39 PM	1:09 PM	EW	401	1	4	1
28	1	1560	12:54 PM	1:20 PM	WE	113	1	3	1
29	1	1500	12:33 PM	12:58 PM	WE	882	1	4	1
30	1	1440	9:43 AM	10:07 AM	EW	2166	2	5	1
31	1	1320	3:44 PM	4:06 PM	WE	1625	2	4	2
32	1	1320	6:15 PM	6:37 PM	EW	2687	1	1	1
33	1	1260	8:30 PM	8:51 PM	EW	897	1	3	1
34	1	1260	6:20 PM	6:41 PM	WE	2756	1	4	1
35	1	1260	5:24 PM	5:45 PM	EW	2376	1	2	1
36	1	1260	3:35 PM	3:56 PM	WE	2417	1	3	3
37	1	1140	8:44 AM	9:03 AM	EW	2081	1	4	5
38	1	1140	6:45 PM	7:04 PM	WE	2656	2	4	6
39	1	1080	1:45 PM	2:03 PM	WE	73	2	3	2
40	1	1080	6:26 AM	6:44 AM	EW	1184	1	1	2
41	1	1020	9:04 PM	9:21 PM	EW	68	2	4	1
42	1	1020	6:30 PM	6:47 PM	EW	411	1	3	1
43	1	1020	3:08 PM	3:25 PM	EW	1228	2	2	2
44	1	900	1:17 PM	1:32 PM	WE	1655	2	4	1
45	1	840	12:00 PM	12:14 PM	WE	2163	2	3	4
46	1	840	7:38 PM	7:52 PM	EW	158	1	3	17
47	1	780	6:54 AM	7:07 AM	EW	1847	1	2	3
48	1	780	2:47 PM	3:00 PM	WE	307	1	2	1
49	1	720	9:07 PM	9:19 PM	WE	1078	2	2	9
50	1	660	4:15 PM	4:26 PM	WE	380	2	4	1
51	1	660	1:08 PM	1:19 PM	EW	1635	2	2	3
52	1	660	8:09 PM	8:20 PM	EW	97	2	2	1

6.8. Simulating Collision and No-Collision scenarios in TMM

Having defined the collision scenarios as described in the previous section, it is necessary to determine how many collision and non-collision simulations to conduct

For the no-collision scenarios, each weather category was replicated five times (with different random seeds) at each demand level to impart randomness to simulation procedure. Considering the 16 weather categories and five demand levels, 400 simulation runs were done in total. Also, we replicated each collision scenario five times with different random seeds at the assigned demand level and weather category which resulted in 260 simulation runs in total. We used the default values for all VISSIM input parameters except the 11 parameters listed in Table 6-2.

Measurement points were located at each origin and destination node in the network to capture individual vehicle O-D travel times. These travel times, along with the origin, destination, and departure time were recorded to a database for subsequent processing.

We encountered an issue with the simulation of collision scenarios that required specific data post processing. Depending on the characteristics of the collision being modelled, it was possible for congestion to form and the ensuring queue spilled back to one or more of the network origins. When this occurred, vehicles that were scheduled to enter the network could not do so. In some cases, when the collision was very severe (i.e. complete blockage of the roadway), no vehicles were recorded as entering the network at that origin during a given 30-minute interval and consequently no travel times for that time period were obtained. This absence of travel time data would distort the travel time distribution.

Figure 6-7 shows a shockwave diagram for a freeway section on which a collision occurs at time $t_1$reducing the capacity of the freeway to zero. According to the shockwave theory, it takes until t_2 that the queue backs up and reaches to the measurement point at the origin. The collision clears at $t_3$and again it requires some time (until t_4) for the queue to clear and traffic starts to move again at the measurement point. No vehicles pass the measurement point between times t_2 and t_4 and, as it is shown in the lower diagram (travel time diagram), no travel time data is captured during that period of time even though a very high travel time should be reported.

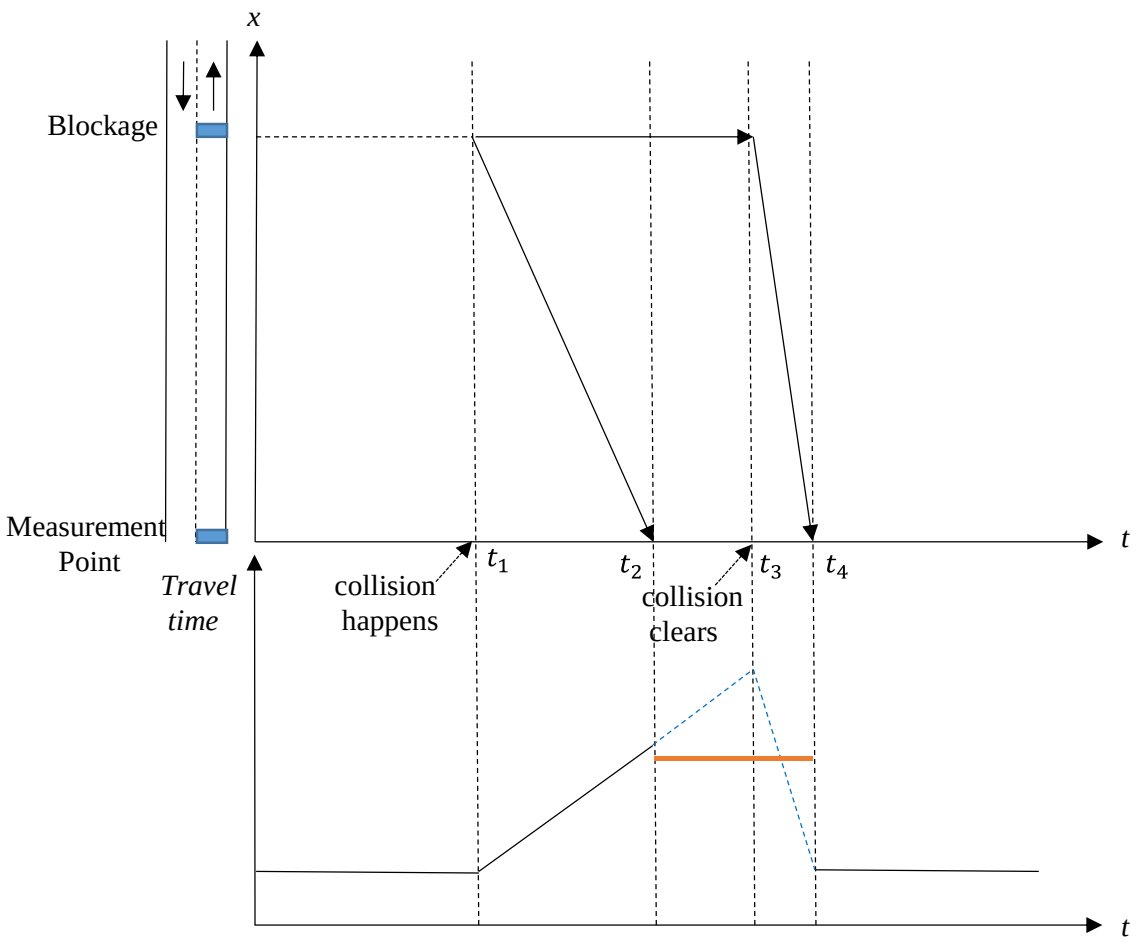

Figure 6-7-Shockwave and travel time diagram of the full blockage collisions

In an effort to mitigate the impact of this absence of data, we identified the time intervals from the simulation travel time data base in which this problem occurred and then we changed the traffic volume in those intervals from 0 vehicles to 1 vehicle and approximated the travel time for the interval as a very large value. There were 32 thirty-minute departure intervals in one-day (from 6 AM to 10 PM) simulation for each route. Considering the 12 routes in the simulation network, 52 collision scenarios and 5 replications, we have 99,840 thirty-minute intervals in the simulated collision scenarios for each alternative; however, we encountered the abovementioned issue in a very small number of intervals: 32 intervals in the Alternative 1 and 37 intervals in the Alternative 2.

6.9. Compute travel time distribution

The evaluation of the cost of travel time (un) reliability is based on the distribution of travel times. This distribution reflects the day to day variation in the travel times experienced by vehicles departing a given origin during a specific time period and en-route to a given destination. In this network, there are 12 O-D pairs and we chose to discretize the departure time to 30-minute time intervals. Given that we simulate from 6:00 AM to 10:00 PM, there are 32 departure time intervals for which travel time distributions are required for each O-D pair.

It is not appropriate to simply combine all the individual vehicle travel time data obtained from the 660 simulation runs which were performed because the number of simulation runs associated with each condition (e.g. weather category, collision vs no-collision, etc.) is not proportional to the probability of that condition occurring in the real world. Consequently, we generate the travel time distributions by sampling from the simulation runs according to the probability of occurrence.

Our weather categories include diurnality (i.e. day versus night). The number of hours of daylight changes throughout the year and therefore we computed the probability of being day and night for each 30-minute time interval between 6 AM and 10 PM. For example, the time interval of 6:30 AM to 7:00 AM is *night* during 126 days of the year (126/365 = 35%) and is *day* during the rest of the year (65%). Therefore, when generating the travel time distribution for this time interval we wish to have 35% of the samples taken from simulation runs reflecting *night* weather conditions (i.e. from the 7 *night* categories in Table 6-1) and 65% from *day* weather conditions (i.e. from the 9 *day* categories in Table 6-1).

We use the same approach for sampling from the collision versus no-collision simulation runs. We took 52/365 = 14% of the samples from the collision simulation runs and 86% from the no collision runs.

This sampling approach to generate the final travel time distribution for the time interval of 6:30 AM to 7:00 AM is shown in Figure 6-8.

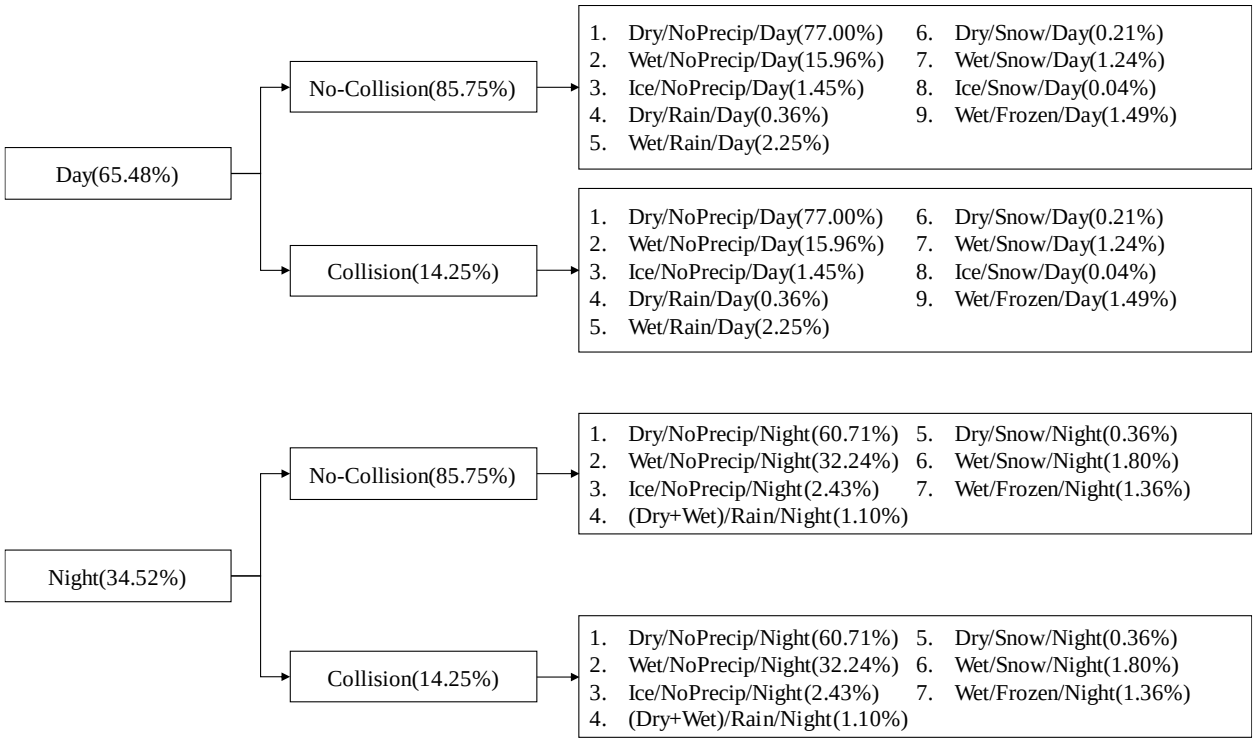

Figure 6-8-Sampling from simulation results to generate TT distribution at the time interval of 6:30 AM to 7:00 AM

The travel time distribution of the vehicles in route 1 departing the origin between 6:30 AM and 7:00 AM is shown in Figure 6-9 along with the distribution of travel times at the same route between 10:30 AM and 11:00 AM.

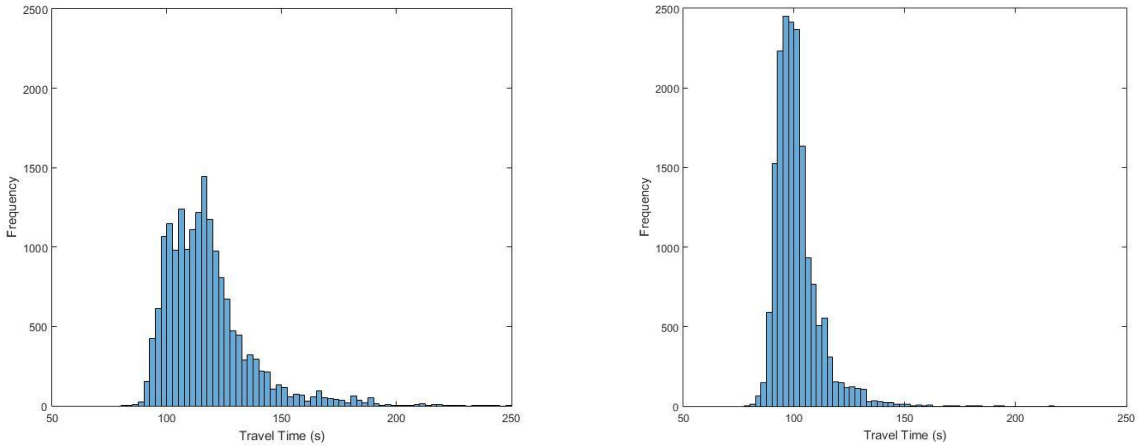

Figure 6-9- Distribution of Travel Time of the route 1 for interval 6:30 - 7:00 AM (left) and 10:30 - 11:00AM (right)

6.10. Compute travel time reliability cost

The travel time reliability cost is computed for each of the 12 O-D pairs and each of the 32 departure time intervals using Equation (5-2) in Chapter 5, which is reproduced below.

$$TTR_{cost} = \left[n_1 \cdot \int_{\tau_f}^{\hat{\tau}} |\tau - \tilde{\tau}| \cdot c(\tau) \cdot P(\tau) d\tau \right] + \left[n_2 \cdot \int_{\hat{\tau}}^{\tau_{max}} (\hat{\tau} - \tilde{\tau}) \cdot VSDL \cdot P(\tau) d\tau \right] \qquad (6\text{-}1)$$

where τ_f is free-flow travel time, $\tilde{\tau}$ is the anticipated travel time, n_1 is the number of vehicles which travel times are shorter than the extreme travel time threshold (i.e. $\hat{\tau}$) and n_2 is the number of vehicles which travel times are longer than the extreme travel time threshold P is the probability density of travel time, and $c(\tau)$ is the cost function.

For each alternative, we compute $\tilde{\tau}$ and $\hat{\tau}$ for each time interval/O-D pair using the method presented in Chapter 5. Table A in Appendix 2 shows these values. For each 30-minute interval, the free-flow travel time was considered as the 15th travel time percentile, and the extreme travel time threshold was 1.83 times of the free-flow travel time. To compute the anticipated travel time, we truncated the travel time distribution at the extreme travel time threshold, and computed the 80% percentile of the truncated distribution as the anticipated travel time.

We use the values of schedule delay early and late (i.e. VSDE and VSDL) estimated by Tseng et al. (2005). Since the values reported by Tseng were in 2004 Euros, we converted those values to the

equivalent in 2014 US dollars. To calculate that we first found the conversion rate of Euro to US$ in 2004 (OANDA, 2016), and then used the consumer price index (CPI-U) last updated on September 16, 2016 by the U.S. Department of Labor Bureau of Labor Statistics to compute the cumulative rate of inflation to calculate the equivalent of one US$ of 2004 in the year 2014. The average CPI-U is 188.9 and 236.7 in 2004 and 2014 respectively (Bureau of Labor Statistics, 2016). Therefore, the cumulative inflation rate of 2004 to 2014 is calculated accordingly:

$$Cumulative\ inflation\ rate = \frac{236.7 - 188.9}{188.9} = 0.253$$

Therefore, $1 in 2004 is equivalent to $1.253 in 2014. The values reported by Tseng and the associated estimated values for the year 2014 are listed in Table 6-6.

Table 6-6-Values of VOT, VSDE and VSDL

	Euro 2004 €/hour/person	**USD2004 $/hour/person**	**USD2014 $/hour/person**
Value of Time (VOT)	8.47	10.31	12.89
Value of Schedule Delay – Early (VSDE)	12.07	14.70	18.37
Value of Schedule Delay – Late (VSDL)	14.88	18.12	22.65

Table 6-7 illustrates the computation of the (un)reliability cost for the route 1 in three departure time intervals during the morning time for Alternative 1 in a single day simulation run. We disaggregate the travel time distribution into 100 one-percent sections and compute the costs at each disaggregated section. For instance, to compute the travel time reliability cost of the 1st percentile at route 1 and time interval of 7:00 AM- 7:30 AM we compute the difference of the average travel time at that percentile (91.8 s) and the anticipated travel time at that interval (124.6 s). Then, since it is an "early" travel time (because 91.8s is shorter than $\tilde{\tau}$ at that interval (i.e. 124.6 s)) we multiply this difference (i.e. 124.6-91.8=32.8 s=0.0091 h) by the value of schedule delay early (i.e. $18.37) which results in $0.17/person. In the absence of vehicle occupancy data, we assume that each vehicle is occupied by only by one person; therefore, the unit can be changed to $/vehicle. This cost will be experienced by 1% of the traffic volume of this interval. Therefore, to compute the total unreliability cost at this interval, Equation (6-2) is used:

$$TTR_{cost}^{t} = \sum_{p=1}^{100}\left(TTR_{u\_cost}^{t,p} \times \frac{q^t}{100}\right) = \frac{q^t}{100} \times \sum_{p=1}^{100}\left(TTR_{u\_cost}^{t,p}\right) \quad (6\text{-}2)$$

where:

TTR_{cost}^{t}: cost of the travel time reliability at the time interval *t* ($)

$TTR_{u\_cost}^{t,p}$: unit cost of the travel time reliability at the p^{th} travel time distribution percentile of the time interval *t* ($/veh)

q^t: traffic volume at the time interval *t* during the computation period (veh)

We are computing the travel time reliability cost for one of the single day simulation runs for illustration purposes; therefore, we use the value of traffic volume (q^t) reported by VISSIM software in that simulation instance. Then, the travel time reliability cost at the 1st time interval of the Table 6-7 for a single day simulation instance is computed accordingly:

$$(0.17 + 0.16 + \cdots + 0.37 + 0.37) \times \frac{128}{100} = \$11.23$$

This value shows it is expected that each vehicle should expect 11.23/128=$0.088 of unreliability cost in average when traversing route 1 between 7 AM and 7:30 AM. It should be noted that it is a very short route and the anticipated travel time to traverse it is small; therefore, having small values of travel time reliability cost is not surprising.

Table 6-7- Illustration of TTR Cost/day Computation of Three Time Intervals of Alternative 1

Route	Time Interval	Volume	τ_f (s)	$\bar{t}$ (s)	$\hat{t}$ (s)	Travel time of percentiles (s)					Cost of percentiles ($/veh)					Total unreliability cost of interval ($)
						1st	2nd	…	99th	100th	1	2	…	99	100	
1	7:00-7:30	128	100.5	124.6	184.0	91.8	93.5		197.0	426.0	0.17	0.16		0.37	0.37	$11.23
1	7:30-8:00	121	98.8	122.8	180.7	91.2	92.8		184.4	441.4	0.16	0.15		0.36	0.36	$ 10.13
1	8:00-8:30	122	96.7	120.8	177.0	89.5	91.3		168.4	245.2	0.16	0.15		0.30	0.35	$9.75

Once the reliability cost was computed for all intervals at each route, we summed them up to compute the travel time reliability cost of that route. Then, the travel time reliability cost of all routes was summed up to obtain the travel time reliability cost of the alternative. Table 6-7 computes the travel time reliability cost in three time intervals using the traffic volume of one day. To compute the travel time reliability cost over the whole year we need to use the traffic volume of each interval during the year. To obtain the annual traffic volume at each interval we sampled 365 traffic volume values from the simulated scenarios proportionate to their probability of occurrence and summed them up.

Figure 6-10 illustrates the cost of travel time reliability in different routes for both alternatives at the time intervals (a) 7:30-8:00 AM and (b) 10:00 -10:30 AM. We observe from Figure 6-10 that TTR cost varies substantially across different routes (for the same time of day). This is expected as different routes have different volumes, and experience different levels of unreliability.

The TTR cost ($/year) of different routes/time intervals is listed in Table A in Appendix 2.

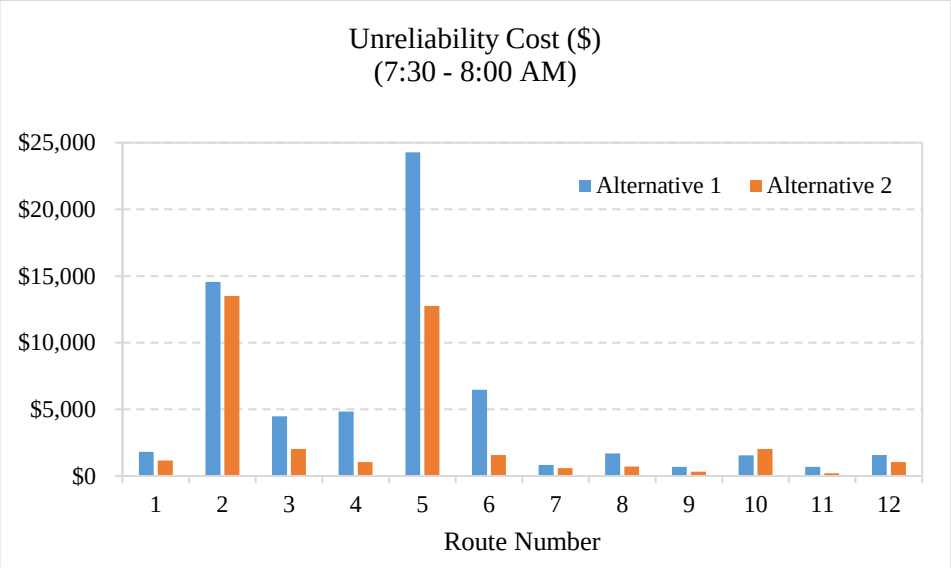

(a)

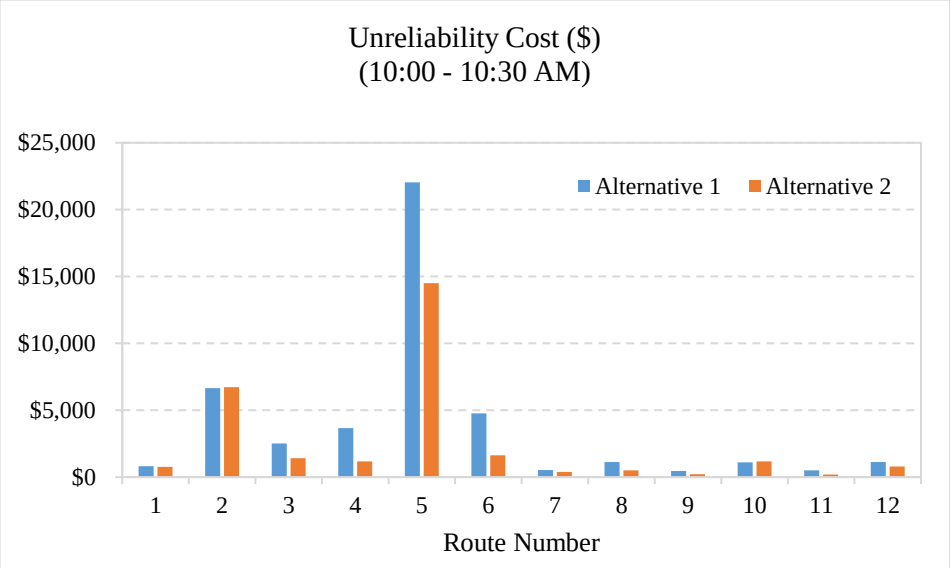

(b)

Figure 6-10- Annual cost of travel time (un)reliability at time intervals 7:30-8:00 AM (a), and 10:00:10:30 AM (b)

To compare the alternatives, we also need to compute the travel time cost at each O-D/time interval. Equation (6-3) is used to compute the travel time cost.

$$TT_{cost} = \left[n_1 \cdot VOT \cdot \int_{\tau_f}^{\hat{\tau}} \tau \cdot P(\tau) \cdot d\tau\right] + \left[n_2 \cdot \hat{\tau} \cdot VSDL \int_{\hat{\tau}}^{\tau_{max}} P(\tau) d\tau\right] \quad (6\text{-}3)$$

where all parameters were defined earlier.

The user cost is computed by summing up the travel time cost and travel time reliability cost. Figure 6-11 shows the annual users' cost for two time intervals 7:30-8:00 AM and 10:00-10:30 AM.

The annual users' cost is computed and illustrated for all time intervals/routes in Table A in Appendix 2. Table 6-8 shows the summary of the alternative analysis. Alternative 2 results in lower total user costs than Alternative 1. This is not unexpected given that the full cloverleaf interchange design from Alterative 2 provides greater capacity and therefore provides improvements (reductions) in the average travel times and improvements in the travel time reliability.

Table 6-8- Summary of Alternative Analysis Results

	Alternative 1	Alternative 2
TTR Cost	$ 1,714,385	$ 1,032,186
TT Cost	$ 8,282,449	$ 7,442,994
Sum	$ 9,996,834	$ 8,475,180

6.11. Mean travel time cost

As mentioned earlier, the common practice in alternative analysis is to compare average travel time costs of different alternatives under ideal conditions. To have a better understanding about the relative size of the cost values in each approach (i.e. the common practice and the method presented in this research), we simulated both alternatives for no-collision no-precipitation dry surface condition and computed the average travel time at each interval and multiplied it by the number of vehicles at that interval × the value of time (VOT) obtained from Table 6-6. We aggregated all time intervals/O-D costs. The result is shown in Table 6-9.

Table 6-9- Alternative Analysis Results (values for 16 hour simulated time in one year)

Alternatives	Mean Travel Time Cost (common practice)	TT Cost +TTR Cost (Method presented at this research)
Alternative 1	$ 7,546,703	$ 9,996,834
Alternative 2	$ 6,551,631	$ 8,475,180

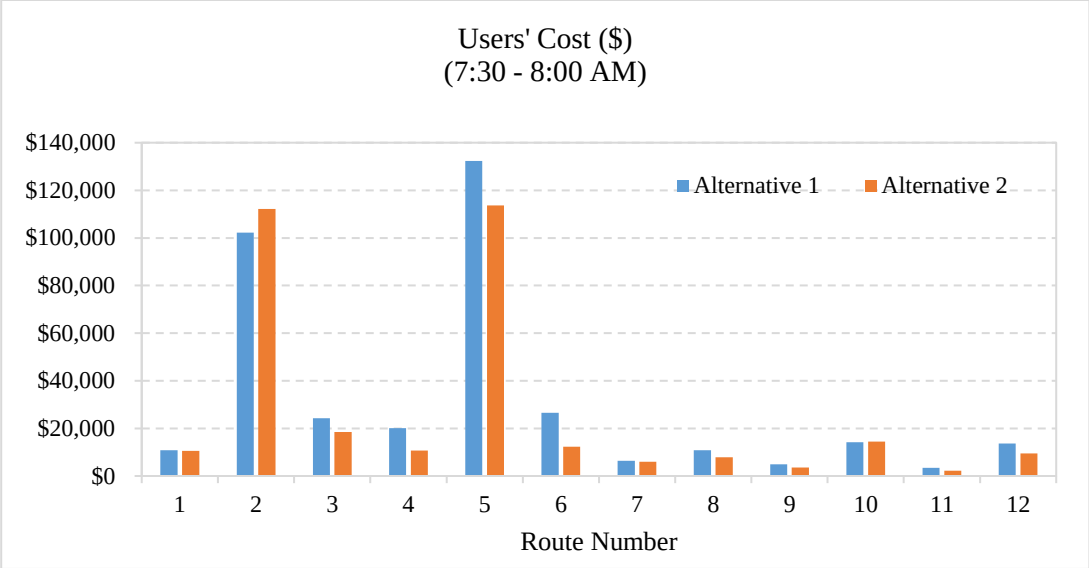

(a)

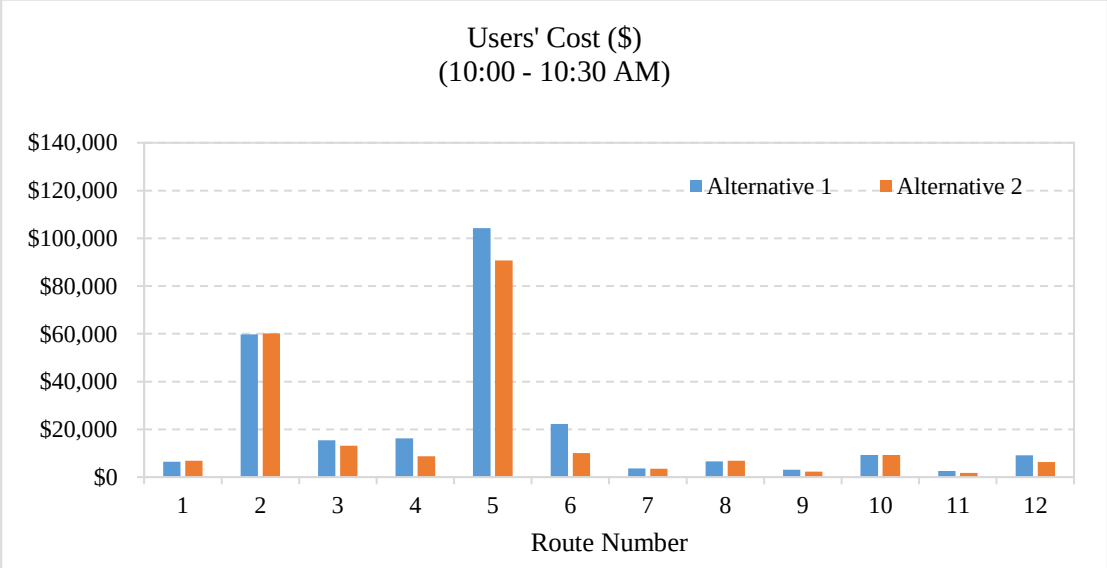

(b)

Figure 6-11- Annual users' cost at time intervals 7:30-8:00 AM (a), and 10:00:10:30 AM (b)

It should be noted that the values of TT cost in Table 6-8 are different from the mean travel time cost (common practice) shown in Table 6-9 for several reasons:

5- The traffic volume used in common practice is computed based on the single/multiple simulation runs representing “ideal” conditions (i.e. no-collision no-precipitation scenario). However, in the proposed method, the traffic volume considers the variations in traffic

demands that occur throughout the year. Therefore, the traffic volumes used at each of the above methods are different. Considering all routes and time intervals, the total volume used in common practice method is 1% higher than our method; however, the magnitude of the difference of volumes varies between different routes / time intervals and the standard deviation of the difference is 7%.

6- The travel time used in common practice is the average travel time of no-collision no-precipitation scenario; however, we use the travel time distribution to compute the travel time cost using Equation (6-3). Therefore, the travel time values are also different in the above methods.

6.12. Conclusion

In this chapter, we illustrated how the research modules that were presented in previous chapters can be combined to carry out an evaluation of two alternatives considering the travel time reliability. We used the method presented in Chapter 3 to determine the distinct weather categories available in the study area. Then we used the method presented in Chapter 4 to estimate the VISSIM microsimulation model input parameters required to simulate the study area under different prevailing weather conditions. Then we used the methods presented in Chapter 5 to calculate the anticipated travel time at each departure time interval and thereby to compute and monetize the cost of travel time (un)reliability.

It should be noted that although the network that we used in this demonstration was a small one, the method explained here is transferrable and applicable to any network size.

Chapter 7

Conclusions and Recommendations

7.1. Introduction

Travel time reliability has gained significant attention among the transportation researchers and practitioners recently. In this research, we aimed to implement traffic microsimulation models in order to model travel time reliability. To reach to this goal we found that several questions should be answered:

1- What factors contribute to the day-to-day variation of travel time?
2- How should these factors be modeled in traffic microsimulation models?
3- Adverse weather conditions can be an important contributor to travel time variability but how can we determine the distinct weather conditions that need to be captured in the simulation model?
4- How can we find the microsimulation input parameter values needed to reflect each of these weather conditions within the simulation model?
5- How should we quantify the variability of travel time based on the simulation results?
6- How do travelers determine their anticipated travel time and how can this information be used to determine the cost of travel time (un)reliability?

7.2. Research Contributions

In this thesis, we have answered the above questions. In some cases, we have made use of existing practices and solutions in the literature, and in other we have created novel solutions. The contributions of this research can be listed as the following:

Developed a technique to distinguish road weather categories that have a significant impact on traffic behavior

Previous work has examined the impact of weather on the characteristics of the speed-flow-density relationship has defined the weather conditions a priori and then attempted to determine the macroscopic traffic stream characteristics for these categories. However, for the purposes of modeling travel time reliability, it is necessary to only capture those weather conditions for which the associated macroscopic characteristics are statistically different. To determine these distinct weather categories, we proposed an innovative method. We first suggested to incorporate different environmental factors when the initial "weather" categories are determined. Then we considered different arrangements for grouping the initial categories. We then applied the bootstrapping technique to create the confidence interval around the estimated traffic parameters of each weather category combined with statistical tests to determine if the difference between the traffic flow parameters of two or more weather categories was statistically significant. Finally, we suggested some measures to select the best arrangement and thereby the preferred set of distinct weather categories.

Evaluated the impact of observation point dispersion on the accuracy of estimated traffic flow parameters and developed a tool to select the preferred van Aerde's model calibration approach in terms of the parameter estimation error

The process of determining macroscopic traffic stream characteristics requires the calibration of a macroscopic speed-flow-density model to field data. In employing this approach, we observed that the errors associated with the estimated parameters are impacted by the number and distribution of the observation points that used to calibrate the model. Therefore, we developed models to estimate the corresponding errors of the estimated traffic parameters and found that for most practical applications, the estimation of the jam density is most sensitive to the distribution of the calibration data. As a result, we suggested some specific conditions for which the jam density value should be assumed *a priori* rather than calibrated on the basis of the available field data. Doing this improves the calibration accuracy and results in more reliable parameter estimates.

Developed a Model to Estimate VISSIM Input Parameters Based on the Known Traffic Flow Parameters

Practitioners sometimes need to simulate the overall drivers' behavior in a roadway so that some specific traffic flow parameters would be obtained. One of the instances of this need appeared in this research. We wanted to be able to model specific weather categories. We knew the traffic flow parameters of those weather conditions from the field data and we wanted the same traffic characteristics to be simulated in the traffic microsimulation model. Therefore, we proposed and evaluated a method to map the traffic flow characteristics to the TMM input parameters using a neural network model. The model developed in this research is not only applicable to simulate different weather categories, but also can be used to simulate any traffic condition -within the acceptable range of the model- when the traffic flow parameters are known.

Developed a Model to Determine Travelers' Anticipated Travel Time

Most of the existing research considers some characteristics of the travel time distribution to quantify the travel time reliability. In contrast, we have approached this problem with the goal of monetizing travel time (un)reliability. To do this we have adopted the unreliability cost in terms of the costs of arriving early or arriving late. This approach has been widely used to quantify the costs of unreliability of public transport system. Of course, this construct requires that we know the *scheduled travel time* which, from the user's perspective is the *anticipated* travel time. For public transport problems this is known as it is a function of the published schedule. However, for road transport the anticipated travel time is not defined by a schedule. Road users consider a route as variable/unreliable when they frequently experience travel times different from their anticipation. So, the main question is: "what is the anticipated travel time?". We carried out a stated preference survey to estimate the anticipated travel time based on the travel time distribution. On the basis of the survey responses we proposed two models in which travelers ignore unusually long travel times when determining their anticipated travel time.

Created a framework method for estimating cost of travel time unreliability using micro-simulation models

Finally, we incorporated all of these findings to create an approach for quantify the cost of travel time (un)reliability using traffic microsimulation tools. We demonstrate this approach to evaluate two road improvement alternatives. We used the traffic simulation model VISSIM to compare these two alternatives based on the travel time cost and travel time reliability cost together.

7.3. Recommendations

Below are the recommendations for further studies:

1- The neural network model developed to estimate the VISSIM input parameter values needed to model a specific traffic stream was calibrated on the basis of data for a freeway with two lanes at each direction. It is recommended that the impact of the number of lanes be investigated to determine if the existing model is transferable to freeway sections with more than two lanes in each direction. Also, this neural network model was calibrated just for freeways. We recommend that the model also be calibrated for other facility types (e.g. urban streets).

2- The model developed to compute the cost of travel time reliability -which is an input to the alternative analysis project- can be used along with any existing cost functions. As a recommendation for further research we suggest that research be done specifically to investigate the schedule delay costs associated with travel times that exceed the extreme value threshold.

3- We recommend the anticipated travel time model developed in this research be validated.

References

Avineri, E., & Prashker, J. N. (2006). The impact of travel time information on travelers' learning under uncertainty. *Transportation, 33*(4), 393-408.

Bindel, D., & Goodman, J. (2009). *Principles of scientific computing*. New York: New York University.

Boer, E. R., Caro, S., Cavallo, V., & Arcueil, F. (2007). A cybernetic perspective on car following in fog. *Proceedings of the Fourth International Driving Symposium on Human Factors in Driver Assessment, Training and Vehicle Design,* 9-12.

Brilon, W., & Ponzlet, M. (1996). Variability of speed-flow relationships on german autobahns. *Transportation Research Record: Journal of the Transportation Research Board,* (1555), 91-98.

Broughton, K. L., Switzer, F., & Scott, D. (2007). Car following decisions under three visibility conditions and two speeds tested with a driving simulator. *Accident Analysis & Prevention, 39*(1), 106-116.

Bureau of Labor Statistics. (2016). Consumer price index. Retrieved from http://www.bls.gov/cpi/

Cambridge Systematics, I. (2013). *Analytical procedures for determining the impacts of reliability mitigation strategies.* (No. L03). Washington: Transportation Research Board.

Campolongo, F., Cariboni, J., & Saltelli, A. (2007). An effective screening design for sensitivity analysis of large models. *Environmental Modelling & Software, 22*(10), 1509-1518.

Caro, S., Cavallo, V., Boer, E., & Vienne, F. (2007). The influence of fog on motion discrimination thresholds in car following. *4th International Symposium on Human Factors in Driver Assessment, Training, and Vehicle Design,* 446-451.

Casello, J., Nour, A., & Hellinga, B. (2009). Quantifying impacts of transit reliability on user costs. *Transportation Research Record: Journal of the Transportation Research Board,* (2112), 136-141.

Chen, C., Skabardonis, A., & Varaiya, P. (2003). Travel-time reliability as a measure of service. *Transportation Research Record: Journal of the Transportation Research Board, 1855*(1), 74-79.

Dervisoglu, G., Gomes, G., Kwon, J., Horowitz, R., & Varaiya, P. (2009). Automatic calibration of the fundamental diagram and empirical observations on capacity. *Transportation Research Board 88th Annual Meeting, , 15*

Do, M., & Kobayashi, K. (2000). Hypothesis testing on divers' rational expectations: An experimental approach. *KSCE Journal of Civil Engineering, 4*(1), 1-10.

Edie, L. C. (1961). Car-following and steady-state theory for noncongested traffic. *Operations Research, 9*(1), 66-76.

Edwards, J. B. (1999). Speed adjustment of motorway commuter traffic to inclement weather. *Transportation Research Part F: Traffic Psychology and Behaviour, 2*(1), 1-14.

Eliasson, J. (2007). The relationship between travel time variability and road congestion. *11th World Conference on Transport Research,*

FHWA. (2015). Reducing non-recurring congestion. Retrieved from http://ops.fhwa.dot.gov/program_areas/reduce-non-cong.htm

Fujii, S., & Kitamura, R. (2000). Anticipated travel time, information acquisition, and actual experience: Hanshin expressway route closure, osaka-sakai, japan. *Transportation Research Record: Journal of the Transportation Research Board, 1725*(1), 79-85.

Ge, Q., & Menendez, M. (2012). Sensitivity analysis for calibrating VISSIM in modeling the zurich network. *12th Swiss Transport Research Conference,* Monte Verità / Ascona.

Gomes, G., May, A., & Horowitz, R. (2004). Calibration of VISSIM for a congested freeway. *California Partners for Advanced Transit and Highways (PATH),*

Greenberg, H. (1959). An analysis of traffic flow. *Operations Research, 7*(1), 79-85.

Greenshields, B., Channing, W., & Miller, H. (1935). A study of traffic capacity. *Highway Research Board Proceedings, , 1935*

Hahn, U. (2014). Experiential limitation in judgment and decision. *Topics in Cognitive Science, 6*(2), 229-244.

Haykin, S. (Ed.). (1999). *Neural networks A comprehensive foundation* (2nd ed.). Delhi, India: Pearson Education.

Heaton, J. (2008). *Introduction to neural networks with java* Heaton Research, Inc.

Ibrahim, A. T., & Hall, F. L. (1994). Effect of adverse weather conditions on speed-flow-occupancy relationships. *Transportation Research Record,* (1457), 184-191.

Jin, L., & McLeod, D. S. (2013). Comparison of travel time indexes and other travel Time Reliability measures using florida freeway spot speed data. Paper presented at the *TRB 92nd Annual Meeting,* Washington D.C.

Jolliffe, I. (2002). *Principal component analysis* (2nd ed.). New York: Springer-Verlag.

Kittelson & Associates, Inc., Parsons Brinckerhoff, Inc., KFH Group, Inc., Texas A&M Transportation Institute, & Arup. (2013). *Transit capacity and quality of service manual.* (No. Transit Cooperative Highway Research Program (TCRP) Report 165). Washington, D.C.: Transportation Research Board.

Kittelson and Associates, I. (2012). *Incorporation of travel time reliability into the highway capacity manual.* (Draft Final No. SHRP2-L08). Washington D.C.: Transportation Research Board. Retrieved from http://onlinepubs.trb.org/onlinepubs/shrp2/RFPL38/L08finalreport.pdf

Kwon, J., Barkley, T., Hranac, R., Petty, K., & Compin, N. (2011). Decomposition of travel time reliability into various sources. *Transportation Research Record: Journal of the Transportation Research Board, 2229*(1), 28-33.

Kyte, M., Khatib, Z., Shannon, P., & Kitchener, F. (2001). Effect of weather on free-flow speed. *Transportation Research Record: Journal of the Transportation Research Board, 1776*(1), 60-68.

Lam, T. C., & Small, K. A. (2001). The value of time and reliability: Measurement from a value pricing experiment. *Transportation Research Part E: Logistics and Transportation Review, 37*(2), 231-251.

Lownes, N. E., & Machemehl, R. B. (2006). VISSIM: A multi-parameter sensitivity analysis. *Simulation Conference, 2006. WSC 06. Proceedings of the Winter,* 1406-1413.

Mahmassani, H. S., & Chang, G. (1985). Dynamic aspects of departure-time choice behavior in a commuting system: Theoretical framework and experimental analysis. *Transportation Research Record: Journal of the Transportation Research Board,* (1037), 88-101.

Margiotta, R., Lomax, T. J., Hallenbeck, M. E., Turner, S. M., Skabardonis, A., Ferrell, C., & Eisele, W. L. (2006). *Guide to effective freeway performance measurement* (Contractor Final Report ed.) Transportation Research Board.

Mathworks Inc. (2016). Matlab documentation. Retrieved from: http://www.mathworks.com/help/matlab/

Minnesota department of transportation (MnDOT). Retrieved from http://www.dot.state.mn.us/

MnDPS. (2015). *Minnesota traffic crashes in 2014.* (). Saint Paul, MN: Minnesota Department of Public Safety, Department of Public Safety.

Morris, M. D. (1991). Factorial sampling plans for preliminary computational experiments. *Technometrics, 33*(2), 161-174.

Muth, J. F. (1961). Rational expectations and the theory of price movements. *Econometrica: Journal of the Econometric Society,* 315-335.

Nam, D., & Mannering, F. (2000). An exploratory hazard-based analysis of highway incident duration. *Transportation Research Part A: Policy and Practice, 34*(2), 85-102.

OANDA. (2016). Currency coverter. Retrieved from https://www.oanda.com/currency/converter/

Park, B., & Qi, H. (2006). Microscopic simulation model calibration and validation for freeway work zone network-a case study of VISSIM. *Intelligent Transportation Systems Conference, 2006. ITSC'06. IEEE,* 1471-1476.

Park, B., & Schneeberger, J. (2003). Microscopic simulation model calibration and validation: Case study of VISSIM simulation model for a coordinated actuated signal system. *Transportation Research Record: Journal of the Transportation Research Board,* (1856), 185-192.

Park, S., Rakha, H., & Guo, F. (2010). Calibration issues for multistate model of travel time reliability. *Transportation Research Record: Journal of the Transportation Research Board, 2188*, 74-84. doi:10.3141/2188-09

Rakha, H. A., & Gao, Y. (2008). Calibration of steady-state car-following models using macroscopic loop detector data. *Symposium on the Fundamental Diagram: 75 Years,* Woods Hole, Massachusetts.

Rakha, H. A., Krechmer, D., Cordahi, G., Zohdy, I., Sadek, S., & Arafeh, M. (2009). *Microscopic analysis of traffic flow in inclement weather.* (No. FHWA-JPO-09-066).FHWA, U.S. Department of Transportation.

Rakha, H. A., & Arafeh, M. (2007). Tool for calibrating steady-state traffic stream and car-following models. *Transportation Research Board 86th Annual Meeting,* (07-0506)

Rakha, H., & Arafeh, M. (2010). Calibrating steady-state traffic stream and car-following models using loop detector data. *Transportation Science, 44*(2), 151-168.

Rakha, H., Farzaneh, M., Arafeh, M., Hranac, R., Sterzin, E., & Krechmer, D. (2007). *Empirical studies on traffic flow in inclement weather* Virginia Tech Transportation Institute.

Richardson, A., & Taylor, M. (1978). Travel time variability on commuter journeys. *High Speed Ground Transportation Journal, 12*(1)

Small, K. A. (1999). *Valuation of travel-time savings and predictability in congested conditions for highway user-cost estimation* Transportation Research Board.

Smith, K., & Smith, B. L. (2002). *Incident duration forecasting.* (No. STL-2001-01). Center for Transportation Studies, University of Virginia.

Stern, A. D., Shah, V., Goodwin, L., & Pisano, P. (2003). Analysis of weather impacts on traffic flow in metropolitan washington DC. *Proceedings of the 19th International Conference on Interactive Information and Processing Systems (IIPS) for Meteorology, Oceanography, and Hydrology,*

Tipping, M. E. (2001). Sparse bayesian learning and the relevance vector machine. *Journal of Machine Learning Research, 1*(Jun), 211-244.

Trope, Y., & Liberman, N. (2010). Construal-level theory of psychological distance. *Psychological Review, 117*(2), 440.

Tseng, Y., & Verhoef, E. T. (2008). Value of time by time of day: A stated-preference study. *Transportation Research Part B: Methodological, 42*(7), 607-618.

Tseng, Y., Ubbels, B., & Verhoef, E. (2005). Value of time, schedule delay, and reliability–Estimation results of a stated choice experiment among dutch commuters facing congestion. *45th Congress of European Regional Science Association,*

Tu, H., van Lint, H., & van Zuylen, H. (2008). The effects of traffic accidents on travel time reliability. *Intelligent Transportation Systems, 2008. ITSC 2008. 11th International IEEE Conference On,* 79-84.

U.S. Federal Highway Administration (FHWA). (2009). Travel time reliability:Making it there on time, all the time. Retrieved from: http://ops.fhwa.dot.gov/publications/tt_reliability/TTR_Report.htm#WhatisTTR

Underwood, R. T. (1961). Speed, volume, and density relationships. *Quality and Theory of Traffic Flow*, New Haven , CT. , *1* 141-188.

Van Aerde, M., & Rakha, H. (1995). Multivariate calibration of single regime speed-flow-density relationships. *Proceedings of the 6th 1995 Vehicle Navigation and Information Systems Conference, , 334* 341.

Van Lint, J., van Zuylen, H. J., & Tu, H. (2008). Travel time unreliability on freeways: Why measures based on variance tell only half the story. *Transportation Research Part A: Policy and Practice, 42*(1), 258-277.

Van Winsum, W. (1999). The human element in car following models. *Transportation Research Part F: Traffic Psychology and Behaviour, 2*(4), 207-211.

Warffemius, P. (2013). *The social value of shorter and more reliable travel times.* (No. KiM-13-A03). The Netherlands: KiM Netherlands Institute for Transport Policy Analysis. Retrieved from http://www.kimnet.nl/en/publication/social-value-shorter-and-more-reliable-travel-times

Weifeng, L., Zhengyu, D., & Gaohua, G. (2013). Research on travel time distribution characteristics of expressways in shanghai. *Procedia-Social and Behavioral Sciences, 96*, 339-350.

Appendices

Appendix 1

Computing codes of the PCA+RVM model in R programming language is shown below:

```
# Start of the Code
# ------------------------------------------
# Load necessary libraries
library(dplyr)
library(plyr)
library(base64)
library(qmap)
library(hydroGOF)
library(kernlab)
library(e1071)
library(xlsx)
library(rJava)
library(psych)
rm(list=ls(all=TRUE))
# Import dataset:
setwd("C:/Users/Reza/Dropbox/paper/FinalPapers/3-CongestedData/modelsR")
data<-read.csv ("freekj1.csv",header=TRUE, sep=",")
err = subset(data, select = colnames(data) == "Error")

## Extracting Principal components using PCA
fit <- princomp(data[,-1], cor=TRUE)
plot(fit,type="lines")
pca<- fit$scores[,1:5]
```

```
  data<- cbind(err, pca)


  # Using K-Fold-Cross-validation method in selecting training and testing
subsets;
  splitdf <- function(dataframe, seed=NULL) {
    if (!is.null(seed)) set.seed(seed)
    index <- 1:nrow(dataframe)
    trainindex <- sample(index, trunc(length(index)*.75))
    train <- dataframe[trainindex, ]
    test <- dataframe[-trainindex, ]
    list(train=train,test=test)
  }
  split <- splitdf(data, seed=44)
  trainset <- split$train
  testset <- split$test
  length(trainset[,1])
  length(testset[,1])
  srange <- sigest(Error~.,data = trainset)
  srange
  s <- srange[2]
  s
  # Developing an RVM model:
  modelPcp <- rvm(Error~., data = trainset, type="regression",
kernel="rbfdot", kpar="automatic",   alpha=ncol(as.matrix(trainset)),
var=0.1, var.fix=FALSE, iterations=100, verbosity=0, tol=.Machine$double.eps,
minmaxdiff=1e-3, cross=0, fit=FALSE)


  #Model characteristics:
  summary(modelPcp)
```

```
  # Training Plot:
  modelPcp
  prediction <- predict(modelPcp, trainset[,-1])
  sim1<-prediction[,]
  obs1<-trainset[,1]
  plot1<- ggof(sim=sim1, obs=obs1, ftype="dm", FUN=mean)

  # Plot for testing subset:
  prediction2 <- predict(modelPcp, testset[,-1])
  sim2<-prediction2[,]
  obs2<-testset[,1]
  plot2<- ggof(sim=sim2, obs=obs2, ftype="dm", FUN=mean)
  performance<- gof(sim=sim2, obs=obs2, ftype="dm", FUN=mean)
  modelPcp

  # Getting Predicted and Observed data on validation data:
  write.table (sim2, "sim2.csv", sep=",")
  write.table (obs2, "obs2.csv", sep=",")

  # Project the Target variable (Error in this case) based on new
observations
  # import the new dataset:
  new <-read.csv ("New-Data.csv",header=TRUE, sep=",")
  fit2<- predict(fit, new[,-1])
  pca2<- fit2[,1:5]
  prediction3 <- predict(modelPcp, pca2)
  sim3<-prediction3[,]
  obs3<-new [,1]
  write.table (sim3, "sim3.csv", sep=",")
```

```
write.table (obs3, "obs3.csv", sep=",")

plot3<- ggof(sim=sim3, obs=obs3, ftype="dm", FUN=mean)

performance<- gof(sim=sim3, obs=obs3, ftype="dm", FUN=mean)

# ------------------------------------------

# End of the Code
```

Appendix 2

Table A-Travel time and travel time reliability cost for each Route/time interval for Alternatives 1 and 2

Route	Time Interval	Alternative 1					Alternative 2				
		τ_f (s)	$\tilde{\tau}$(s)	$\hat{\tau}$(s)	TTR Cost	TT Cost	τ_f (s)	$\tilde{\tau}$(s)	$\hat{\tau}$(s)	TTR Cost	TT Cost
1	6:00-6:30	96.1	113.2	175.9	$1,288	$9,435	96.1	113.2	175.9	$996	$8,208
1	6:30-7:00	100.6	126.5	184.1	$1,993	$9,987	100.6	126.5	184.1	$1,198	$9,768
1	7:00-7:30	100.5	124.6	184	$1,905	$9,298	100.5	124.6	184	$1,209	$9,728
1	7:30-8:00	98.8	122.8	180.7	$1,808	$9,044	98.8	122.8	180.7	$1,171	$9,421
1	8:00-8:30	96.7	120.8	177	$1,817	$8,400	96.7	120.8	177	$1,217	$8,998
1	8:30-9:00	95.7	119.7	175.1	$1,653	$10,140	95.7	119.7	175.1	$1,212	$8,810
1	9:00-9:30	94.9	119.2	173.7	$1,781	$9,402	94.9	119.2	173.7	$1,171	$8,080
1	9:30-10:00	93.5	113.1	171.1	$1,399	$8,330	93.5	113.1	171.1	$973	$7,212
1	10:00-10:30	91.7	105.1	167.9	$810	$5,606	91.7	105.1	167.9	$758	$6,066
1	10:30-11:00	92.8	106.5	169.9	$784	$7,202	92.8	106.5	169.9	$713	$4,729
1	11:00-11:30	92.3	105.1	169	$760	$7,139	92.3	105.1	169	$738	$6,265
1	11:30-12:00	92.4	106.3	169.1	$877	$7,709	92.4	106.3	169.1	$764	$6,773
1	12:00-12:30	93.2	105.6	170.5	$754	$7,585	93.2	105.6	170.5	$711	$6,655
1	12:30-13:00	94.1	106.4	172.1	$816	$8,404	94.1	106.4	172.1	$756	$5,711
1	13:00-13:30	93.8	107.8	171.7	$921	$8,228	93.8	107.8	171.7	$776	$8,725
1	13:30-14:00	95.2	109.9	174.1	$1,065	$7,355	95.2	109.9	174.1	$904	$8,989
1	14:00-14:30	95.8	113.9	175.3	$1,356	$10,194	95.8	113.9	175.3	$998	$8,239
1	14:30-15:00	97.6	121.3	178.6	$1,938	$11,821	97.6	121.3	178.6	$1,176	$9,430
1	15:00-15:30	98.1	120	179.4	$1,665	$10,914	98.1	120	179.4	$1,139	$8,022
1	15:30-16:00	96.9	123.7	177.3	$2,188	$9,666	96.9	123.7	177.3	$1,241	$9,551
1	16:00-16:30	96.8	119.7	177.1	$1,716	$10,248	96.8	119.7	177.1	$1,201	$6,776
1	16:30-17:00	96.4	119.9	176.4	$1,667	$8,431	96.4	119.9	176.4	$1,236	$9,087
1	17:00-17:30	96.8	118.4	177.2	$1,588	$8,356	96.8	118.4	177.2	$1,197	$9,082
1	17:30-18:00	96.7	120.4	176.9	$1,724	$8,197	96.7	120.4	176.9	$1,187	$6,829
1	18:00-18:30	95.5	117.3	174.8	$1,514	$9,388	95.5	117.3	174.8	$1,144	$8,119
1	18:30-19:00	93.9	111.6	171.8	$1,249	$8,277	93.9	111.6	171.8	$1,037	$5,631
1	19:00-19:30	92.3	105.8	169	$788	$6,583	92.3	105.8	169	$766	$5,781
1	19:30-20:00	91	104.6	166.5	$650	$5,622	91	104.6	166.5	$625	$4,957
1	20:00-20:30	90.8	102.9	166.1	$573	$5,284	90.8	102.9	166.1	$590	$4,682
1	20:30-21:00	90.8	103	166.1	$513	$5,055	90.8	103	166.1	$557	$4,480
1	21:00-21:30	90.8	103.3	166.1	$498	$4,923	90.8	103.3	166.1	$523	$4,352
1	21:30-22:00	90.1	101.9	164.8	$417	$4,222	90.1	101.9	164.8	$451	$3,760

2	6:00-6:30	94.9	110.2	173.7	$10,646	$73,778	94.9	110.2	173.7	$9,995	$72,038
2	6:30-7:00	100.4	120.7	183.7	$13,997	$97,509	100.4	120.7	183.7	$12,785	$96,472
2	7:00-7:30	98.7	120	180.6	$13,809	$90,623	98.7	120	180.6	$12,553	$98,219
2	7:30-8:00	97.8	119.8	179	$14,552	$87,624	97.8	119.8	179	$13,511	$98,638
2	8:00-8:30	96.3	118.4	176.2	$14,841	$80,530	96.3	118.4	176.2	$13,985	$79,805
2	8:30-9:00	94.8	117.4	173.5	$14,540	$98,774	94.8	117.4	173.5	$14,137	$98,439
2	9:00-9:30	92.3	116.1	168.9	$14,680	$89,162	92.3	116.1	168.9	$14,273	$88,744
2	9:30-10:00	91.4	108.6	167.3	$11,350	$65,902	91.4	108.6	167.3	$11,636	$64,755
2	10:00-10:30	89.8	100.4	164.3	$6,662	$53,168	89.8	100.4	164.3	$6,736	$53,375
2	10:30-11:00	91.5	102.8	167.4	$6,898	$55,420	91.5	102.8	167.4	$6,856	$55,325
2	11:00-11:30	90.6	101.7	165.9	$7,086	$59,831	90.6	101.7	165.9	$6,906	$58,870
2	11:30-12:00	90.9	103.2	166.3	$7,677	$64,088	90.9	103.2	166.3	$7,529	$63,448
2	12:00-12:30	91.7	102.8	167.9	$6,768	$63,878	91.7	102.8	167.9	$6,619	$63,299
2	12:30-13:00	92.9	103.5	170	$7,027	$65,146	92.9	103.5	170	$6,995	$65,148
2	13:00-13:30	92.8	104.5	169.8	$7,764	$64,836	92.8	104.5	169.8	$7,611	$76,753
2	13:30-14:00	94.4	107.6	172.8	$9,263	$70,285	94.4	107.6	172.8	$8,996	$95,072
2	14:00-14:30	94.7	109.2	173.3	$11,010	$93,247	94.7	109.2	173.3	$11,064	$92,521
2	14:30-15:00	96.7	116	177	$14,380	$106,953	96.7	116	177	$13,826	$87,946
2	15:00-15:30	97.2	118	177.8	$15,233	$108,130	97.2	118	177.8	$13,703	$90,007
2	15:30-16:00	96.2	118.2	176.1	$14,582	$84,041	96.2	118.2	176.1	$13,614	$82,580
2	16:00-16:30	95.9	117.5	175.5	$14,178	$82,184	95.9	117.5	175.5	$13,711	$81,304
2	16:30-17:00	95.3	117	174.3	$14,335	$78,548	95.3	117	174.3	$13,410	$78,049
2	17:00-17:30	96	116.4	175.7	$14,199	$81,373	96	116.4	175.7	$13,504	$80,702
2	17:30-18:00	95.9	117.8	175.6	$14,682	$80,131	95.9	117.8	175.6	$13,977	$79,408
2	18:00-18:30	94.4	115.6	172.7	$14,184	$73,306	94.4	115.6	172.7	$13,771	$72,429
2	18:30-19:00	92.3	107.3	168.9	$10,797	$64,055	92.3	107.3	168.9	$11,020	$64,331
2	19:00-19:30	90.6	101.1	165.8	$6,451	$50,905	90.6	101.1	165.8	$6,594	$51,474
2	19:30-20:00	89.3	99.6	163.3	$5,398	$43,770	89.3	99.6	163.3	$5,040	$45,194
2	20:00-20:30	88.7	98	162.4	$4,576	$39,727	88.7	98	162.4	$4,749	$40,265
2	20:30-21:00	88.9	97.8	162.8	$3,902	$37,219	88.9	97.8	162.8	$4,111	$37,529
2	21:00-21:30	89.4	98.4	163.7	$3,830	$37,712	89.4	98.4	163.7	$3,866	$37,114
2	21:30-22:00	88.2	97.1	161.4	$3,244	$31,532	88.2	97.1	161.4	$3,013	$31,382
3	6:00-6:30	143.4	178.9	262.5	$3,252	$17,742	143.4	178.9	262.5	$1,693	$13,507
3	6:30-7:00	151	192.8	276.4	$4,633	$22,361	151	192.8	276.4	$2,014	$16,683
3	7:00-7:30	151.8	190.7	277.7	$4,550	$21,901	151.8	190.7	277.7	$2,136	$19,712
3	7:30-8:00	146.3	190.5	267.8	$4,475	$19,782	146.3	190.5	267.8	$2,039	$16,409
3	8:00-8:30	145.7	185.5	266.6	$4,029	$18,708	145.7	185.5	266.6	$2,049	$16,937
3	8:30-9:00	144.5	181.7	264.5	$3,611	$21,462	144.5	181.7	264.5	$2,097	$16,972

3	9:00-9:30	141.3	179.8	258.5	$3,684	$20,058	141.3	179.8	258.5	$2,155	$15,712
3	9:30-10:00	138.7	175.2	253.8	$3,353	$17,700	138.7	175.2	253.8	$1,751	$13,893
3	10:00-10:30	136.6	170.3	250	$2,521	$12,878	136.6	170.3	250	$1,402	$11,800
3	10:30-11:00	138.4	170	253.3	$2,412	$15,814	138.4	170	253.3	$1,290	$12,501
3	11:00-11:30	137.7	169.1	252.1	$2,327	$13,262	137.7	169.1	252.1	$1,348	$10,418
3	11:30-12:00	137.8	168.7	252.2	$2,600	$14,385	137.8	168.7	252.2	$1,424	$11,240
3	12:00-12:30	137.3	169.5	251.2	$2,448	$16,006	137.3	169.5	251.2	$1,221	$12,664
3	12:30-13:00	139.6	169.1	255.5	$2,577	$15,253	139.6	169.1	255.5	$1,279	$11,590
3	13:00-13:30	140.4	174.8	257	$2,849	$17,591	140.4	174.8	257	$1,400	$11,853
3	13:30-14:00	142.5	174.1	260.7	$2,925	$19,123	142.5	174.1	260.7	$1,526	$16,152
3	14:00-14:30	142.7	176.9	261.1	$3,353	$21,008	142.7	176.9	261.1	$1,793	$15,659
3	14:30-15:00	145.4	185.9	266	$4,423	$24,416	145.4	185.9	266	$2,091	$17,995
3	15:00-15:30	147.9	183.1	270.6	$3,749	$22,877	147.9	183.1	270.6	$2,092	$16,159
3	15:30-16:00	146.2	189.4	267.5	$4,619	$20,649	146.2	189.4	267.5	$2,036	$14,740
3	16:00-16:30	145.6	182.9	266.4	$3,641	$18,361	145.6	182.9	266.4	$1,988	$13,706
3	16:30-17:00	146	182.1	267.1	$3,811	$19,069	146	182.1	267.1	$2,106	$14,215
3	17:00-17:30	143.7	181.2	263	$3,614	$18,324	143.7	181.2	263	$1,976	$13,750
3	17:30-18:00	144.5	185	264.4	$3,876	$18,674	144.5	185	264.4	$2,062	$14,096
3	18:00-18:30	142.7	179.2	261.2	$3,286	$19,694	142.7	179.2	261.2	$1,982	$12,653
3	18:30-19:00	139.7	173.5	255.6	$2,916	$14,748	139.7	173.5	255.6	$1,761	$11,306
3	19:00-19:30	136.4	170.1	249.5	$2,374	$13,906	136.4	170.1	249.5	$1,318	$9,891
3	19:30-20:00	133.6	167.2	244.5	$1,948	$11,837	133.6	167.2	244.5	$1,119	$9,422
3	20:00-20:30	133.6	167.5	244.4	$1,917	$9,775	133.6	167.5	244.4	$1,068	$9,146
3	20:30-21:00	132.3	164	242.1	$1,630	$10,469	132.3	164	242.1	$936	$8,394
3	21:00-21:30	133.7	165	244.7	$1,640	$10,600	133.7	165	244.7	$999	$8,488
3	21:30-22:00	131.6	165.2	240.8	$1,457	$8,620	131.6	165.2	240.8	$779	$6,933
4	6:00-6:30	111.1	156.9	203.4	$3,222	$10,753	111.1	156.9	203.4	$992	$8,207
4	6:30-7:00	125.7	191.9	230.1	$4,753	$14,032	125.7	191.9	230.1	$1,133	$9,308
4	7:00-7:30	129.9	205.7	237.7	$4,956	$15,074	129.9	205.7	237.7	$1,044	$9,314
4	7:30-8:00	129.3	201.1	236.6	$4,846	$15,311	129.3	201.1	236.6	$1,048	$9,666
4	8:00-8:30	123.8	190.5	226.5	$4,871	$16,332	123.8	190.5	226.5	$1,066	$7,756
4	8:30-9:00	126.6	197.4	231.6	$4,831	$14,340	126.6	197.4	231.6	$1,034	$7,152
4	9:00-9:30	122.3	195	223.7	$4,657	$14,816	122.3	195	223.7	$1,067	$9,012
4	9:30-10:00	121.3	195.3	221.9	$4,733	$14,573	121.3	195.3	221.9	$1,201	$6,706
4	10:00-10:30	110.4	162.6	202	$3,652	$12,603	110.4	162.6	202	$1,170	$7,585
4	10:30-11:00	109.8	153.9	201	$3,330	$12,472	109.8	153.9	201	$1,135	$6,200
4	11:00-11:30	109.4	153.8	200.2	$3,343	$12,404	109.4	153.8	200.2	$1,127	$5,968
4	11:30-12:00	111.2	154.9	203.5	$3,257	$10,568	111.2	154.9	203.5	$1,127	$7,813

4	12:00-12:30	107.7	156.3	197	$3,471	$12,568	107.7	156.3	197	$1,130	$7,960
4	12:30-13:00	111	159.4	203.2	$3,505	$12,036	111	159.4	203.2	$1,131	$8,593
4	13:00-13:30	110.7	157.7	202.5	$3,528	$11,099	110.7	157.7	202.5	$1,086	$7,952
4	13:30-14:00	117.6	171	215.3	$4,278	$16,459	117.6	171	215.3	$1,179	$10,380
4	14:00-14:30	119.1	175.2	218	$4,325	$16,463	119.1	175.2	218	$1,173	$10,576
4	14:30-15:00	127.9	201.4	234.1	$5,045	$17,866	127.9	201.4	234.1	$1,105	$9,563
4	15:00-15:30	131.3	208	240.2	$5,147	$17,938	131.3	208	240.2	$1,084	$9,789
4	15:30-16:00	136.7	219.7	250.2	$5,236	$18,800	136.7	219.7	250.2	$1,107	$10,675
4	16:00-16:30	132.3	211.4	242	$5,045	$16,931	132.3	211.4	242	$1,093	$10,402
4	16:30-17:00	130.4	200.7	238.7	$5,072	$17,726	130.4	200.7	238.7	$1,138	$9,810
4	17:00-17:30	126.6	194.7	231.6	$4,838	$16,802	126.6	194.7	231.6	$1,059	$9,550
4	17:30-18:00	127.9	202.4	234.1	$5,109	$14,945	127.9	202.4	234.1	$1,069	$7,586
4	18:00-18:30	124.1	184.4	227.1	$4,818	$16,544	124.1	184.4	227.1	$1,073	$9,443
4	18:30-19:00	119.6	183.9	218.8	$4,474	$15,809	119.6	183.9	218.8	$1,104	$9,194
4	19:00-19:30	115.6	179	211.6	$4,107	$14,643	115.6	179	211.6	$1,067	$8,602
4	19:30-20:00	109.5	167.2	200.4	$3,638	$13,069	109.5	167.2	200.4	$1,124	$7,553
4	20:00-20:30	100.9	147.2	184.7	$2,454	$9,297	100.9	147.2	184.7	$990	$6,008
4	20:30-21:00	102	146.7	186.6	$2,416	$9,087	102	146.7	186.6	$972	$5,945
4	21:00-21:30	101.8	144.9	186.3	$2,381	$9,085	101.8	144.9	186.3	$988	$5,976
4	21:30-22:00	99.6	144.9	182.3	$2,079	$7,712	99.6	144.9	182.3	$875	$5,125
5	6:00-6:30	96.3	114.2	176.2	$14,662	$78,791	96.3	114.2	176.2	$11,710	$77,520
5	6:30-7:00	101.8	130.9	186.2	$23,225	$99,826	101.8	130.9	186.2	$13,323	$93,847
5	7:00-7:30	102.7	145.9	187.9	$30,726	$107,946	102.7	145.9	187.9	$12,176	$98,117
5	7:30-8:00	103.1	135.6	188.7	$24,290	$108,016	103.1	135.6	188.7	$12,750	$100,958
5	8:00-8:30	100.6	130.5	184.1	$22,233	$101,888	100.6	130.5	184.1	$12,042	$95,739
5	8:30-9:00	100	139.5	183	$27,390	$104,772	100	139.5	183	$11,740	$95,418
5	9:00-9:30	96.8	145.4	177.2	$30,457	$98,785	96.8	145.4	177.2	$11,735	$87,426
5	9:30-10:00	96.7	141.5	176.9	$28,854	$94,564	96.7	141.5	176.9	$13,451	$84,664
5	10:00-10:30	92.6	125.1	169.4	$22,051	$82,145	92.6	125.1	169.4	$14,494	$76,219
5	10:30-11:00	93.8	121.5	171.7	$21,126	$80,416	93.8	121.5	171.7	$13,704	$77,137
5	11:00-11:30	94.6	119.4	173	$18,484	$78,727	94.6	119.4	173	$14,231	$76,133
5	11:30-12:00	95.1	119.7	174	$19,167	$78,388	95.1	119.7	174	$13,498	$75,644
5	12:00-12:30	95.1	120.4	174	$19,406	$81,385	95.1	120.4	174	$14,151	$78,384
5	12:30-13:00	95.1	120.6	174.1	$20,142	$89,598	95.1	120.6	174.1	$13,981	$81,166
5	13:00-13:30	95.4	122.3	174.6	$21,492	$85,132	95.4	122.3	174.6	$13,438	$84,869
5	13:30-14:00	96.7	126.2	177	$24,148	$121,346	96.7	126.2	177	$14,811	$116,845
5	14:00-14:30	98	130.4	179.4	$24,788	$130,256	98	130.4	179.4	$13,597	$125,205
5	14:30-15:00	102.4	144.6	187.4	$31,331	$124,872	102.4	144.6	187.4	$13,611	$115,156

5	15:00-15:30	104.4	138.7	191	$25,539	$103,763	104.4	138.7	191	$12,693	$117,299
5	15:30-16:00	107	149.2	195.8	$30,514	$112,892	107	149.2	195.8	$13,455	$102,119
5	16:00-16:30	102.9	143.4	188.3	$28,317	$108,887	102.9	143.4	188.3	$13,158	$100,251
5	16:30-17:00	101.7	139.4	186.1	$28,069	$105,917	101.7	139.4	186.1	$12,436	$99,579
5	17:00-17:30	101.6	137.6	185.9	$26,609	$105,437	101.6	137.6	185.9	$12,846	$96,831
5	17:30-18:00	102	140	186.7	$27,092	$106,504	102	140	186.7	$11,739	$98,461
5	18:00-18:30	100.6	140.8	184	$28,481	$104,651	100.6	140.8	184	$11,962	$97,184
5	18:30-19:00	97.4	136.2	178.3	$25,759	$98,731	97.4	136.2	178.3	$12,263	$91,538
5	19:00-19:30	94.2	132.2	172.5	$23,771	$88,665	94.2	132.2	172.5	$11,672	$82,903
5	19:30-20:00	92	134.4	168.3	$24,170	$77,310	92	134.4	168.3	$13,008	$69,918
5	20:00-20:30	90.2	119.1	165	$16,863	$58,727	90.2	119.1	165	$12,632	$56,374
5	20:30-21:00	90.6	119.1	165.9	$16,932	$57,924	90.6	119.1	165.9	$13,183	$57,494
5	21:00-21:30	90.4	118.6	165.5	$16,434	$56,551	90.4	118.6	165.5	$12,932	$54,810
5	21:30-22:00	89.4	118.3	163.6	$14,411	$49,851	89.4	118.3	163.6	$11,631	$48,329
6	6:00-6:30	92.2	130.3	168.6	$4,235	$13,749	92.2	130.3	168.6	$1,358	$11,720
6	6:30-7:00	102.4	155.9	187.4	$6,125	$18,354	102.4	155.9	187.4	$1,628	$9,953
6	7:00-7:30	106.8	166.8	195.4	$6,512	$20,871	106.8	166.8	195.4	$1,629	$10,884
6	7:30-8:00	108.2	176.5	197.9	$6,466	$20,146	108.2	176.5	197.9	$1,575	$10,742
6	8:00-8:30	103.1	156.3	188.7	$5,931	$18,021	103.1	156.3	188.7	$1,458	$9,957
6	8:30-9:00	101.9	159	186.6	$6,136	$19,448	101.9	159	186.6	$1,544	$10,120
6	9:00-9:30	97.9	151.9	179.1	$5,891	$19,545	97.9	151.9	179.1	$1,547	$9,705
6	9:30-10:00	97.1	149.3	177.8	$5,928	$19,202	97.1	149.3	177.8	$1,662	$9,309
6	10:00-10:30	89.7	128.7	164.1	$4,763	$17,440	89.7	128.7	164.1	$1,636	$8,395
6	10:30-11:00	89.2	124.1	163.3	$4,275	$14,202	89.2	124.1	163.3	$1,600	$8,403
6	11:00-11:30	89.6	123.3	164	$3,979	$12,862	89.6	123.3	164	$1,497	$10,845
6	11:30-12:00	90.8	127.3	166.1	$4,247	$13,796	90.8	127.3	166.1	$1,586	$8,355
6	12:00-12:30	89	124.1	162.8	$4,294	$13,573	89	124.1	162.8	$1,566	$8,293
6	12:30-13:00	91.8	129.7	168	$4,499	$15,938	91.8	129.7	168	$1,548	$12,412
6	13:00-13:30	91.8	124.4	168	$4,575	$14,963	91.8	124.4	168	$1,585	$10,922
6	13:30-14:00	97	139.1	177.5	$5,412	$21,454	97	139.1	177.5	$1,641	$12,730
6	14:00-14:30	99	148.3	181.2	$5,480	$21,661	99	148.3	181.2	$1,641	$14,475
6	14:30-15:00	107.2	169	196.2	$6,508	$23,767	107.2	169	196.2	$1,590	$13,535
6	15:00-15:30	109.5	176.2	200.3	$6,485	$23,616	109.5	176.2	200.3	$1,538	$13,690
6	15:30-16:00	115.4	187	211.2	$6,577	$21,674	115.4	187	211.2	$1,468	$12,923
6	16:00-16:30	109.3	176.1	199.9	$6,248	$20,108	109.3	176.1	199.9	$1,553	$14,296
6	16:30-17:00	109.4	172.8	200.3	$6,558	$20,172	109.4	172.8	200.3	$1,556	$12,191
6	17:00-17:30	108.2	168.5	198	$6,307	$22,230	108.2	168.5	198	$1,433	$9,890
6	17:30-18:00	104.9	162.8	192.1	$6,215	$19,523	104.9	162.8	192.1	$1,537	$10,259

6	18:00-18:30	103.2	153.3	188.9	$6,053	$18,854	103.2	153.3	188.9	$1,498	$9,886
6	18:30-19:00	97.1	148.5	177.8	$5,401	$17,390	97.1	148.5	177.8	$1,507	$9,719
6	19:00-19:30	92	143.6	168.4	$4,931	$16,510	92	143.6	168.4	$1,475	$9,135
6	19:30-20:00	87.8	133.3	160.7	$4,499	$17,423	87.8	133.3	160.7	$1,539	$7,845
6	20:00-20:30	81.6	115.7	149.4	$3,102	$10,034	81.6	115.7	149.4	$1,339	$8,631
6	20:30-21:00	82.4	110.6	150.7	$3,003	$9,951	82.4	110.6	150.7	$1,340	$8,713
6	21:00-21:30	82.7	111.5	151.3	$2,783	$11,359	82.7	111.5	151.3	$1,306	$5,933
6	21:30-22:00	80.6	109.9	147.4	$2,500	$7,939	80.6	109.9	147.4	$1,108	$5,121
7	6:00-6:30	96.9	123	177.4	$755	$4,668	96.9	123	177.4	$535	$4,588
7	6:30-7:00	101.5	125.2	185.8	$948	$6,451	101.5	125.2	185.8	$736	$6,297
7	7:00-7:30	101.7	125.2	186.1	$890	$5,959	101.7	125.2	186.1	$665	$5,838
7	7:30-8:00	101	125.1	184.8	$840	$5,500	101	125.1	184.8	$597	$5,367
7	8:00-8:30	98.9	123.1	181	$795	$5,296	98.9	123.1	181	$501	$5,190
7	8:30-9:00	99.2	123.2	181.5	$760	$5,212	99.2	123.2	181.5	$566	$5,074
7	9:00-9:30	95.8	121.2	175.3	$652	$4,117	95.8	121.2	175.3	$439	$4,060
7	9:30-10:00	96.8	119.9	177.2	$604	$4,098	96.8	119.9	177.2	$462	$4,012
7	10:00-10:30	92.8	118.9	169.9	$526	$3,141	92.8	118.9	169.9	$378	$3,058
7	10:30-11:00	94.4	120.5	172.8	$631	$3,921	94.4	120.5	172.8	$453	$3,814
7	11:00-11:30	95.1	120.1	174	$610	$3,772	95.1	120.1	174	$437	$3,696
7	11:30-12:00	95.5	119.4	174.7	$626	$4,007	95.5	119.4	174.7	$459	$3,916
7	12:00-12:30	96.1	119.6	175.9	$572	$3,825	96.1	119.6	175.9	$412	$3,744
7	12:30-13:00	96.4	121	176.4	$697	$4,416	96.4	121	176.4	$535	$4,298
7	13:00-13:30	96.5	122.3	176.6	$679	$4,252	96.5	122.3	176.6	$481	$4,161
7	13:30-14:00	97.9	122.5	179.2	$763	$5,586	97.9	122.5	179.2	$589	$5,444
7	14:00-14:30	99.5	122.7	182.1	$742	$5,751	99.5	122.7	182.1	$569	$5,576
7	14:30-15:00	100.1	125.1	183.2	$916	$6,092	100.1	125.1	183.2	$706	$5,901
7	15:00-15:30	99.5	125.7	182.1	$1,001	$6,207	99.5	125.7	182.1	$676	$6,098
7	15:30-16:00	102.8	126.4	188.2	$900	$6,082	102.8	126.4	188.2	$706	$5,914
7	16:00-16:30	100.9	125.4	184.6	$887	$5,929	100.9	125.4	184.6	$662	$5,822
7	16:30-17:00	99.6	123.3	182.3	$789	$5,278	99.6	123.3	182.3	$602	$5,232
7	17:00-17:30	100.5	123.8	183.8	$764	$5,281	100.5	123.8	183.8	$588	$5,182
7	17:30-18:00	99	124.1	181.1	$789	$5,084	99	124.1	181.1	$596	$4,965
7	18:00-18:30	98.3	122.7	179.9	$710	$4,723	98.3	122.7	179.9	$510	$4,670
7	18:30-19:00	96.8	120.6	177.1	$635	$4,146	96.8	120.6	177.1	$473	$4,097
7	19:00-19:30	93.8	120.4	171.7	$533	$3,167	93.8	120.4	171.7	$358	$3,111
7	19:30-20:00	92.4	119.8	169.1	$539	$3,127	92.4	119.8	169.1	$386	$3,048
7	20:00-20:30	91.4	117.7	167.2	$431	$2,546	91.4	117.7	167.2	$328	$2,489
7	20:30-21:00	91	115.4	166.6	$414	$2,513	91	115.4	166.6	$328	$2,480

7	21:00-21:30	91.1	117.9	166.8	$490	$2,809	91.1	117.9	166.8	$363	$2,734
7	21:30-22:00	90.4	118.9	165.4	$407	$2,262	90.4	118.9	165.4	$307	$2,209
8	6:00-6:30	69	85.6	126.2	$1,475	$7,701	69	85.6	126.2	$697	$6,123
8	6:30-7:00	70.4	85.9	128.9	$1,792	$10,183	70.4	85.9	128.9	$754	$11,708
8	7:00-7:30	70.4	86.5	128.8	$1,813	$10,162	70.4	86.5	128.8	$791	$7,926
8	7:30-8:00	69.3	85.7	126.8	$1,700	$9,169	69.3	85.7	126.8	$699	$7,174
8	8:00-8:30	68.9	85.5	126.2	$1,735	$9,260	68.9	85.5	126.2	$710	$7,266
8	8:30-9:00	68.7	86.2	125.8	$1,706	$8,870	68.7	86.2	125.8	$698	$6,937
8	9:00-9:30	66.9	83.9	122.4	$1,294	$6,741	66.9	83.9	122.4	$569	$5,334
8	9:30-10:00	67.3	83.8	123.2	$1,339	$6,960	67.3	83.8	123.2	$566	$5,524
8	10:00-10:30	65.3	83.5	119.5	$1,131	$5,397	65.3	83.5	119.5	$512	$6,385
8	10:30-11:00	66.7	83.7	122.1	$1,263	$6,327	66.7	83.7	122.1	$551	$7,406
8	11:00-11:30	66.5	82.9	121.7	$1,253	$6,391	66.5	82.9	121.7	$573	$5,101
8	11:30-12:00	66.6	83.7	122	$1,302	$6,518	66.6	83.7	122	$600	$7,654
8	12:00-12:30	66.3	83.6	121.4	$1,283	$6,355	66.3	83.6	121.4	$594	$7,482
8	12:30-13:00	67.8	84.6	124.1	$1,384	$7,008	67.8	84.6	124.1	$562	$5,545
8	13:00-13:30	67.3	84.2	123.2	$1,365	$9,600	67.3	84.2	123.2	$573	$5,563
8	13:30-14:00	68.7	85.5	125.7	$1,517	$7,898	68.7	85.5	125.7	$680	$6,235
8	14:00-14:30	67.9	84.2	124.2	$1,543	$8,369	67.9	84.2	124.2	$685	$6,630
8	14:30-15:00	70.3	86.1	128.7	$1,725	$12,312	70.3	86.1	128.7	$813	$10,072
8	15:00-15:30	69.8	87.5	127.8	$2,053	$14,057	69.8	87.5	127.8	$795	$11,761
8	15:30-16:00	69.1	86.6	126.5	$1,871	$10,057	69.1	86.6	126.5	$832	$7,680
8	16:00-16:30	68.9	85.2	126.1	$1,751	$9,439	68.9	85.2	126.1	$795	$7,406
8	16:30-17:00	69.1	84.4	126.5	$1,549	$8,880	69.1	84.4	126.5	$658	$6,950
8	17:00-17:30	69.4	85.4	126.9	$1,622	$8,792	69.4	85.4	126.9	$623	$6,936
8	17:30-18:00	69	86.2	126.2	$1,657	$8,470	69	86.2	126.2	$693	$6,600
8	18:00-18:30	67.9	84.4	124.3	$1,517	$8,001	67.9	84.4	124.3	$671	$6,370
8	18:30-19:00	67.5	84.5	123.5	$1,384	$7,102	67.5	84.5	123.5	$613	$5,626
8	19:00-19:30	66.7	84.9	122.1	$1,148	$5,550	66.7	84.9	122.1	$521	$4,425
8	19:30-20:00	66.2	85.1	121.1	$1,158	$5,338	66.2	85.1	121.1	$536	$6,224
8	20:00-20:30	64.7	84.8	118.4	$980	$6,003	64.7	84.8	118.4	$445	$5,166
8	20:30-21:00	64.2	83.4	117.4	$945	$6,013	64.2	83.4	117.4	$481	$5,226
8	21:00-21:30	66	84.6	120.7	$1,021	$6,526	66	84.6	120.7	$488	$5,588
8	21:30-22:00	65.1	84.1	119.1	$863	$4,083	65.1	84.1	119.1	$440	$4,855
9	6:00-6:30	69.3	89.6	126.9	$627	$3,866	69.3	89.6	126.9	$315	$2,951
9	6:30-7:00	72.5	92.1	132.6	$778	$5,001	72.5	92.1	132.6	$370	$3,765
9	7:00-7:30	72.1	91.9	132	$726	$4,707	72.1	91.9	132	$352	$3,539
9	7:30-8:00	71.4	92.2	130.6	$683	$4,231	71.4	92.2	130.6	$333	$3,170

9	8:00-8:30	70.9	90.8	129.7	$675	$4,282	70.9	90.8	129.7	$299	$3,217
9	8:30-9:00	68.9	89.2	126.2	$659	$4,127	68.9	89.2	126.2	$305	$3,142
9	9:00-9:30	68.3	87.4	125	$511	$3,247	68.3	87.4	125	$258	$2,481
9	9:30-10:00	67.1	87.7	122.8	$554	$3,258	67.1	87.7	122.8	$263	$2,493
9	10:00-10:30	65.9	85.6	120.7	$447	$2,706	65.9	85.6	120.7	$220	$2,075
9	10:30-11:00	66.8	86.6	122.2	$488	$2,955	66.8	86.6	122.2	$237	$2,259
9	11:00-11:30	66.6	85.9	121.8	$518	$3,169	66.6	85.9	121.8	$258	$2,422
9	11:30-12:00	68.3	86.1	125	$476	$3,123	68.3	86.1	125	$264	$2,387
9	12:00-12:30	67.4	87.3	123.3	$520	$3,197	67.4	87.3	123.3	$255	$2,442
9	12:30-13:00	69.2	88.8	126.6	$557	$3,428	69.2	88.8	126.6	$271	$2,600
9	13:00-13:30	68.1	87.8	124.7	$545	$3,476	68.1	87.8	124.7	$296	$2,656
9	13:30-14:00	70	88.8	128.1	$563	$3,713	70	88.8	128.1	$284	$2,829
9	14:00-14:30	69.8	90.6	127.8	$682	$4,015	69.8	90.6	127.8	$288	$3,015
9	14:30-15:00	71.6	92	131	$733	$4,586	71.6	92	131	$369	$3,431
9	15:00-15:30	71.5	91.9	130.8	$731	$4,771	71.5	91.9	130.8	$353	$3,561
9	15:30-16:00	71.6	91.3	131	$731	$4,719	71.6	91.3	131	$383	$3,537
9	16:00-16:30	71.5	90.8	130.9	$675	$4,398	71.5	90.8	130.9	$326	$3,306
9	16:30-17:00	71.4	90.2	130.7	$645	$4,188	71.4	90.2	130.7	$314	$3,162
9	17:00-17:30	71.2	89.9	130.4	$629	$4,178	71.2	89.9	130.4	$320	$3,154
9	17:30-18:00	70.5	90.1	128.9	$609	$3,932	70.5	90.1	128.9	$323	$2,967
9	18:00-18:30	69.3	90	126.8	$610	$3,700	69.3	90	126.8	$284	$2,798
9	18:30-19:00	68.1	87.6	124.6	$522	$3,297	68.1	87.6	124.6	$265	$2,523
9	19:00-19:30	66.3	86.1	121.3	$420	$2,559	66.3	86.1	121.3	$202	$1,966
9	19:30-20:00	65.7	85.6	120.2	$401	$2,358	65.7	85.6	120.2	$200	$1,815
9	20:00-20:30	64.5	85.7	118	$353	$1,980	64.5	85.7	118	$172	$1,534
9	20:30-21:00	64.8	85	118.7	$338	$1,971	64.8	85	118.7	$174	$1,531
9	21:00-21:30	65.1	86.6	119.2	$390	$2,199	65.1	86.6	119.2	$198	$1,693
9	21:30-22:00	64.9	85.1	118.7	$328	$1,867	64.9	85.1	118.7	$171	$1,457
10	6:00-6:30	93.2	107.5	170.6	$1,275	$9,734	93.2	107.5	170.6	$1,531	$9,862
10	6:30-7:00	95.9	109.6	175.5	$1,377	$11,305	95.9	109.6	175.5	$1,947	$12,658
10	7:00-7:30	95.8	109.8	175.2	$1,486	$12,305	95.8	109.8	175.2	$1,985	$12,271
10	7:30-8:00	94.7	109	173.2	$1,544	$12,698	94.7	109	173.2	$2,026	$12,420
10	8:00-8:30	94.7	107.7	173.3	$1,300	$13,850	94.7	107.7	173.3	$1,760	$11,254
10	8:30-9:00	94.6	107.8	173.1	$1,319	$10,794	94.6	107.8	173.1	$1,791	$10,887
10	9:00-9:30	92.3	106.6	168.9	$1,182	$9,475	92.3	106.6	168.9	$1,595	$9,672
10	9:30-10:00	92.5	106.2	169.2	$1,145	$9,712	92.5	106.2	169.2	$1,399	$11,992
10	10:00-10:30	89.3	104.7	163.4	$1,100	$8,100	89.3	104.7	163.4	$1,165	$8,046
10	10:30-11:00	92	106	168.4	$1,105	$9,031	92	106	168.4	$1,401	$8,911

10	11:00-11:30	91.2	105.5	166.9	$1,093	$10,940	91.2	105.5	166.9	$1,230	$8,364
10	11:30-12:00	91.2	104.4	167	$1,036	$8,668	91.2	104.4	167	$1,363	$8,657
10	12:00-12:30	91.9	105.2	168.3	$1,126	$9,479	91.9	105.2	168.3	$1,458	$9,386
10	12:30-13:00	91.9	105.9	168.2	$1,155	$9,003	91.9	105.9	168.2	$1,531	$9,089
10	13:00-13:30	91.8	107.2	167.9	$1,282	$9,609	91.8	107.2	167.9	$1,411	$9,537
10	13:30-14:00	93.2	107.1	170.6	$1,219	$14,272	93.2	107.1	170.6	$1,757	$14,605
10	14:00-14:30	93.8	108.5	171.7	$1,417	$15,466	93.8	108.5	171.7	$1,812	$15,715
10	14:30-15:00	94.1	108.3	172.2	$1,464	$15,160	94.1	108.3	172.2	$2,094	$15,465
10	15:00-15:30	95.2	109.7	174.2	$1,507	$14,647	95.2	109.7	174.2	$1,942	$14,564
10	15:30-16:00	97	112.2	177.6	$1,733	$13,414	97	112.2	177.6	$2,611	$13,759
10	16:00-16:30	96.3	111	176.3	$1,632	$13,467	96.3	111	176.3	$2,319	$13,339
10	16:30-17:00	95	108	173.8	$1,417	$12,844	95	108	173.8	$2,312	$12,785
10	17:00-17:30	95	108.6	173.9	$1,457	$11,859	95	108.6	173.9	$1,920	$11,950
10	17:30-18:00	95.7	109.5	175.1	$1,448	$11,974	95.7	109.5	175.1	$1,988	$13,487
10	18:00-18:30	94.6	108.6	173.2	$1,352	$13,948	94.6	108.6	173.2	$1,795	$12,305
10	18:30-19:00	93.8	107	171.6	$1,192	$10,134	93.8	107	171.6	$1,525	$10,274
10	19:00-19:30	91.4	105.3	167.3	$929	$7,338	91.4	105.3	167.3	$1,162	$9,203
10	19:30-20:00	90.3	104.3	165.2	$809	$7,867	90.3	104.3	165.2	$976	$7,746
10	20:00-20:30	88.2	103.8	161.3	$768	$6,753	88.2	103.8	161.3	$767	$6,641
10	20:30-21:00	87.9	102.3	160.8	$694	$6,339	87.9	102.3	160.8	$759	$6,248
10	21:00-21:30	88.1	103.7	161.2	$732	$6,247	88.1	103.7	161.2	$769	$6,108
10	21:30-22:00	89.3	104.7	163.5	$697	$6,212	89.3	104.7	163.5	$750	$6,030
11	6:00-6:30	72.4	109.9	132.5	$546	$2,206	72.4	109.9	132.5	$203	$1,607
11	6:30-7:00	75.7	109.9	138.6	$605	$2,614	75.7	109.9	138.6	$215	$1,885
11	7:00-7:30	73.7	108.9	134.9	$654	$2,829	73.7	108.9	134.9	$227	$2,041
11	7:30-8:00	73.8	109.2	135.1	$678	$2,790	73.8	109.2	135.1	$215	$2,007
11	8:00-8:30	73.2	111.8	133.9	$635	$2,575	73.2	111.8	133.9	$238	$1,851
11	8:30-9:00	75.6	108.9	138.4	$630	$2,738	75.6	108.9	138.4	$235	$1,992
11	9:00-9:30	72.7	110.2	133.1	$601	$2,422	72.7	110.2	133.1	$232	$1,780
11	9:30-10:00	72.4	109.9	132.6	$594	$2,425	72.4	109.9	132.6	$209	$1,761
11	10:00-10:30	71.9	107.5	131.6	$513	$2,079	71.9	107.5	131.6	$184	$1,502
11	10:30-11:00	72.5	110.6	132.7	$595	$2,308	72.5	110.6	132.7	$228	$1,685
11	11:00-11:30	71	107.1	129.9	$535	$2,166	71	107.1	129.9	$202	$1,591
11	11:30-12:00	70.3	106.3	128.6	$530	$2,327	70.3	106.3	128.6	$212	$1,692
11	12:00-12:30	75.1	112.3	137.4	$632	$2,511	75.1	112.3	137.4	$213	$1,795
11	12:30-13:00	74.6	110.4	136.4	$587	$2,405	74.6	110.4	136.4	$216	$1,725
11	13:00-13:30	74	109.6	135.4	$606	$2,554	74	109.6	135.4	$245	$1,854
11	13:30-14:00	73.1	107.8	133.8	$611	$2,557	73.1	107.8	133.8	$210	$1,864

11	14:00-14:30	75	109	137.2	$608	$2,679	75	109	137.2	$213	$2,112
11	14:30-15:00	73.8	111	135.1	$724	$2,994	73.8	111	135.1	$239	$2,232
11	15:00-15:30	76.7	114	140.4	$732	$2,838	76.7	114	140.4	$247	$2,037
11	15:30-16:00	75.4	110.8	137.9	$696	$3,024	75.4	110.8	137.9	$270	$2,185
11	16:00-16:30	76	110	139.1	$752	$3,159	76	110	139.1	$279	$2,292
11	16:30-17:00	73.9	108.4	135.2	$672	$2,868	73.9	108.4	135.2	$250	$2,072
11	17:00-17:30	74.1	111.6	135.5	$690	$2,835	74.1	111.6	135.5	$235	$2,037
11	17:30-18:00	76.5	112	140	$703	$2,904	76.5	112	140	$229	$2,084
11	18:00-18:30	73.5	110.1	134.4	$651	$2,697	73.5	110.1	134.4	$236	$1,960
11	18:30-19:00	72.1	108.1	131.9	$582	$2,405	72.1	108.1	131.9	$208	$1,755
11	19:00-19:30	71.3	109.4	130.5	$441	$1,766	71.3	109.4	130.5	$159	$1,281
11	19:30-20:00	70.6	108.8	129.1	$391	$1,529	70.6	108.8	129.1	$156	$1,117
11	20:00-20:30	69.9	107.4	128	$319	$1,458	69.9	107.4	128	$134	$978
11	20:30-21:00	68.9	105	126.1	$289	$1,500	68.9	105	126.1	$137	$907
11	21:00-21:30	68	105.4	124.4	$269	$1,396	68	105.4	124.4	$112	$1,093
11	21:30-22:00	68.1	107.3	124.5	$303	$1,494	68.1	107.3	124.5	$129	$1,176
12	6:00-6:30	92.5	113.5	169.4	$1,350	$9,810	92.5	113.5	169.4	$927	$6,853
12	6:30-7:00	96.4	116.3	176.5	$1,509	$9,317	96.4	116.3	176.5	$1,001	$8,196
12	7:00-7:30	95.6	116.2	174.9	$1,593	$11,913	95.6	116.2	174.9	$973	$8,361
12	7:30-8:00	95.3	114.7	174.4	$1,573	$12,087	95.3	114.7	174.4	$1,053	$8,412
12	8:00-8:30	94.6	113.4	173.1	$1,430	$8,938	94.6	113.4	173.1	$924	$7,846
12	8:30-9:00	93.4	113.8	170.8	$1,512	$11,285	93.4	113.8	170.8	$1,015	$8,074
12	9:00-9:30	91.2	111.5	167	$1,298	$9,727	91.2	111.5	167	$847	$6,819
12	9:30-10:00	90.4	111.5	165.5	$1,346	$7,629	90.4	111.5	165.5	$861	$6,739
12	10:00-10:30	88.7	109.8	162.4	$1,134	$8,020	88.7	109.8	162.4	$785	$5,570
12	10:30-11:00	91.2	112.3	166.9	$1,288	$7,573	91.2	112.3	166.9	$828	$8,475
12	11:00-11:30	88.7	109.5	162.3	$1,254	$8,823	88.7	109.5	162.3	$810	$6,502
12	11:30-12:00	90.3	110	165.2	$1,237	$7,657	90.3	110	165.2	$857	$6,791
12	12:00-12:30	91.1	110.3	166.7	$1,286	$9,779	91.1	110.3	166.7	$855	$7,145
12	12:30-13:00	91.4	109.9	167.3	$1,208	$8,252	91.4	109.9	167.3	$861	$8,662
12	13:00-13:30	91.8	110.8	167.9	$1,323	$7,987	91.8	110.8	167.9	$922	$7,037
12	13:30-14:00	92.2	113.3	168.7	$1,418	$8,280	92.2	113.3	168.7	$926	$9,571
12	14:00-14:30	93.4	113.4	170.9	$1,470	$11,672	93.4	113.4	170.9	$1,002	$11,235
12	14:30-15:00	95.2	115.1	174.3	$1,655	$12,535	95.2	115.1	174.3	$1,091	$11,655
12	15:00-15:30	95.2	115.3	174.2	$1,580	$11,964	95.2	115.3	174.2	$1,041	$10,821
12	15:30-16:00	97.2	116.3	177.8	$1,637	$10,368	97.2	116.3	177.8	$1,120	$9,245
12	16:00-16:30	96.8	115.9	177.2	$1,664	$10,416	96.8	115.9	177.2	$1,085	$9,042
12	16:30-17:00	94.3	114.9	172.5	$1,666	$9,663	94.3	114.9	172.5	$1,071	$11,068

12	17:00-17:30	94.8	114.3	173.4	$1,552	$9,529	94.8	114.3	173.4	$1,051	$8,425
12	17:30-18:00	95.7	114.9	175.1	$1,571	$9,975	95.7	114.9	175.1	$1,074	$9,368
12	18:00-18:30	94	114	172	$1,487	$9,212	94	114	172	$1,012	$10,341
12	18:30-19:00	91.3	112.1	167.1	$1,354	$7,755	91.3	112.1	167.1	$885	$8,920
12	19:00-19:30	89.1	110.6	163	$1,067	$6,150	89.1	110.6	163	$745	$6,903
12	19:30-20:00	86.8	109.5	158.9	$979	$6,431	86.8	109.5	158.9	$657	$5,908
12	20:00-20:30	86	109.1	157.4	$880	$5,620	86	109.1	157.4	$594	$5,202
12	20:30-21:00	85.3	108.6	156	$783	$5,063	85.3	108.6	156	$546	$4,672
12	21:00-21:30	86.1	110.5	157.6	$820	$5,052	86.1	110.5	157.6	$543	$4,617
12	21:30-22:00	85.3	109.8	156	$762	$4,841	85.3	109.8	156	$527	$4,459
				Sum	**$1,714,385**	**$8,282,449**			**Sum**	**$1,032,186**	**$7,442,994**